UNIVERSITY OF CYPRUS

DEPARTMENT OF HISTORY AND ARCHAEOLOGY

MA Programme in Field Archaeology on Land and Under the Sea

A digital approach to micro-stratigraphy: the case of Mazotos Shipwreck

Master's dissertation by

Irene Maritsa Katsouri

Thesis supervisor: Dr. Stella Demesticha

Nicosia, May 2021

I hereby declare that all opinions in this paper are my own, and that the text does not reflect official opinions of the University of Cyprus.

Acknowledgements

This thesis would not have been possible without the support of many people.

First and foremost, I am immensely grateful to my supervisor, Dr. Stella Demesticha, for suggesting and helping me pursue this topic, but also for her continuous guidance, encouragement and patience. I would also like to thank her for the privilege of working on the Mazotos and other projects and for granting me access to the Mazotos dataset.

I would also like to express my deep appreciation to the members of my committee, Professor Maria Iacovou and Professor Apostolos Sarris, as well as to the Department of Antiquities for permitting the use of certain photographs as part of this thesis. My sincerest thanks are also extended to Dr. Eleni Loizides and Constantina Hadjivasili, whose work played a key role in this study.

In the course of this work I have benefited greatly from discussions with Dr. Massimiliano Secci, who took the time to read chapters and provide both guidance and a sounding board on numerous occasions. I would also like to acknowledge the valuable technical advice provided by Andonis Neophytou.

I am indebted to my friends and colleagues for their kindness and moral support during my study, but most especially to Georgia-Dimitra Kyriakou for her friendship and for sharing this otherwise lonely endeavour with me.

Lastly, my family deserves endless gratitude, for their understanding and infinite support throughout this process. For all the sacrifices that you've made on my behalf, thank you Christofore.

This thesis is lovingly dedicated to Christoforos, Georgia, Ella, Paris and Phivos.

Table of Contents

List of Tables

List of Figures

1. Introduction

Understanding and reconstructing the wreck site formation processes (WSFP) and events that have transformed a ship into an archaeological site is an established area of research in shipwreck archaeology and an essential prerequisite to the interpretation of any shipwreck. However, the scarcity of coherent and undisturbed ancient shipwreck sites, but also the only recent advancements of underwater mapping techniques (in terms of efficiency, accuracy and detail) have prevented archaeologists from comprehensively examining and reconstructing such complex procedures (i.e. WSFP) in ancient shipwrecks.

The process of identifying and describing the WSFP is achieved through the documentation, study and analysis of the surviving material and their associations. Even evidence that may at first appear unexciting or insignificant need to be objectively and accurately recorded, to ensure that all information and meaning that may be extracted from the study of the site, feeds into its reconstruction and interpretation, giving a basis secure enough to justify conclusions.

With this in mind, even the isolated and fragmentary finds within the broader site can contribute in explaining the spatial disposition and relational aspects that characterize the site assemblage. The potential information that may be derived from the spatial analysis of such micro-scale evidence (i.e. small finds and pottery fragments) in shipwreck sites, however, has yet to be fully explored.

The present thesis explores the use of 3D modelling and visualization for intra-site stratigraphic analysis, using as its case study the Mazotos shipwreck site, a coherent shipwreck site, dated to the 4th century BC and located southwest of Larnaca, Cyprus. A workflow for mapping micro-stratigraphic evidence in a 3D environment is proposed, using the digital documentation and excavation data of the Mazotos Shipwreck Project. The aim of this research is to evaluate the potential of the 3D approach of mapping the spatial disposition of small artefacts, in the stratigraphic analysis of shipwreck sites and the study of WSFP.

Thus, the research objectives of this study are as follows:

1. To develop a methodological approach for the plotting and visualization of sherds and small finds in a 3D environment, during and post fieldwork.
2. To apply the methodology to specific finds and evaluate the potential of the method, for the study of the shipwreck's stratigraphy.

3. To assess the results of the case studies, in comparison with potential results and knowledge gained through conventional analytical methods.

The process followed to achieve the objectives listed above, involves both literature-based research and a practical component. First, I discuss the stratigraphy of shipwreck sites and the WSFP that transform a ship into an archaeological site. As this thesis focuses on the post-processing of 3D spatial data, research will also involve a focused discussion on 3D recording and modelling techniques as research tools in the field of Maritime Archaeology.

In Chapter 3, I present the case study for this research, the Mazotos shipwreck site, currently being excavated by the University of Cyprus under the direction of Dr. Stella Demesticha. This chapter includes an overview of the project and the established documentation methods at the site, but also of the data produced during and post fieldwork. An overview of the published analysis regarding the site formation processes at the bow of the ship is also provided, as the present study focuses on examining and mapping some of the artefacts deposited in this specific area.

The proposed methodological approach is presented in Chapter 4, before describing its implementation for the spatial analysis of twelve artefact reconstructions that form the basis of this work. The existing Mazotos 3D Site Model (3DSM), augmented with the plotted fragments and information derived from the conservation work, already completed before this research started, will then serve to evaluate the potential of this added 3D information in enhancing the study of the site. The spatial analysis is conducted with the intent of determining whether insights may be acquired into the stratigraphy and WSFP of the Mazotos shipwreck site.

Chapter 5 focuses on discussing and evaluating the proposed methodology as well as the findings of this study. The use of a virtual 3D environment will be appraised, on whether it can facilitate a more comprehensive analysis and interpretation of the site. The meaning, importance and relevance of the results are considered in order to answer the question of whether micro-stratigraphic evidence can contribute and in what manner in the study and understanding of a coherent shipwreck site.

Finally, Chapter 6 summarizes the conclusions of this dissertation. An Appendix follows, with information on the artefacts involved in the twelve reconstructions.

2. Shipwreck Archaeology

Shipwrecks can offer unique insights into the past (Gibbins & Adams 2001: 281). Even though shipwreck sites vary in extent, environmental conditions and complexity, it is crucial that their archaeological investigation is always conducted using controlled, scientific methods. A careful and systematic approach is necessary for both the study of the remains of the ship (structure and cargo) and the wreck site itself (geomorphological context); this prevents the loss of valuable archaeological information and leads to the reconstruction of the past based on appropriate interpretation of the archaeological record (Gould 2011: 2-3).

2.1 The Stratigraphy of Shipwreck Sites

Shipwreck sites are distinctly different from other archaeological sites, in a number of ways. Firstly, we must recognize that a ship and its contents were once mobile, able to move freely over large distances of water. In the event of wrecking, the ship and its remains come to rest in a location, environment and manner that was not selected nor intended, quite possibly away from its place of origin (Martin 2011: 1-2; Adams 2013: 19-20). In this respect shipwreck stratigraphy is very different to the stratified deposits encountered on land sites, a result of post-depositional factors, including re-occupation or reuse of the site (Gibbins 1990: 377; Gould 2011: 53-54; Adams 2013: 19-20). As Gibbins and Adams explain, the accidental nature of shipwreck sites 'results in a contemporaneous assemblage of material lost in use' (2001: 205). This means that the vessel and its contents are contemporaneous in reference to the wrecking event and consequently, "we have a much better chance of being able to discern relationships between individual objects, between assemblages of objects and between these assemblages and the structures within which they were stored or used" (Adams 2013: 20). Certainly the coherence and integrity of the assemblage must be established first, before assuming these attributes are applicable.

Most shipwreck sites show no evidence of stratified deposits over long periods of time, except in the case of ship smears: when multiple wreck depositions are evident at the same site. At most shipwreck sites, archaeologists encounter superposition and a kind of internal stratigraphy, which usually relates to a single event in time (the wrecking sequence). Thus the stratigraphy of a shipwreck may have little or no temporal significance but instead a particular spatial significance (Green 2004: 244; Gould 2011: 53-54), and in this regard "limited to three primary layers: the surface that more often consists of disturbed finds and

depositional sediment, the layer of the ship deposition, and the sterile layer of the seabed where the ship lies" (Demesticha et al. 2014: 137).

Green (2004:244) warns that careful excavation and documentation is necessary at all times, in order to detect subtle changes in colour, texture, compaction or artefact content, which may indicate different stratigraphic layers. The task of recording stratigraphy under water is an extremely difficult one. Maritime archaeologists are rarely able to excavate vertical cross-sections (except in compact mud), as the sediment can seldom hold a vertical wall, instead collapsing with the sides infilling. Therefore a site is excavated (in small sections or larger areas), systematically in both the horizontal and vertical directions, proceeding downwards layer by layer, documenting the three-dimensional coordinate location of all artefacts as well as their associations (Green 2004: 236-237; Gould 2011: 53).

As Adams (2013: 20) illustrates "a ship arrives at its place of wrecking with an onboard stratigraphy"- its components (hull structure, ballast, cargo, other assemblages, fixtures and fittings) constitute a stratigraphic sequence. From the moment of its deposit on the seafloor, the natural and cultural processes that affect and transform it, result in the creation of a unilinear and not a multilinear stratigraphic sequence (Harris 1989: 128-129; Demesticha et al. 2014: 137). As Harris (1989: 129) defines: "A multilinear stratigraphic sequence is, therefore, usually composed of a series of unilinear sequences which do not have superpositional links, the one to the other. The chronological relationships between these separate parts of a multilinear stratigraphic sequence must be determined by the analysis of non-stratigraphic data". Non-stratigraphic data, are derived from reliable radiocarbon dates or evidence from the geoarchaeological characteristics, site-formation processes, or from the study of the artefacts contained in each deposit. This information ultimately serves to divide the multilinear stratigraphic sequence into phases and/or periods, by grouping all those units belonging to the same period of time. A site is described as having a unilinear stratigraphic sequence when successive layers accumulate one after the other, following the law of superposition, producing a single chain of chronological events.

With this in mind, the stratigraphy of a shipwreck site may have more of a spatial significance rather than a long-term temporal one. Consequently, archaeologists need to fully record and investigate the 'spatial dimension' of the site, the exact location each artefact is found, in relation to its surroundings. Next, it must deduced whether the *in situ* location is in fact the artefact's original position, or can be directly associated to the onboard stratigraphy

or if instead may provide information on different phases of the site's formation process (Green 2004: 244-245; Spooner 2004: 27-28; Gould 2011: 53-54). These different phases are outlined by Demesticha et al. (2014: 135) as being: "those that were moved during the unstable phase of the wreckage (either while on the surface or during the wrecking of the ship on the seabed), finds that were moved during the stable phase of the hull disintegration and the shipwreck site formation processes, and lastly, those that were moved because of anthropogenic causes (e.g., disturbance from divers, boats, fishing nets, etc.)". A similar line of investigation is to be followed to examine the site's second dimension, its 'formal dimension', which considers the condition of each artefact, as it was found in the archaeological record. For instance, a fragmentary artefact could have been broken at any point, prior, during or after the wrecking process (Spooner 2004: 28-29).

To return to the topic of the spatial association of artefacts, Gould (2011: 58-60) proposes the concept of primary, secondary and tertiary associations according to the degree of physical integrity of the material associations at the site. Primary associations occur when we find elements of the ship's structure directly attached to each other or when elements of the ship's cargo are found in their original position and in direct contact with the ship's structural remains. Secondary associations can offer information of the post-depositional process affecting a site, as these occur when elements of structure are detached from their original position and associations, but can be reconnected. Lastly, tertiary associations "usually occur in highly dispersed contexts and may indicate mixed deposits from overlapping debris fields or isolated objects derived from other wrecks" (Gould 2011: 60). Of course, some associations cannot be explained, either because the archaeological record is incomplete (fragile items disappearing from the site) or due to the inherent inability of fully and completely understanding human behavior of the past (Green 2004: 351; Gould 2011: 60-61).

An additional differentiation of shipwreck sites, is highlighted by Bowens (2009: 27, 58), who states that the nature of stratification under water, where sediments are mobile, is likely to be very different and even more complex that in the stable contexts of terrestrial sites. Thus, maritime archaeologists need to investigate a shipwreck alongside its environment and never separately, if they are to "understand the complex mechanisms of destruction, dispersal, reordering, decay, and stabilization with which the relevant area of seafloor has reacted to the intrusion of a wreck" (Martin 2011: 2) which is essential in retracing and understanding how a site is formed, as well as the archaeological material it preserves. These mechanisms, which can be either natural or cultural and "transform a sinking vessel into a

site as it is archaeologically observable" (Gibbins 1990: 382), constitute the WSFP, the complexities of which are examined next.

2.2 Wreck – Site Formation Processes

Archaeologists cannot study past human behavior directly; instead they must study the material culture found in the archaeological record, from which past behavior can be inferred. This is not an easy task, as the archaeological record (even though likened to a 'time capsule') seldom represents a moment frozen in time, but is instead affected by various factors and processes, from its original deposition and subsequently until any archaeological recovery is made (Muckelroy 1978: 56; Murphy 1997: 386; Stewart 1999: 587; Adams 2013: 20). As a definition, Bahn (2001: 165) states that archaeological formation processes are: "the total sum of processes, natural and cultural, acting individually or in concert, that results in the archaeological record as it exists today". Archaeologists recognized the importance and necessity of systematically investigating the formation processes which can potentially cause distortion and hinder interpretive reliability (Clarke 1973; Schiffer 1976,1987,1996; Murphy 1997: 386-387).

In the same manner as sites on land, underwater sites and shipwrecks also undergo complex formation processes (Stewart 1999: 585). Maritime archaeologists, by observing and documenting the archaeological site - the surviving material and their associations - need to then identify and describe the WSFP and events which intervened, in order to understand a ship's original state and context (Dumas 1962; Throkmorton 1965; Muckelroy 1978: 157; Delgado 1997: 259; Harpster 2009: 75; Martin 2011: 8). The thorough study of WSFP is also vital in that it informs the strategy to be followed to protect and preserve an archaeological site, as well as the conservation and stabilization of elements that constitute the site (Oxley & Keith 2016: 2).

Frederic Dumas's 'Deep-water Archaeology' (1962), was the first attempt at comparing different wreck-site environments and discussing "post-depositional processes such as burial rates and biological activity, as well as depositional impact on amphoras and wood hulls" (Murphy 1997: 387); but it solely focused on observations of Mediterranean wreck formations (Muckelroy 1978: 160).

The first systematic study of WSFP, was conducted in the mid-1970s by Keith Muckelroy,

who examined a number of environmental variables (offshore fetch, winds, tides, water movement, depth, slope, topography, sediment composition) of twenty wreck sites around the British Isles, to determine how these affected the state of preservation of the archaeological remains (1978: 160-165).

Muckelroy's work and ideas were heavily influenced by contemporary research into site formation processes on terrestrial sites, and his time in Cambridge, under the tutelage of Grahame Clark and more notably David Clarke (Harpster 2009: 65-70; Martin 2011: 8). In his seminal book Maritime Archaeology (1978), Muckelroy sought to "create an interpretive framework to guide maritime archaeologists through their investigations of shipwrecks" (Harpster 2009: 75), by developing a model specific to the formation processes of shipwreck sites. He was the first to advocate a theory in Maritime Archaeology and propose a three-tier hierarchy: 1) the archaeology of shipwrecks; 2) the archaeology of ships; and 3) the archaeology of maritime cultures (Muckelroy 1975, 1978).

Regarding the archaeology of shipwrecks, the wreck site and its environment needs to be assessed, in order to comprehend the wrecking process (Delgado 1997: 259). Muckelroy created a model on the evolution of a shipwreck (Fig. 1), in which he identified: the process of wrecking; salvage operations; the disintegration of perishables; seabed movement; and the characteristics of excavation methodologies (1978: 158). Central to Muckelroy's model are two processes, operative on every site: that of extracting filters and scrambling devices, which an archaeologist needs to take into consideration to make an accurate analysis of artefacts found on the seabed and which can lead to insights regarding the ship itself (Muckelroy 1978: 165-182; Gould 1997; Stewart 1999; O'Shea 2002; Martin 2011).

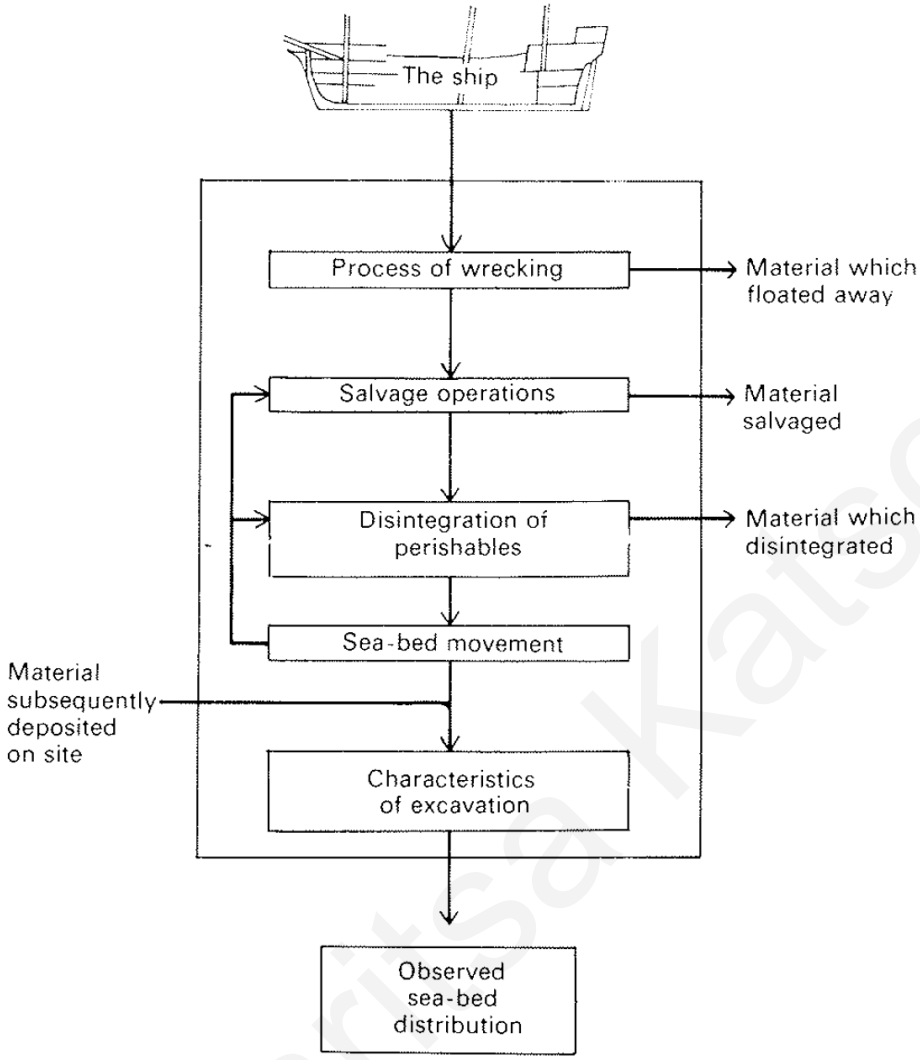

Figure 1: 'Flow Diagram representing the evolution of a shipwreck (Muckelroy 1976: 158, Fig. 5.1).

Extraction filters, describe the mechanisms that remove materials from their primary context or may even cause the loss of material; this can be due to the actual wrecking process, salvage operations throughout the shipwreck's lifetime and the disintegration of perishables caused by the marine environment.

Scrambling devices are the processes that in effect, re-arrange the vessel's elements, causing the alteration of the archaeological context. Such movements of the archaeological material can be due to the sinking event and the initial impact and by the continued disintegration of the ship's structure until it becomes a part of the seascape. Examples of such devices, affecting the site post-depositionaly, are the activities of marine creatures and the forces acting on the site, such as water movement (currents and wave action), which can cause sediment instability, disturbance or accumulation, as well as affect its stratigraphy. Muckelroy (1978: 181) highlights the importance of marine geomorphological and biological

study in the interpretation of a wreck-site, further to the thorough recording and understanding of a site and its stratigraphy, in order to decipher the processes that have shaped them in the passing of time.

When discussing the seabed distribution of wreck-sites, Muckelroy (1978: 182) divided shipwrecks into two types: continuous (sites with artefacts and ship remains relatively localised) and discontinuous (sites with their elements widely scattered). These types are effectively created by either the wrecking process and/or post depositional seabed movements and other site formation processes at work at each site.

Since Muckelroy's untimely death in 1980, his model on 'the evolution of a shipwreck' has been adjusted and enriched by scholars (Beltrame 1998: 143; Stewart 1999; Martin 2011), while others have used his work and ideas as a starting point, from which to address related topics (Ferrari 1995; MacLeod 1995; Gregory 1995, 1996; Ward et al. 1999; O'Shea 2002; Quinn 2006; Gibbs 2006), but no one has attempted a comprehensive study and analysis of WSFP (Martin 2011: 9).

2.2.1 Pre-deposition

As Martin describes: "no two wreck-site formations are the same, since the complex and interacting variables that constitute the environmental setting, the nature of the ship, and the circumstances of its loss will combine to create a set of attributes unique to each site" (2011: 2). In broad terms, shipwreck sites can be the result of either an unintentional catastrophic event (for example due to a collision or a vessel's structural fault) or deliberate abandonment (such as ship-burials and ship-graveyards).

The purpose of Gibbs' 2006 paper was to analyse in greater detail the cultural processes affecting catastrophic shipwreck sites, following John Leach's five major stages of a disaster: pre-impact, impact, recoil, rescue and post-trauma (Gibbs 2006: 4-8). Decisions and actions during the pre-impact phase have the potential of not only causing a shipwreck but also to affect the archaeological record. It is during this phase that the voyage and its planning begins; what type of vessel was used and how it was designed, constructed and perhaps modified, who the people on board were (the crew and passengers), what was the purpose of the trip, its destination, route and the time of sailing, what cargo and equipment was on board and how these were stowed. Another important moment of the pre-impact phase, is when danger approaches – and whether this is realized or not. If it is, how do people on board react and respond - do they change course or velocity, become more alert, ready equipment, secure

cargo, or take other steps to avoid it? If their actions at avoiding the imminent danger and disaster are unsuccessful, does the crew result in more radical measures? Do they attempt to lighten the vessel's load by jettisoning equipment or cargo, or if in great peril, do they abandon ship?

Thus moments prior to the disaster need to be investigated, "from either the historical record, the location of the wreck, or the nature and disposition of the archaeological deposits" (Gibbs 2006: 7).

2.2.2 Deposition

Once the vessel is in immediate danger, the sinking phase begins, which can be swift or go on for hours, depending on the nature of the catastrophic event. During this time, similar steps as those outlined in the pre-depositional phase can still be taken to avert disaster; but disaster studies have shown, that the majority of people act mechanically during this stage, with thinking and effective response severely impaired. The crew at this point would have to evaluate the situation and strategize to save human lives, save cargo and/or save the vessel (Gibbs 2006: 8-9). Whether such strategic steps were decided and followed, can again be inferred from the location of the ship and distribution of its contents in the archaeological record. For instance, are there human remains or were the people on board able to escape, taking with them their valuables and personal items? Is there evidence of an attempt at repairing the vessel, or of jettisoning items and ship's fittings?

As Stewart (1999: 568-569) points out, the archaeological record can also inform us of the wrecking process. If the ship sunk relatively intact, the deposit is fairly coherent in nature and buoyant items may be trapped, long enough to become waterlogged. Instead if the vessel disintegrated on the surface then many lighter objects may be lost and the deposit will be scattered (Muckelroy 1978: 166). Finally if the ship capsized, the objects that were on deck may be deposited in one location and the remainder of the ship and its contents in another.

2.2.3 Post-deposition

Cultural / Anthropogenic transforms

Once the disaster event has concluded, the post-deposition stage begins. During this period, survivors may find refuge or be rescued and leave behind some historical account of what came to pass. If the wreck-site is accessible, then there may be evidence of attempted salvage or looting either in antiquity or in more recent times (Stewart 1999: 574; McCarthy 2001: 93; Gibbs 2006: 10-11).

Underwater sites can also be disturbed or damaged by a number of other anthropogenic factors: a) the construction of new structures (piers, jetties, harbours, oil drilling platforms) and their maintenance (dredging of harbours), b) fishing activities and c) from later refuse disposal, which means material not belonging to the wreck, is deposited to it at a later stage (Stewart 1999: 576-578).

The term C-transforms, encompasses all the deliberate or accidental, anthropogenic formation processes (such as: use, discard, loss, reuse, salvage). They are responsible for the transformation and redistribution of material culture, after the initial period of use, when their context shifts from systemic to archaeological (Schiffer 1996). Such processes can transform a site, altering the stratigraphy and archaeological context and need to be investigated in depth, along with the natural formation processes, described next.

Natural / Environmental transforms

Natural formation processes, are all natural or environmental events (such as chemical, biological and physical agents) that affect the burial and preservation of the archaeological record (Schiffer 1996).

Once on the seabed, the ship's remains are subjected to an unstable, dynamic phase, in which they can be transformed by physical, chemical or biological formation processes, regulated by the actions of three main agents: the water, the substrate and living organisms. To assess the effect of the first agent, it is necessary to monitor variables such as temperature, light, salinity, pH, its concentration of oxygen and nutrients, as well as current intensity and direction. Substrates are divided into hard and soft and they need to be characterized according to their hardness, chemical composition, granulometry, content of organic material and level of potential oxidation-reduction (redox) reaction. Lastly, living organisms are the flora and fauna present at the site and which may affect it (Ward et al. 1999: 562-563; Bastida et al. 2010: 270).

The chemical composition and physical properties of the water can cause several reactions in artefacts, especially to metals (MacLeod 1995; Martin 2011: 3). Organic material is particularly susceptible to the effects of water penetration, variations in temperature and light, as well as the action of biological organisms.

It is obvious that the site's topography can also affect its stratigraphy, as it can cause different materials to move in different ways. For instance, gravity affects artefacts on slopes, with heavy equipment such as anchors most likely to remain close to their original deposition,

whereas pottery items can easily roll downwards to another location (Stewart 1999: 583-584; Ford et al. 2016: 23).

Seafloor conditions also play an important role in both the formation and preservation of a site. Shipwreck studies have demonstrated that materials are best preserved when they are quickly buried, as they are protected from wave and current action, as well as biological factors (Muckelroy 1978: 53, Ford et al. 2016: 19). The state of preservation is also better when the environmental conditions are more stable (Schiffer 1996).

Tides, surges, currents and wave action can cause lighter materials to relocate (either within the wreck or away from it), damage the ship's structure and disperse its contents (Martin 2011: 2-3). Stewart (1999: 582) notes that it is difficult to form a clear picture of the currents and tides that affected the newly deposited wreck – as these change significantly over time.

"Fundamental processes driving site formation are therefore dependent upon the complex erosion (net sediment loss) and accretion (net sediment deposition) history of wreck sites", which can threaten the stability of shipwreck sites and accelerate physical degradation (Quinn 2006: 1420-1421). Shipwrecks form obstacles on the seafloor, altering the flow velocity and turbulent intensity of the prevailing hydrodynamic regime/s (currents, waves or combined waves and currents), often resulting in scour signatures and deposition patterns on the seabed. Scour pits may be dug near the wreck as the water speeds up around it and/or sediment may mound up around the wreck. These marks need to be systematically investigated and recorded, during the study and excavation of a site, in order to more accurately understand possible artefact displacements and other changes to said site (Quinn 2006: 1429-1431).

Submerged and shipwreck sites, apart from being obstacles on the seafloor, also become artificial reefs, attracting a variety of flora and fauna, which can in turn cause changes to the site, in a process called bioturbation. For instance, marine borers, such as teredo worms found in warm seas, are known for their detrimental effect to wooden shipwrecks. Animals that burrow, fish and octopuses can cause sediment disturbance and the displacement of artefacts. Marine plants, such as sea grass can also move artefacts with their roots (Easton 1997; Stewart 1999: 578-581; Leino et al. 2011). Muckelroy (1978: 181) proposed that information on the overall environmental circumstances of a wreck-site can be gleamed by studying the life cycles of certain fouling organisms, known to exist and thrive in very specific conditions.

2.3 3D recording and mapping

Archaeology is the academic discipline concerned with understanding, reconstructing and explaining the human past, through the identification, recording, study and interpretation of the surviving physical evidence (Bowens 2009: 2). Archaeologists retrieve and document the collection of evidence present at a site, through the systematic processes of archaeological excavation and recording. This procedure is often referred to as a process of controlled destruction, as it inevitably leads to the destruction and loss of context, but it also provides a singular opportunity to precisely record a site and all that it contains. Once this process is completed and the evidence analysed, archaeologists are able to offer interpretations regarding the past human activities occurring at a site and how these change over time (Harris 1989; Barker 1993; Bowens 2009: 3).

Consequently, diligent recording of each stratigraphic unit or context and its relation to those around it (stratigraphic relationship), is essential to correctly understand the order in which these contexts were created over the course of time (stratigraphic sequence) and to interpret a site properly (Bowens 2009: 58-60). Keeping objective, meticulous and accurate records of all the surviving evidence on an archaeological site, no matter how unexciting or insignificant they may first appear, ensures and enables archaeologists to extract all information and meaning that may be gleaned from its study (Bowens 2009: 23, 55). In this manner, the information and data are preserved and accessible not only for the present, but also for future generations, permitting the 'reconstruction' of the site from the archive, the assessment and replication of its interpretation, the comparison with related evidence and lastly the answering of future questions that may arise (Bowens 2009: 53; Holtorf 2014: 6128).

As the underwater environment imposes significant constraints (lighting conditions, visibility, depth, current, temperature) and demands economy of bottom time, the discipline was driven to search for a fast and accurate technique of mapping finds and features (Bass 1966: 118; Green et al. 1971; Muckelroy 1978: 33; Bass and van Doorninck 1982: 19–28). Photogrammetry is a digital documentation technique that has become widely used in a number of fields, including archaeology, both on land and underwater (Ballard et al. 2001; Green et al. 2002; Green and Gainsford 2003; Sedlazeck et al. 2010; Verhoeven 2011; Olson et al. 2013). The value and potential of this method was recognized in underwater archaeology from as early as the 1960s, when George Bass experimented with

photogrammetry on the recording of the Byzantine shipwreck Yassi Ada (Bass & van Doorninck 1982).

"Photogrammetry is the art, science and technology of obtaining reliable information about physical objects and the environment through the process of recording, measuring, and interpreting photographic images and patterns of electromagnetic radiant energy and other phenomena" (McGlone et al. 2004: 2). An important tool in geoscience, initially developed to provide topographic information for producing maps (Konecny 2014: 9), photogrammetry is a remote technique that uses photographic images taken according to specific parameters to reconstruct physical objects or scenes which can be fully scaled and positioned through a geo-referencing process, finally allowing to extract useful measurements.

Recent advances in technology, such as the automation of many post-processing steps through modern algorithms and improved computer power, have also contributed in establishing this technique as an easy and effective method of digitally recording cultural heritage (Drap et al. 2013: 382; De Reu et al. 2013). The diversity of its potential deliverables (three-dimensional models, orthophotos) affordability, simplicity of implementation and speed of acquisition, has resulted in photogrammetry becoming more popular and being used for both large-scale sites as well as small surveys conducted underwater (Skarlatos et al. 2012; Demesticha et al. 2014; McCarthy & Benjamin 2014; Fulton et al. 2016: 19).

Site recording in three dimensions through the use of photogrammetry, has undisputedly revolutionized underwater archaeological research, documentation and interpretation, as it minimizes the underwater recording time and maximizes the quality and accuracy of the acquired data, producing better results than manual recording methods. Furthermore, this process produces extremely detailed, measurable and versatile digital datasets, which can be migrated and converted, organized and processed in various ways to facilitate the detailed study and accurate reconstruction of shipwreck sites: firstly to analyse the spatial arrangement of a shipwreck's artefact assemblage, secondly to detect the temporal relationship of different units of stratification, and thirdly to investigate and reconstruct the different phases of the site formation processes (Demesticha et al. 2014: 137). Compared to traditional two-dimensional (2D) recording and representation techniques, digital three-dimensional (3D) recording methods allow the reconstruction and representation of sites in their full three-dimensional context. Such methods generate sets of data, which can be further exploited, expanding the potential for new analytical opportunities (see below).

The term Digital Archeology (DA), as discussed in contemporary literature, encompasses a series of digital techniques as well as information and communication technologies applied in the various stages of the archaeological work. DA is also concerned with the debate focusing on the integration of these technologies in a comprehensive manner, creating a bridge between theory, methodology and archaeological practice. As noted by Daly and Evans (2006: 7): "Digital archaeology should exist to assist us in the performance of archaeology as a whole. It should not be a secret knowledge, nor a distinct school of thought, but rather simply seen as archaeology done well, using all of the tools available to aid in better recovering, understanding and presenting the past. In the end, there is no such thing as digital archaeology. What exists, or at least what should exist, are intelligent and practical ways of applying the use of computers to archaeology that better enable us to pursue both our theoretical questions and our methodological applications".

It is in the stages of data collection, documentation, analysis, visualization and sharing, that digital technologies have most directly influenced archaeological work (Hill 1994). Access to 3D recording equipment and techniques, geographic information systems (GIS) and 3D modelling software have altered conventional workflows, enabling massive data collection in a more efficient and integrated way. Digital technologies offer powerful tools for the representation and modelling of the observed world, while enabling the integration of diverse data in virtual narratives of great flexibility, manipulated and transmitted with incredible speed and to a wider audience (Zubrow 2006: 21-23).

The potential of 3D models, resides in the ability to allow viewers to progress from what is observable, (archaeological data and theory), to concepts of what is unobservable, the past (Lock 2003: 13). To this end, as Ware explains (2004: 3-4), the visualization of data can encourage understanding in a number of ways:

1. Visualization provides the ability to comprehend large amounts of data.
2. Visualization facilitates the perception of initially unanticipated patterns or properties.
3. Visualization frequently highlights problems with the data itself or regarding the way in which it was collected.
4. Visualization enables understanding and analysis of both large-scale and small-scale features of data simultaneously.
5. Visualization promotes the formulation of hypotheses.

Even though 3D recording, visualisation, representation and reconstruction of archaeological sites, monuments and artefacts is becoming more widely implemented in archaeology, they have been largely used for documentation and presentation purposes (Tsiafki & Michailidou 2015: 37-38). 3D digital models are a versatile format for disseminating raw data or interpretations and can encourage collaboration, peer review, as well as public engagement. Forms of dissemination based on 3D digital models include museum exhibits, the creation of animation videos, as well as the design of virtual and augmented reality environments. Naturally, Maritime Archaeology has also utilized such tools for the aforementioned objectives (e.g. de Juan Fuertes et al. 2012; Rodriguez Iborra 2012; Secci et al. 2019; Martin & McCarthy 2019; Jézégou et al. 2020) however 3D modelling and visualization has seen increased use as a tool for research and analysis, outlined below.

2.3.1 3D documentation and analysis of artefacts and hull timbers

The method of documenting intact or fragmentary hull timbers has progressed quickly from 2D records into 3D models, as such artefacts are irregular and complex in shape, thus difficult to represent faithfully in 2D (Rose 2014: 104-105). Even though 2D drawings can be used to generate 3D models of timbers using computer aided design (CAD) software, the benefits of a full 3D recording have been demonstrated in projects such as the Newport Medieval Ship (Jones 2009) and the Skuldelev vessels (Ravn et al. 2011). Apart from hull timbers, artefacts found underwater and on land have also been recorded in 3D, as such an approach enables different types of meaningful analysis to be conducted; examples include artefacts such as naval rams (Adams et al. 2013; Polakowski 2016; Murray 2020), column drums (Carlson & Aylward 2010), marble blocks (Parizzi & Beltrame 2020) and amphorae (Radic Rossi 2005; Knapp & Demesticha 2016: Appendix; Hein & Kilikoglou 2020).

3D ship reconstruction

One of the objectives of investigating shipwrecks is the reconstruction of the forms, construction techniques and shipbuilding traditions of the studied vessels. Computer graphics programs are used to extract basic longitudinal and transverse curves from the wooden remains found at a site, from which complex geometries are extrapolated in order to reconstruct the shape of the hull of a vessel. Digital 3D technologies also allow the testing of such reconstructions through hydrodynamic, hydrostatic and seakeeping analysis of the resulting hypothetical reconstructions; they can additionally be used to explore hypotheses relating to the construction and use of vessels, as in the cases of: the Uluburun (Lin 2003), Nossa Senhora dos Mártires (Wells 2008), Kizilburun (Littlefield 2012), Drogheda Boat

(Tanner 2013), Newport (Jones et al. 2013), Vasa (Rose 2014), Egadi 10 (Polakowski 2016), Dramont E (Poveda 2017), Napoli A (Boetto & Poveda 2018), Capo Sagro 2 (Cibecchini et al. 2018), Punta Scifo D, Marzamemi 1, Isolla delle Correnti, Capo Granitola, Capo Taormina, Punta del Francese and Porto Cervo (Parizzi & Beltrame 2020). Furthermore, as most reconstructions are conjectural, digital methods provide greater flexibility in that they allow researchers to reiterate the hypothetical models as new data become available. 3D modelling has also been used to model and examine vessels based on information derived from shipbuilding documents and treatises (Hazlett 2003; Cook 2011; Higgins 2012).

3D site plans

Computer visualization has also been applied in the creation of shipwreck site plans, providing far more detailed information than a conventional archaeological plan. As Demesticha (2014: 138) explains: "Unlike terrestrial sites, where 3D plans are often considered a promotional tool for public archaeology, in cases of densely placed artifacts, like the cargo of a ship, 3D mapping is the only method available for faithfully documenting the spatial arrangement".

Undoubtedly, 3D site plans are also used for the mapping of surveyed sites (e.g. Diamanti & Vlachaki 2015; Royal 2018). However, as the Mazotos Project (an ongoing excavation) is the case study used for this thesis, the pertinent question is to examine different approaches for representing excavated shipwreck sites digitally and how these have been used in their study and analysis.

The first approach concerns the creation of 3D site models using 3D CAD software. The 3D site plans for three shipwrecks, the Tektaş Burnu (Fig. 2), the Kızılburun (Fig. 3) and the Cape Stoba (Fig. 4), were produced through such an approach, by geo-referencing theoretical/generic models of artefacts using the 3D co-ordinates taken from the photogrammetric survey (Green et al. 2002; Catsambis 2006; Beltrame & Costa 2018).

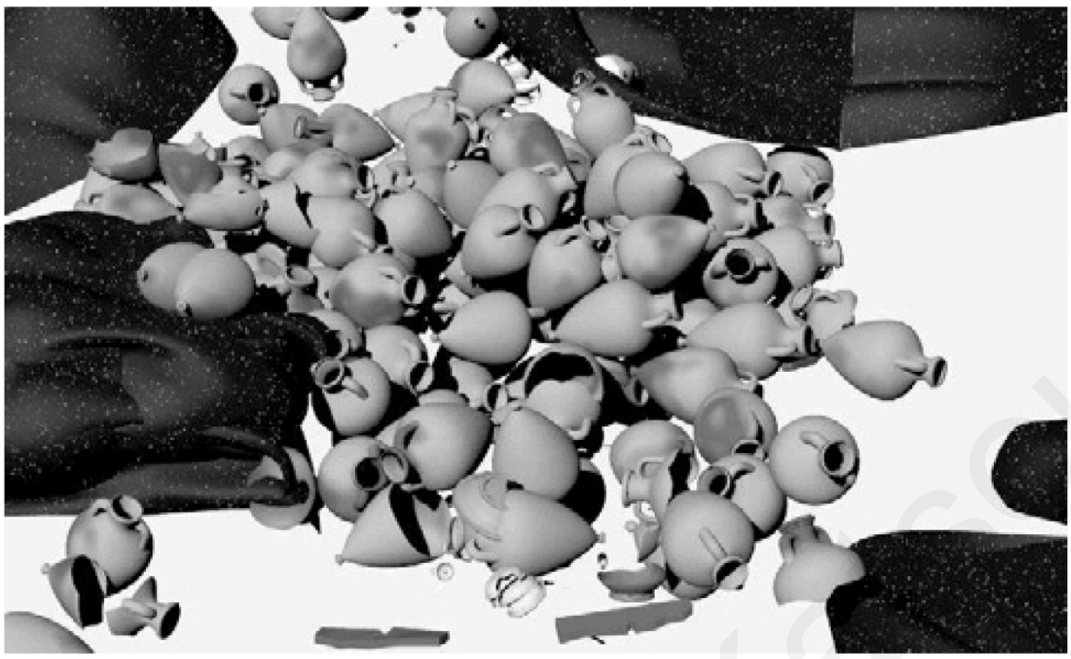

Figure 2: The Tektaş Burnu 3D site plan (Green at al. 2002: 287, Fig. 9).

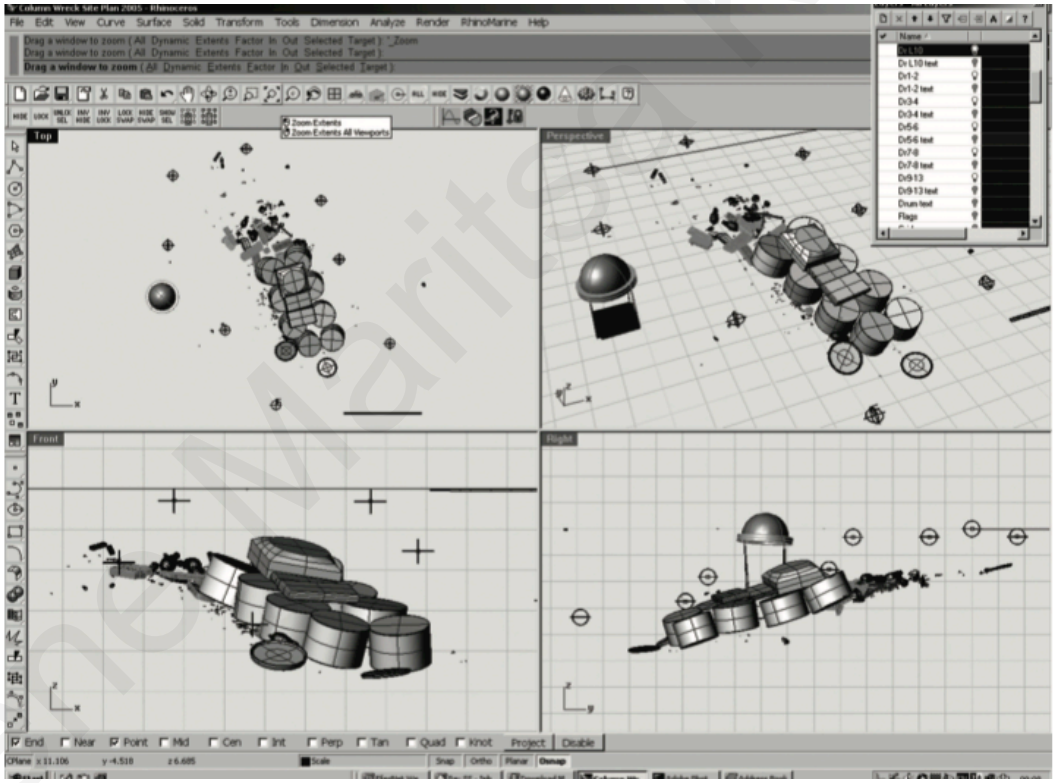

Figure 3: The Kizilburun 3D site plan (Catsambis 2006: 613, Fig. 2)

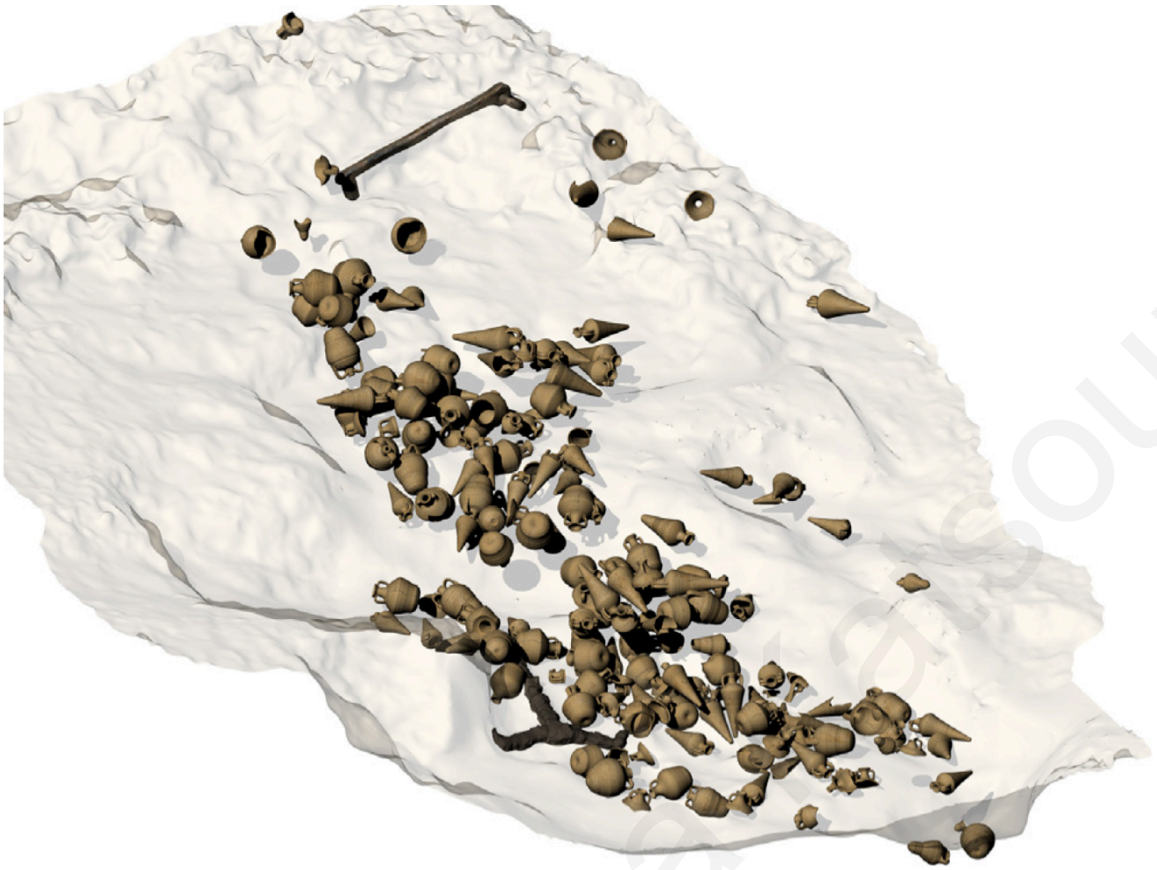

Figure 4: The Cape Stoba 3D site plan (Beltrame & Costa 2018: 87, Fig. 9).

These three 3D site plan examples include the larger artefacts from each site, whereas smaller finds, for instance pottery sherds are seemingly absent. At the Cape Stoba site, Krajl et al. (2016: 53) specifically mention that glassware was found mixed among the amphorae, but could not be recorded precisely during excavation and hence was not included in the 3D site plan. The ballast, lying between and over the amphorae, was not plotted either.

The 3D site plan for the Modi shipwreck is currently being created inside a game engine, utilising the photogrammetric documentation data and 3D modelling techniques. As Vlachaki et al. (2020) describe, this interactive 3D environment (Fig. 5) contains the geo-referenced photogrammetric or theoretical/generic models of intact and fragmentary artefacts. What differentiates this approach from the previous one is that the 3D site plan is linked to the project's database and that each artefact model is accompanied by relevant information.

Figure 5: a) Navigation in the 3D site model of the Modi wreck, b) an example of a 2D view of the excavation trench, generated by the user and c) pop-up window relating brief information regarding a selected artefact (Vlachaki et al. 2020: 9-10, Figs. 7, 9, 10).

The third approach concerns a set of tools (ARPENTEUR) developed from 1998 onward. At different points in its development, ARPENTEUR has been utilised to produce the 3D site plan of three shipwreck sites: the Grand Ribaud F (Fig. 6), the Xlendi (Fig. 7) and the Cala Rossa (Drap et al. 2003; Seinturier et al. 2004; Gambin et al. 2018).

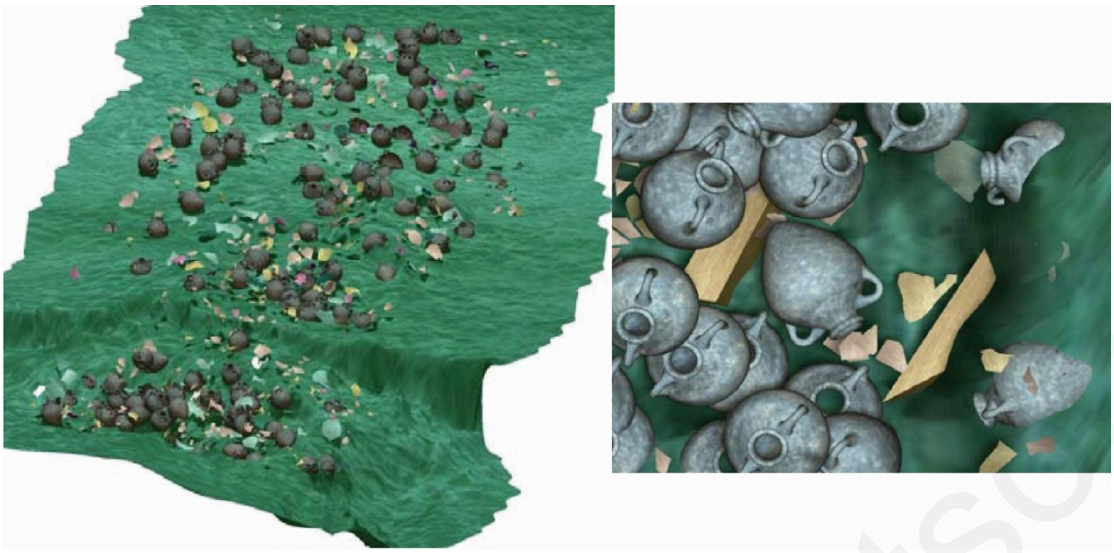

Figure 6: An overview and a close up image of 3D site plan of the Grand Ribaud F, created using ARPENTEUR (Drap et al. 2003: 185, Figs. 11, 12).

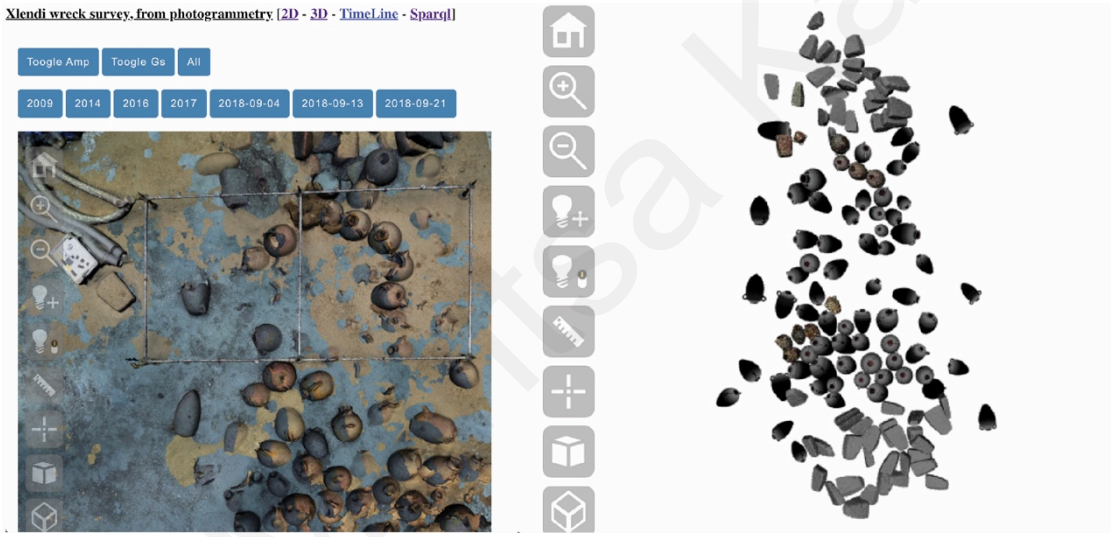

Figure 7: The Xlendi 3D site plan and datasets are also available online, where the visitor can view a timeline of the excavation's progress (Screen captures from the website http://www.lsis.org/groplan/hop/xlendiTimeLine/xlendi.html).

Encompassing a database management system, a 3D measuring tool and a 3D visualization system, ARPENTEUR, enabled archaeologists to study a site, without requiring photogrammetric knowledge or expertise, themselves. An information system was thus created for each site, based on two ontologies: "one dedicated to photogrammetric measurement and the geo-localisation of the measured items, whereas the other is dedicated to the measured items, principally the archaeological artefacts, describing their dimensional properties, ratios between main dimensions, and default values" (Drap et al. 2015: 30374). In simple terms, the approach is as follows (see Drap et al. 2003; Drap 2012; Drap et al. 2015; Ellefi et al. 2018):

- The creation of a 3D model for each amphora type present at a site (theoretical model).
- 2D artefacts are detected in the full orthophoto or photos of the site, either manually or using the Pasquet et al. (2017) deep learning method, which is based on pixel prediction to detect cultural heritage resources in a larger image.
- The 'spatial profile' (derived from the photogrammetric data) of the detected object provides the information that will be used to compute the position, orientation and dimensions of the 3D object that will be generated.
- Information from the photogrammetric data is also used to create the typological profile of said object (according to a set of morphological attributes), which will then propose an ontology for modelling it.
- The artefact is then modelled based on the theoretical model, dimensioned by the photogrammetric measurements.

Thus, a 3D representation (3D site model) of the site and its contents is generated, from which measurements and spatial queries can be made. The application also allows the user to add archaeological comments and observations, through its interface.

Another unique aspect of the ARPENTEUR software is its capability to model and plot pottery fragments. In brief, a fragment's shape is firstly delineated by a set of digital points, which are then used to gather photogrammetric information and measurements for it. The system creates a new 'item' in the database (for this fragment) and through the interface, the user can input information and characteristics to define it, such as: fragment type (belly, bottom, neck) and its related amphora typology. From all this data, the fragment's contour is "fitted' in the theoretical amphora model and part of the latter (matching the fragment's contour) is extracted. Thus the 3D representation of said fragment is achieved (Fig. 8), which is subsequently 3D plotted in its documented position within the site (Seinturier et al. 2004; Drap 2012).

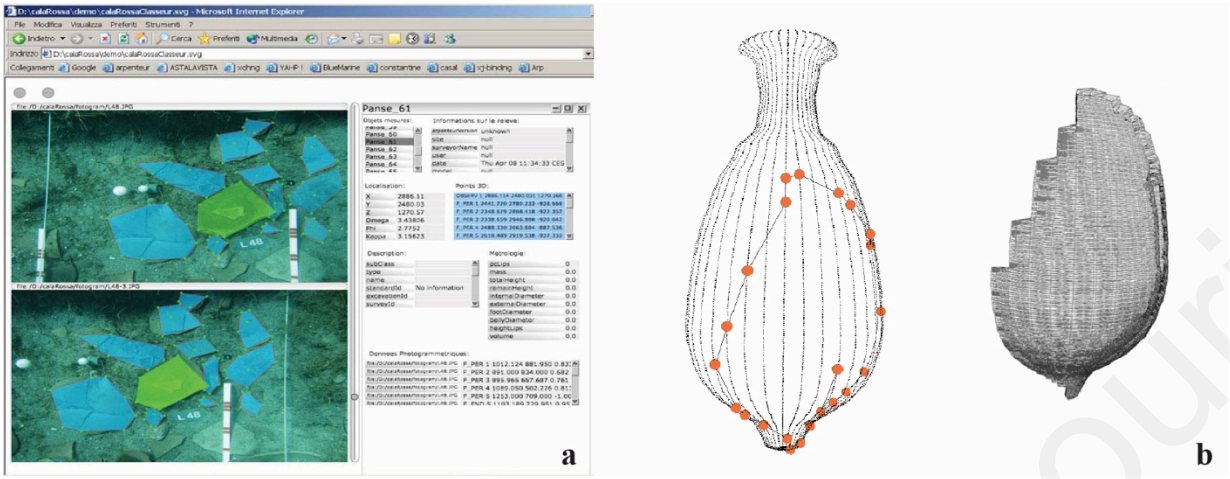

Figure 8: Fragment reconstruction process in ARPENTEUR: a) a fragment's shape is delineated by a set of digital points, whereas information and characteristics to define it are manually added using the system's interface; b) the fragment's contour is "fitted' in the theoretical amphora model and part of the latter (matching the fragment's contour) is extracted (Seinturier et al. 2004: 5, Fig. 3; Drap 2012: 127, Fig. 13).

Apart from 3D site plans, another approach is visualizing and analyzing data from shipwreck sites using Geographical Information Systems (GIS); for instance, the study of the Stella 1 (Bartoli et al. 2012), Gnalić (Casaban et al. 2013; Yamafune et al. 2016) and Mercure (Beltrame & Manfio 2014) shipwrecks is conducted using GIS site plans. In such cases, artefacts are represented using 2D tracings, which are linked to their associated information.

The digital reconstruction of the Stella 1 shipwreck using GIS (Fig. 9) irrefutably enables the visualization of the archaeological site within its wider geographical context, for instance, the exact location of the wreck compared to the remains of the Roman bridge along the Via Annia (Bartoli et al. 2012). It is also evident however, that the 2D documentation and representation of the remains of this small Roman barge, was not sufficient for scholars to understand its hull and construction. To achieve these objectives, two models were created: a physical one in wood at a 1/10 scale and a virtual one (3D) at full size, which will be used further to create "a series of hypothetical reconstructions for several lengths and cargo configurations in order to assess the more plausible ranges of sizes of the original Stella 1 barge" (Castro & Capulli 2016).

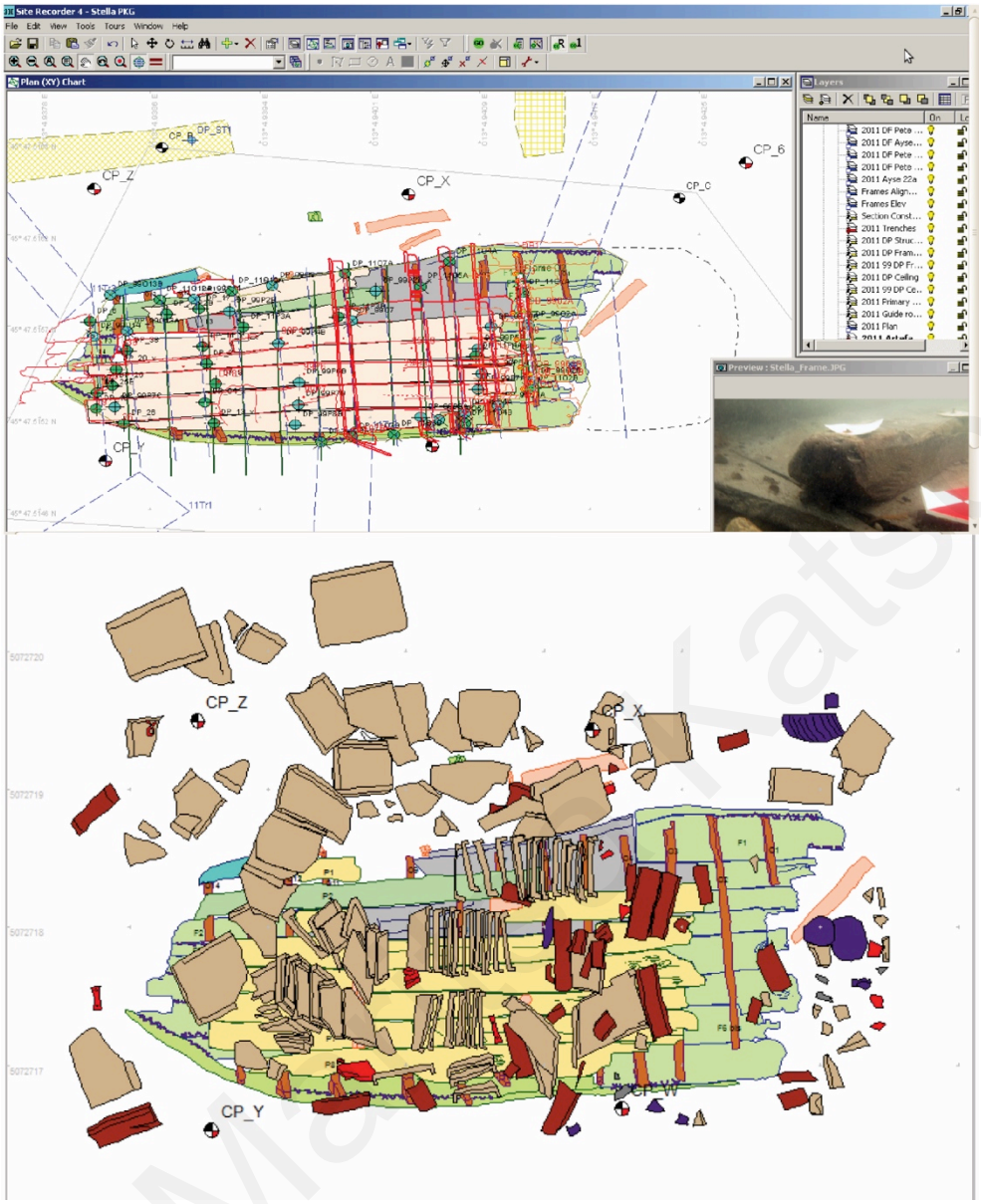

Figure 9: The Stella 1 site plan, created in Site Recorder 4: a) the plotted hull remains of the shipwreck viewed alongside photographs and other information. b) The tiles that were lifted in 1998 and 1999 have also been plotted (Bartoli et al. 2012: 3, 8, Figs. 1, 5).

Further to the GIS site plan (Fig. 10), the study of the Gnalić shipwreck also employs a VR application (Fig. 11) and 3D modelling as tools with which to examine the photogrammetric 3D models of timbers and study the ship remains (Yamafune et al. 2016; Radić Rossi et al. 2019: 61). What is thus inferred is that so far the reconstructions have focused on the hull remains and related artefacts, with the intent of: a) developing a plausible model of the hull shape and b) the ship's structure and construction sequence. It remains unclear however, whether the smaller artefacts from this site (for example, the glass window-panes, glass vessels, beads and mirrors, etc.) have been incorporated either inside the VR application or plotted in the GIS of the site (Yamafune et al. 2016).

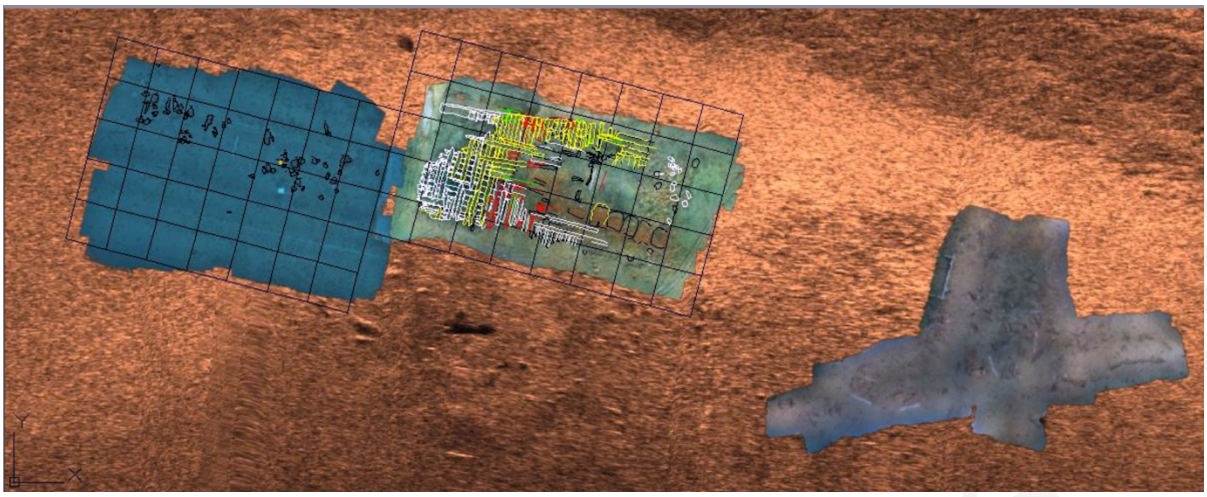

Figure 10: The GIS site plan of the Gnalić Project (Casaban et al. 2013).

Figure 11: Examining recorded timbers, inside the VR Gnalić application (Radić Rossi et al. 2019: 63, Fig. 4.17).

In the case of the Mercure shipwreck, small finds (such as osteological remains and personal objects, etc.) mostly found in Area A of the site, were also included in the GIS site plan (Fig. 12). Beltrame and Manfio (2014: 118-126) explain that as such micro-scale evidence could not be documented using photogrammetry, they were mapped according to their recorded 'topological relationships' (i.e. the relation of an artefact's find spot in comparison to another, using such terms as: "close to", "below" or "above" another artefact). In order to record the discovered depth of small finds, the archaeological deposit was divided into arbitrary strata – with each layer being approximately 15cm. For the purpose of performing statistical analysis

and queries relating to the distribution of such micro-scale evidence, each small find was also plotted as an individual point inside the GIS site plan, and Area A was divided into a grid. This enabled the 2D visualization of the total number of small finds in each grid cell of Area A (Fig. 13).

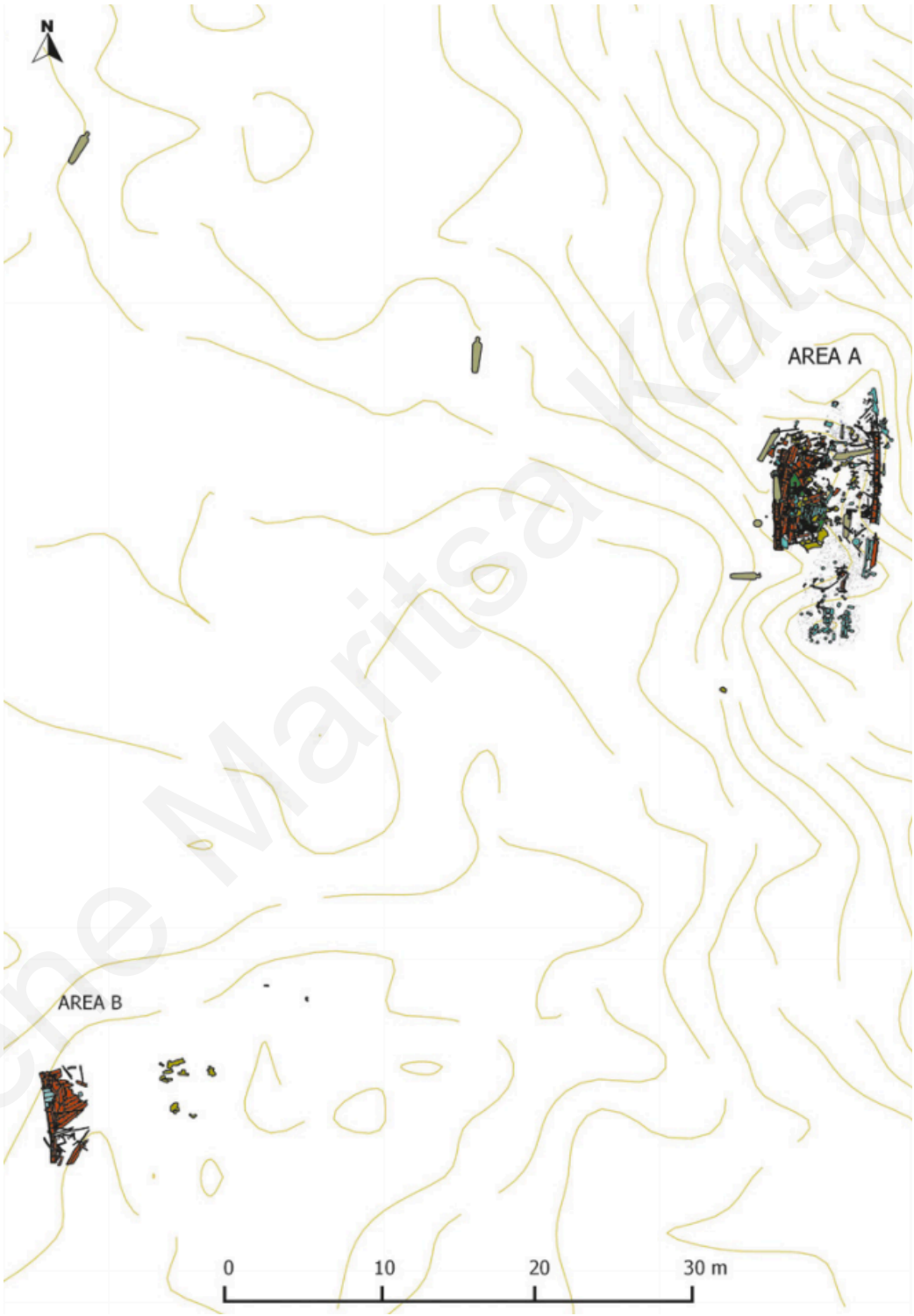

Figure 12: The Mercure GIS site plan: Areas A and B correspond respectively to the bow and stern (Beltrame & Manfio 2014: 114, Fig. 1).

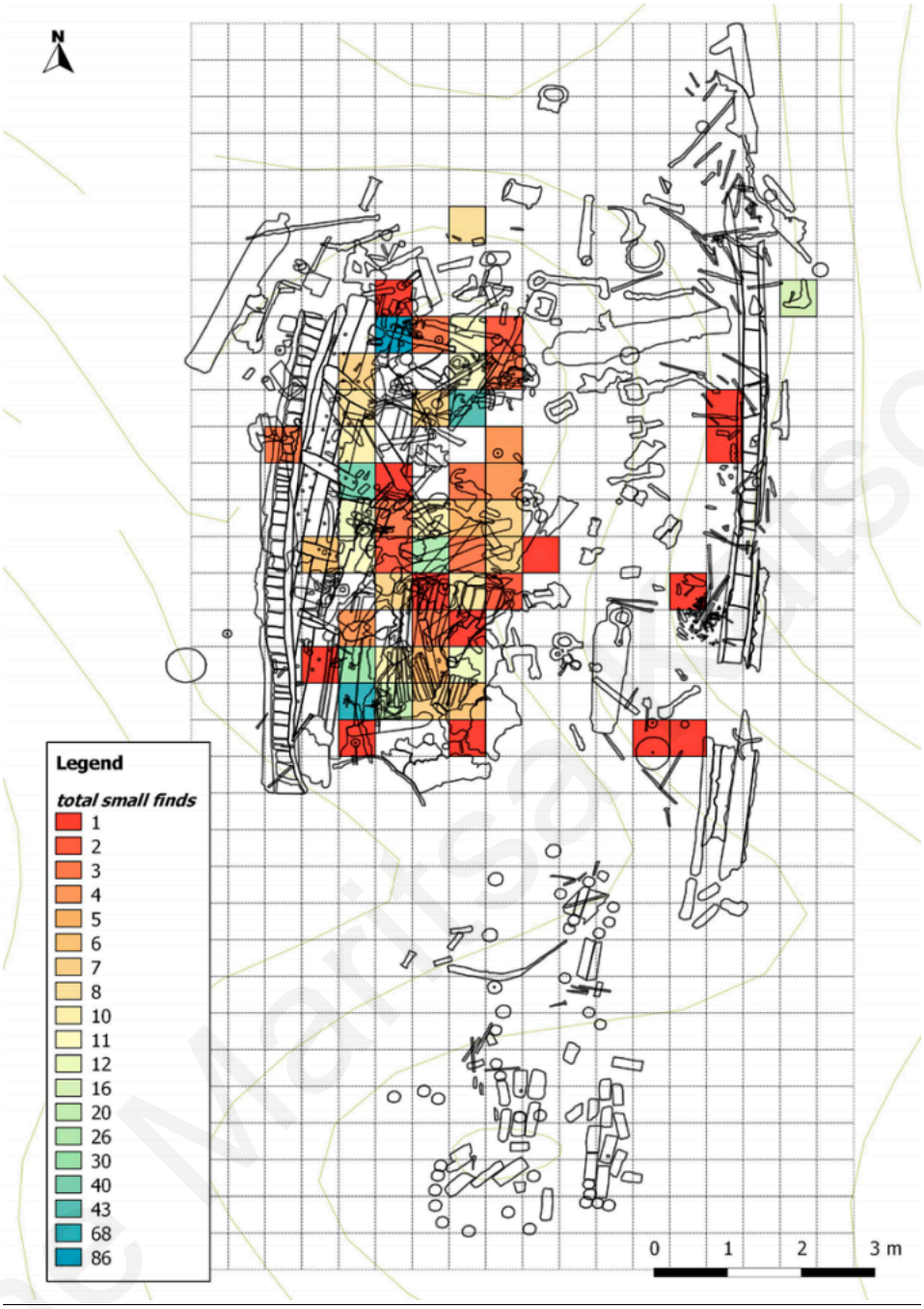

Figure 13: Map of Area A from the Mercure GIS site plan noting the topographical distribution of the small finds: each cell contains a specific number of small finds (Beltrame & Manfio 2014: 124, Fig. 6).

The overview presented in this section, aimed at elaborating on the role and demonstrating the value of 3D recording and modelling techniques as research tools in the field of Maritime Archaeology. Digital models have been used to: visualize and digitally reconstruct entire sites, investigate individual artefacts, calculate their volume as well as that of entire cargoes, reconstruct the original stowage arrangements, reconstruct the actual ships, test their

hydrodynamic, hydrostatic and seakeeping properties and understand their construction methods and traditions. What is also confirmed is that many research teams are utilizing digital photogrammetry, because of its accurate and detailed results, low cost and simplicity of use.

The majority of the discussed 3D site plans, come from ongoing shipwreck excavations, thus only partially investigated and published. The researchers stress that 3D site representations are important for visualizing a site that is being lost through excavation, monitoring the site and the progress of its excavation whilst also assisting in the study and analysis of a site.

At the same time, micro-scale evidence (for instance: ballast, glass or pottery fragments etc.) seem to be mostly missing from the 3D plotting process and subsequent analysis, with most of the site plan examples focusing on the larger artefacts found at each site. What can be surmised is that the potential information that may be derived from the 3D spatial analysis of such evidence, has yet to be fully explored.

In conclusion, many opportunities still remain to better utilize and take full advantage of digital modelling to study a site. This can only happen through experimentation, by exploring the possibilities that 3D models have to offer, as an integral part of the analytical and interpretative process. As researchers become more familiar with the possibilities of these digital techniques and software, 3D visualizations from ‘graphic reproductions’, can become analytical tools with which to formulate and investigate hypotheses and observe otherwise ‘invisible’ phenomena (Piccoli 2018: 67, 84-87).

3. Case study: Mazotos Shipwreck

3.1 The Mazotos Shipwreck

In 2006, a shipwreck was found by divers at a depth of 44 meters off the coast of Mazotos, in the Larnaca district of Cyprus (Fig. 14a). The main visible feature of the site is a 17 x 7 m concentration of amphorae on a sandy, almost flat seabed (Fig. 14b). The oblong mound, almost in the form of a ship, has a north-south orientation and consisted of 500-800 Chian amphorae partly or totally visible, dating to the middle of the 4th century BC (Demesticha 2009; Demesticha et al. 2014).

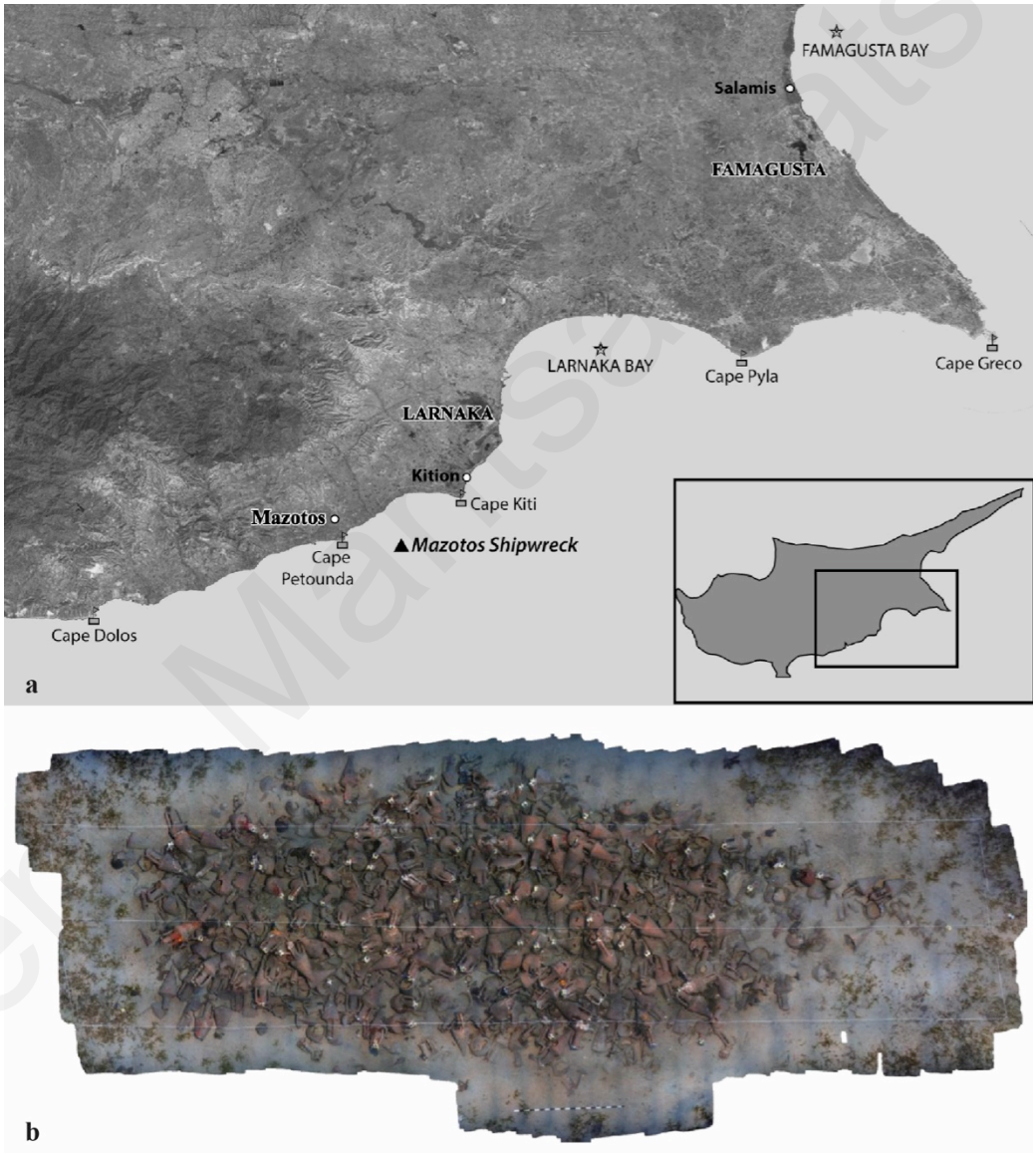

Figure 14: a) Map of Cyprus showing the location of the Mazotos shipwreck (Demesticha 2021: 44, Fig. 1); b) Orthophoto of the 2007 pre-disturbance survey at the Mazotos shipwreck site (Secci et al. 2021: 3, Fig. 1).

The Mazotos shipwreck is the first shipwreck of the 4th century BC located in the South East Mediterranean carrying Chian amphorae, at a depth where divers can work. Its research can shed light on issues concerning shipbuilding and seafaring in antiquity, sea routes and trade relations between the Aegean and the eastern Mediterranean during the late Classical period (Demesticha 2019; Demesticha 2009).

Judging from the upright position of the half-buried amphorae, the cargo of the ship had not been dispersed on the sea floor. Thus it is assumed that the ship landed upright at the time of the wreck, tilted slightly to its starboard side and was gradually half-buried in sand (Demesticha et al. 2014: 139). The high level of the site's preservation classifies it among the rare cases of shipwrecks in the Mediterranean where the internal stratigraphy and the various phases of the site's formation processes can be studied in detail (Demesticha 2009: 2; Demesticha 2017: 293-94).

Its archaeological importance, as well as the immediate need for its protection, triggered the Mazotos Research Project, the first Cypriot underwater archaeological project. The project was conducted by the Archaeological Research Unit (ARU) of the University of Cyprus, firstly under the direction of Dr. Stella Demesticha and Dr. Demetrios Michaelides and subsequently solely directed by Dr. Demesticha, in collaboration with the Department of Antiquities of Cyprus (Demesticha 2009; Demesticha 2010; Demesticha et al. 2014). The desalination, conservation and restoration of all recovered artefacts is conducted at the special laboratory for underwater finds of the Department of Antiquities, based in Larnaca and under the direction of Dr. Eleni Loizides (Demesticha 2011; Loizides 2011: 16-17).

It is important to note at this point, the multidisciplinary nature of the Mazotos project. The photogrammetric mapping of the site in its entirety, as well as the daily documentation of its excavation progress, has been undertaken by Dr. Dimitrios Skarlatos of the Department of Civil Engineering and Geomatics at the Cyprus University of Technology (Demesticha 2011; Demesticha et al. 2014). Since 2011, Enalia Physis, a Cypriot NGO, has been documenting and studying the flora and fauna evident at the Mazotos site, as the shipwreck has acted as an artificial reef on the seabed.

Twelve field seasons have taken place at the site since 2007. Four of them (2007, 2008, 2009 and 2013) were surface surveys, conducted for the purpose of preliminarily mapping the site and the surface finds (Demesticha 2009: 1-2). Excavation was conducted on the site during the remaining eight field seasons (2008, 2010, 2011, 2012, 2015, 2016, 2018 and 2019)

during which the shipwreck was precisely documented using advanced methods and the lifted finds being carefully conserved (Demesticha 2017: 284).

The vast majority of the cargo amphorae of the Mazotos ship belonged to a well-known wine transport container of the 4th century BC, from the Aegean island of Chios, a Greek city-state with eminent sea power. The homogeneity of the Mazotos cargo containers implies that this was a large shipment of the same product — most probably wine — that was loaded at the island of Chios. Some non-Chian containers however were also found in the ship's hold, such as Solokha I or Mushroom-Rim amphorae, Northern Aegean amphorae, Coan amphorae and possibly Lycian amphorae. At least 55 jugs have been excavated among the amphorae found in the aft part of the hold. They have a squat body and a similar fabric to that of the Chian amphorae. These were most probably used for serving wine, the main cargo of the ship (Demesticha 2009: 4-8; Demesticha 2017: 288-91; Demesticha 2021: 41-44).

3.2 The bow area of the ship

The excavation at the southern end of the site has been successfully completed and has exposed the bow area of the ship in its entirety. The fact that a full account of the bow area has been attained, provides the principal reason of the present study's focus and why it was selected to investigate and map some of the smaller artefacts it contained.

The majority of amphorae excavated at the bow area are Chian, but two possibly Lycian, two Solokha I or Mushroom-Rim and one Coan amphorae were also part of this cargo block. Apart from the cargo amphorae, a stone weight, the remains of three anchors, as well as part of the keel and hull of the ship were also found in this area (Demesticha 2021: 41-44). What follows is an overview of the analysis regarding the site formation processes at the bow of the ship, as published by Demesticha (2021) thus far.

In terms of the ancient ship, the cargo amphorae at the bow were loaded in the compartment under its foredeck and are believed to have been stacked in two layers. The impact of the ship reaching the seabed, along with the collapse of the foredeck, resulted in the amphorae stacked in the bow to fall on their sides and to shift slightly from their original positions.

The starboard tilting of the ship and the consequent westward cargo movement, effectively served to better preserve the starboard side of the hull. Furthermore, as the ship tilted to its starboard side and with the collapse of the foredeck, the three anchors fell on the seabed: the

first of the two larger anchors fell on the port side whilst the second on the starboard side of the bow (Fig. 15).

Figure 15: Top view of the excavated part of the bow. The lead cores of the small anchor (M0006-M0003) can be distinguished under the wire-frame models on the right, and the preserved part of the keel under the models on the left. M0308 and M0309 are parts of the starboard bower's stock; M0010 and M0012 are its arm-tips. M0004 and M0057 belong to the port bower (Demesticha 2021: 46, Fig. 9).

Contrary to the remaining western side of the assemblage, the collapsed amphorae at the bow did not spill farther off the concentration – this was most likely prevented by the two larger anchors serving as barriers. As Demesticha writes (2021: 45-47), "the positions of the amphorae support this hypothetical scenario:

1. There is a line of amphorae at the starboard (western) side that has fallen eastwards (rim

to the east and toe to the west), instead of westwards (rim to the west and toe to the east); these must have been stored against the starboard side of the bow, inside of where the anchor was attached. When this part collapsed, it seems to have pushed them eastwards against the rest of the amphorae: these had fallen westwards when the ship tilted.

2. The port side of the cargo shifted into the starboard side and this must have caused some of the breakages found *in situ*. Most of the upper-tier amphorae were found at the port side.

3. In the fore end of the concentration, some amphorae were found broken and turned upside down: perhaps they were bounced from their original positions when the ship reached the seabed and broke open".

The remains of the starboard anchor include two heavily conglomerated, iron arm-tips, which must have been deposited in the position they were found upon the deterioration of the wooden elements of said anchor (Fig. 15). The third and smaller anchor was found near the starboard one, but underneath three fallen amphorae (Fig. 15). Either this anchor was stored inside the hold or that the deposition of the amphorae happened later, with the collapse of the starboard side of the hold. It is deduced from the stratigraphic evidence that the larger anchors were not stored on the deck, but rather outside the gunwale.

3.3 Documentation and mapping of the site

Since its commencement, the Mazotos shipwreck project has employed digital photogrammetry to document, with accuracy and detail, the site, its stratigraphy and the locations of the artefacts (Demesticha et al. 2014: 148). Regarding the methodology followed at Mazotos, a constant effort was made to optimize the various steps or methods in the documentation process, which have been discussed in previous reports (Demesticha 2010; Skarlatos et al. 2012; Demesticha et al. 2014). The photogrammetric recording of the Mazotos site relies on the creation of a network of control points (points with known co-ordinates) which are used as a reference system in order to geo-reference the produced photogrammetric models. In the case of Mazotos, control points are placed both inside the site (targets placed on amphora mouths) and around it (targets affixed on 25kg concrete blocks) which enable the surveyors to accurately map and geo-reference large areas (Demesticha et al. 2014: 142-143).

During the photogrammetry photography dive, both "aerial like" photos from a height and oblique photos closer to the assemblage are taken, thus covering the intended area, gathering information horizontally and vertically, whilst also achieving close-ups of artefacts and information on hidden areas. The more photos taken the better, but the photographer also needs to ensure that the photographs are of a) good quality, b) include plenty of control points and c) achieve a high percentage of overlap between them. These factors enhance the quality and accuracy of the geo-referenced 3D point cloud, orthophoto and mesh models, which are produced from the processing of the photos following workflow tasks in Agisoft Photoscan/Metashape. The created geo-referenced point cloud (made up of million of points, each with specific co-ordinates) can then be used to retrieve metrical and spatial information (Demesticha et al. 2014).

Once labeled amphorae and artefacts are adequately recorded *in situ*, they are removed from the trench and brought on board the support vessel. They are then cleaned and emptied of their contents (which are catalogued separately according to their material), photographed and their dimensions are carefully measured.

In contrast, smaller or loose artefacts are seldomly labeled underwater, as this is both impractical and difficult but also such an undertaking would cause significant delays to the progress of the excavation. As the excavation at Mazotos is conducted in sections, the delineation of each season's trench area and its subdivisions provides the means by which such finds can be easily and quickly recorded. Broken sherds are collected in lots, according to the particular area they were discovered and are assigned a unique identifying number – this is a common practice in most excavations (Green 2004: 280). Artefacts retrieved through sieving are also dealt with in the same manner after they are distinguished according to their material. In order to ensure that digital mapping of individual sherds and small artefacts is possible, the changes made to the trench during excavation are recorded in more than one way: the excavation area is photographed multiple times a day while divers work and it is documented photogrammetrically either at the start or end of each day. All relevant information pertaining to each artefact is also entered in the project's database (Demesticha et al. 2014: 145).

The remainder of this section provides an overview of the excavation and documentation data, produced during and post fieldwork, namely the: a) photogrammetric data, b) information contained in the project's database, c) photographic and video data, concluding

with the presentation of the Mazotos 3DSM.

Photogrammetric data

Photogrammmetry, the recording method and technique employed at the Mazotos excavation, uses flexible low-cost equipment to provide fast, complete and accurate documentation, allowing the excavation work to proceed without delays (Demesticha et al. 2014: 142). The site needs to be fully and accurately documented in its entirety, before any excavation work commences each field season and prior to leaving the site upon the completion of a season (Skarlatos 2011: 14). It is also important that the progress of excavation of each trench is systematically recorded and to ensure that no material is removed from the site without first being documented *in situ*.

(i) Area or site point clouds (ply or obj format)

Each photogrammetry photoshoot produces hundreds of high-quality photos, which are then processed in Agisoft Photoscan/Metashape within the same day, to produce a full three-dimensional model (a dense cloud of millions of points) of the area of interest (Skarlatos 2011: 14; Demesticha et al. 2014: 142). This process has produced 3D photogrammetric models (point clouds) for each day in the field, documenting the state of the site or of a specific trench, as the excavation progresses – fundamental data for both, during fieldwork and for the purpose of analysis.

(ii) Orthophotos and daily plans

From the photogrammetric 3D models of the recorded areas, spatially-referenced 2D orthophotos are also exported, which are orthographic projections of the image dataset, corrected for lens and elevation distortion. These are essential during the field work for producing daily site plans of the area being excavated and are also used above and below the water to co-ordinate divers and tasks (Demesticha et al. 2014: 147).

(iii) Artefact Photogrammetry

Since 2016, photogrammetry has also been utilized to produce 3D models of the retrieved amphorae, to accurately record the environmental and biological markings on these artefacts (Fig. 17). This was pursued in an attempt to understand the dynamic sequence of exposure and burial events that the site has undergone since its initial deposition (Secci et al. 2021).

Database

Each and every person involved in the project is responsible in ensuring that comprehensive records of the work carried out on a daily basis, are systematically and accurately documented in the project's database. This recording system is designed to address the data management requirements of the project, thus able to store and manage diverse information, allowing users to easily and quickly cross-reference its contents.

The database consists of the following data resources: Dive Logs, Excavation Logs, Find Records, Daily Logs, Photographic Archive and the links, or connections between them.

(i) Dive logs

Detailed dive logs are kept and include the objectives assigned to each dive, what was achieved and observations made by the divers. These form an integral part of the project's archive as they are frequently referred to during post-fieldwork processing, offering insights which might have been missed at the time of recording (for example: context details, artefact details, associations and excavation conditions and observations).

(ii) Excavation Logs

Logs created for the purpose of recording information relating to the excavation of a specific area per dive. Such information includes the location, the stratigraphic layer, the total distance excavated, as well as observations regarding sediment condition and changes.

(iii) Find records

The database also includes artefact records, providing a short description of each find, accompanied by photographs of each artefact and all events associated with it (for instance the dates of when it was first labeled, moved, lifted etc.).

(iv) Daily logs

A diary of all activities taking place on dry land, or at sea and onboard the support vessel, are kept in the database. Apart from offering insights on the project's progression on a daily basis, these logs are invaluable in terms of planning, logistical and equipment issues, artefact processing and conservation, as well as work conducted during museum visits.

Photographic Archive

During the course of the excavation, a great number of photographs are taken on a daily basis. Photographs are one of the most important materials of such a project, serving to document the progress and details of the work being carried out, the artefacts themselves and their context. A daily, laborious but imperative task is embedding metadata to each photograph - a process called photo-tagging. This is done prior to adding a new dataset into the project's database enabling the important function of searching for appropriate data rapidly and exactly.

Video footage

This format of documentation is less frequently used during the Mazotos excavation, usually assigned to recording underwater tasks, exciting discoveries and moments.

3DSM

In addition to the photogrammetric recording, the archaeological data are visualized and analysed using the Mazotos 3D site model, inside the Rhinoceros 3D software. All large, labeled artefacts (raised or still underwater) are individually modeled in 3D and plotted in their exact location within the 3DSM to create a digital representation of the site, which is updated after every field season. This is achieved by generating segments from the geo-referenced point clouds depicting each artefact in its *in situ* position, which are then used to align the 3D CAD or photogrammetric model of each artefact.

Additionally, the 3DSM has proved a useful tool for preliminary examining the stowage-system at the fore end of the ship; a study which resulted in three stowage reconstruction suggestions of the 42 amphorae which comprise this cargo block. For two of the three hypothetical stowage reconstructions (Fig. 16c), the 42 amphorae were stowed in the available 3D space in two different configurations, without taking into account their specific find-spots. Instead the remaining hypothetical reconstruction (Figs. 16a and 16b) took into consideration the aforementioned aspect, for the purpose of retracing (where possible) the original stowage position of each container (Demesticha 2021).

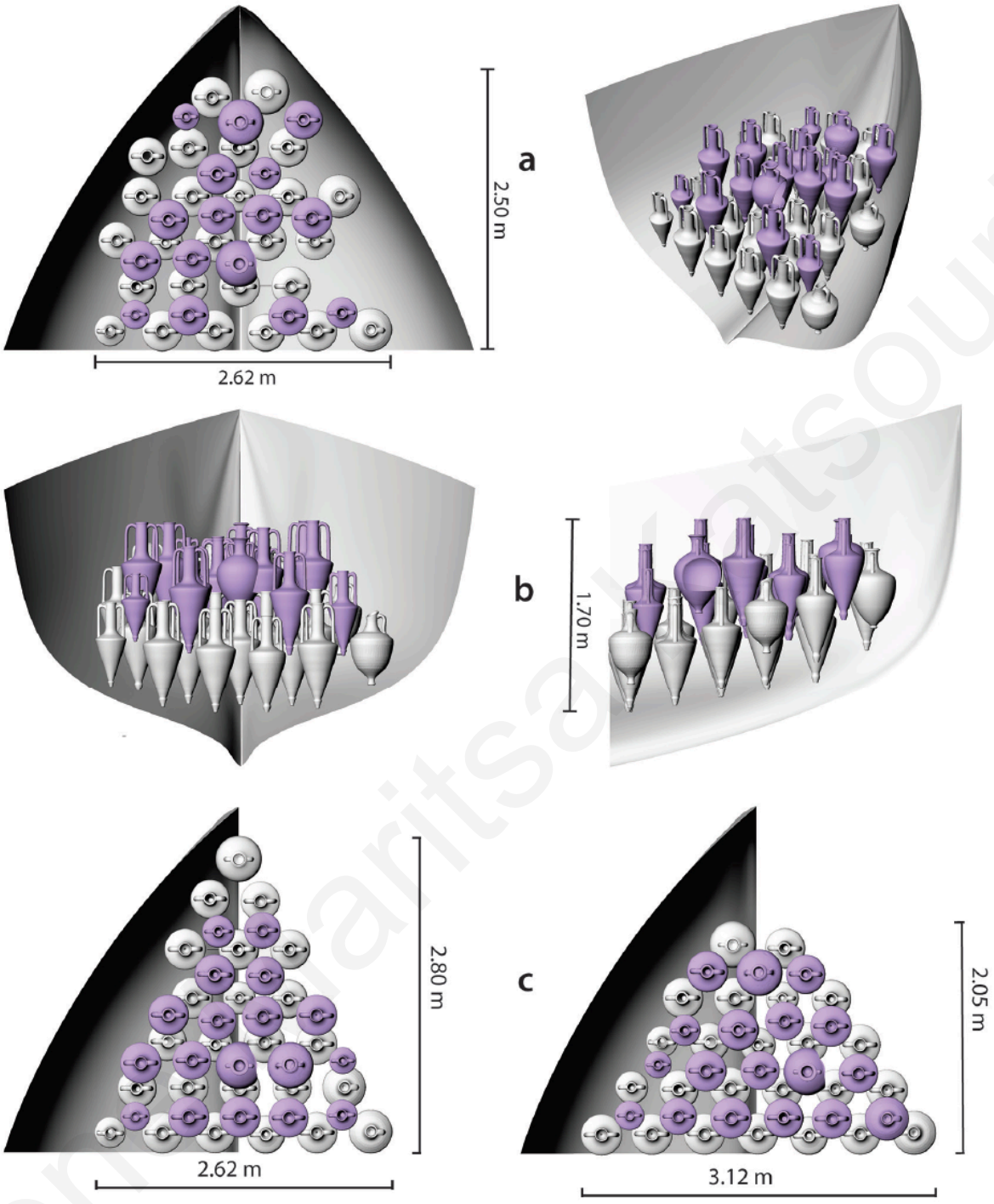

Figure 16: Stowage reconstructions at the bow end: a) and b) top, front and side views of the suggested stowage reconstruction, with the find spots taken into account; c) two different hypothetical reconstructions where find-spots are not taken into account (Demesticha 2021: 50, Fig. 13).

Moreover, the 3DSM has also been used in the investigation of the WSFP (Secci et al. 2021; Demesticha 2021). As mentioned previously, since 2016, raised amphorae have been individually documented using photogrammetry, in order to record the sediment and biogenic horizons marks left on their exterior surface (Fig. 17). Recording and analyzing this evidence

has been the focus of a Post-Doctoral study seeking to understand the depositional history of the site, through the use of three-dimensional recording and modelling, which has already resulted in identifying an older seafloor: “representing a phase of stability, in the sediment accretion at the site, achieved some time after the wreckage” (Secci et al. 2021: 7).

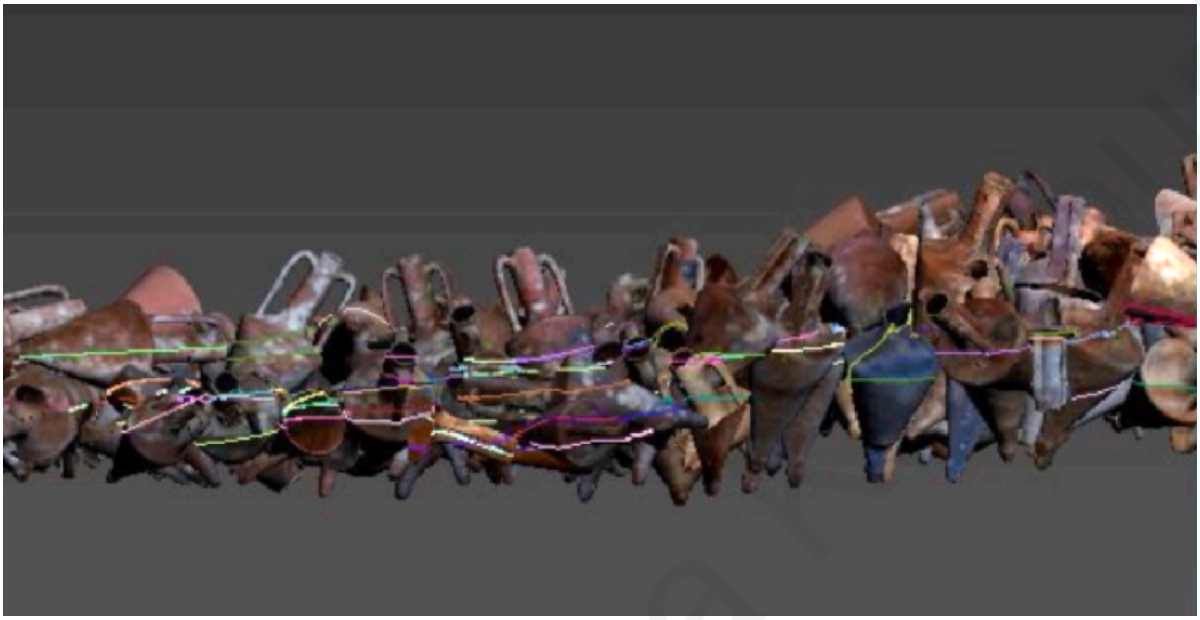

Figure 17: Sediment horizons are identified and plotted on the photogrammetric models of the amphorae (Secci et al. 2021: 9, Fig. 9b).

4. Spatial analysis of reconstructed finds

The first objective of this thesis was to develop a methodological approach for mapping micro-stratigraphical evidence in a 3D environment, using the digital documentation data acquired during the Mazotos Shipwreck Project. As mentioned in section 3.3, the 3DSM has up to this point, mostly included the larger artefacts found at the site; the majority of smaller artefacts and all sherd groups have not been modelled and plotted in the digital reconstruction of the site. The detailed documentation used in the project however, permits the plotting of every lifted find and indeed, as the reconstruction of the WSFP is one of the project's prime objectives, the mapping of micro-stratigraphical evidence was an aspect intended to be further examined (Demesticha et al. 2014: 145-146).

The reconstruction of fragmented artefacts during conservation provided the basis of this investigation. All artefacts excavated at the Mazotos shipwreck site are treated at the Conservation Laboratory for Underwater Finds of the Department of Antiquities. Treatment involves cleaning, stabilization, reinforcement and consolidation as well as groupings and joining together fragments that belong to the same artefact (Loizides 2017; Hadjivasili 2018). This conservation work resulted in 36 reconstructions which were photographically documented during and after each process. However, as the focus of the study was the bow area of the site, only twelve (Table 1) of the thirty-six reconstructions were examined.

Table 1: The twelve Reconstructions resulting from the conservation work and which will be investigated.

Reconstruction Number	Artefact Number	Individual Fragments used in Reconstructions
01	P0371	1 sherd from P0365 (P0365a)
		1 sherd from P0366 (P0366a)
		P0220
02	P0018	A toe from P0320 (P0320a)
03	P0141	1 sherd from P0265 (P0265a)
04	P0151	1 sherd from P0265 (P0265b)
05	P0273	1 handle fragment from P0342 (P0342a)

06	P0357	1 sherd from P0395 (P0395a)
07	P0314	2 sherds from P0292 (P0292e-f)
08	P0310	P0295: 1 sherd broken into two pieces
		4 sherds from P0293 (P0293e-h)
		Adhered fragment comprising of 1 sherd from P0293 (P0293d) and 4 sherds from P0292 (P0292a-d); which the conservators believe belongs to P0310.
		Toe fragment from P0293 (P0293i); which the conservators believe belongs to P0310.
		Adhered fragment comprising of 1 sherd from P0282 (P0282a) and 3 sherds from P0293 (P0293a-c); which the conservators believe belongs to P0310.
09	P0263	2 sherds from P0333 (P0333a-b)
10	P0290	P0362: 1 handle fragment
11	P0385	1 toe from P0404 (P0404a)
		3 sherds from P0395 (P0395b-d)
		1 sherd from P0353 (P0353a)
12	P0384	1 sherd from P0911 (P0911a)
		1 sherd from P0844 (P0844a)
		1 sherd from P0291 (P0291a)
		2 sherds from P0395 (P0395e-f)
Total	**Twelve artefacts already included in the 3DSM prior to this study.**	**Thirty-eight fragments, to be plotted in the 3DSM for the purpose of this thesis.**

The decision to solely examine the information derived from these twelve cases was made for a number of reasons. First and foremost, the fragments in question have already been associated to the broken amphorae they belong to (through the conservation work) and so

their study served as a springboard from which transference patterns could be meaningfully investigated. Additionally, it was estimated that these reconstructed finds would provide ample data for the scope of a master thesis and that through their spatial analysis, a valid proof of concept could be produced, from which to evaluate the efficacy of the proposed methodology, as well as the potential of investigating the micro-stratigraphy of the site and doing so using digital applications.

4.1 Methodology

Thirty-eight individual fragments (Table 1) had to be added to the 3DSM and analysed as part of this thesis. To this end, the process followed involved three major steps:

1. All information regarding the excavation process of each fragment was collected.
2. Fragments were accurately plotted into the 3DSM.
3. Once in the 3DSM, the locations of all artefacts were carefully studied so that they could be stratigraphically and spatially contextualized.

Data gathering

The information derived from the conservation work was correlated to the corresponding information from the excavation and documentation phases. The project's existing database, underwater photographs of artefacts still *in situ* and photogrammetric point clouds documenting the daily progress of excavation, were primarily utilized, in order to accurately plot the fragments in the 3DSM and ensure valid and reliable results.

All information regarding the fragments under investigation was retrieved from the project's database. This included reviewing each individual artefact record (Fig. 18) in conjunction with all relevant dive and daily logs with the aim of extracting the most relevant information regarding each individual artefact. Artefact photographs (prior and after conservation) were inspected in order to identify the fragments used in each Reconstruction, by the conservators. Furthermore for the ease of the reader, the sherds under investigation were given a distinctive code number for this thesis, using letters of the alphabet.

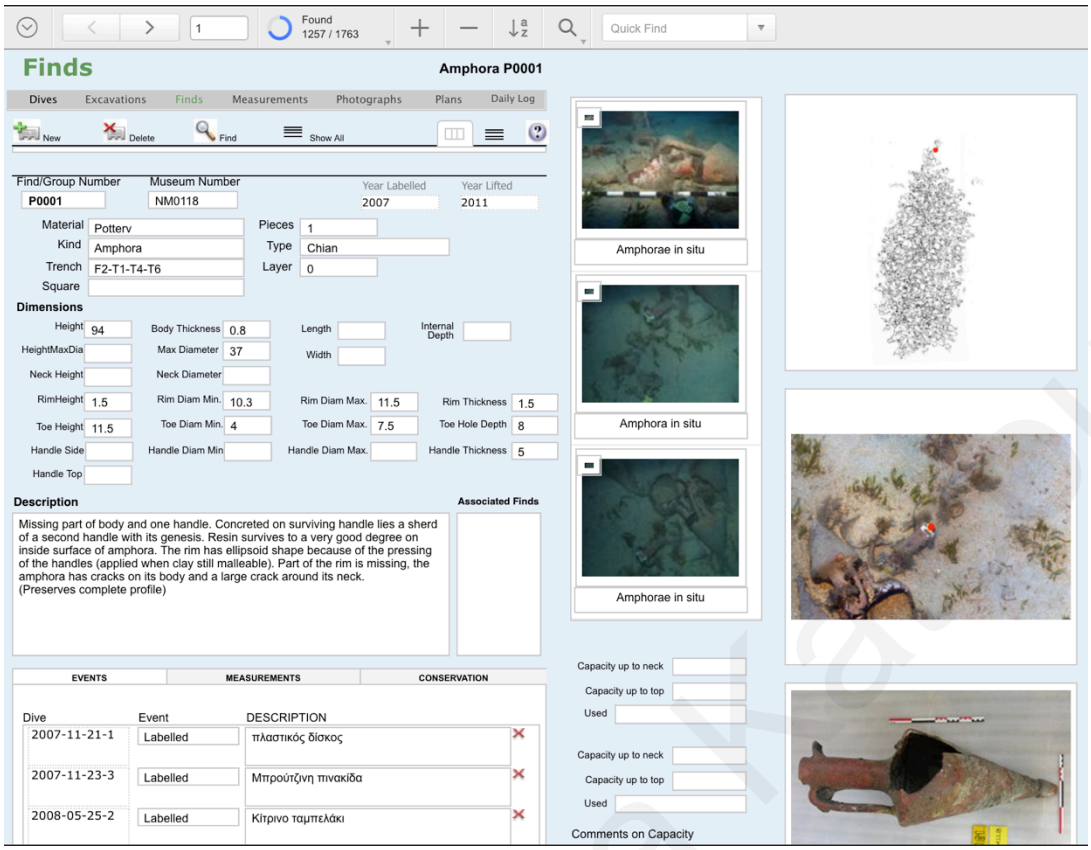

Figure 18: Sample of an artefact record in the database.

Once a visual identification of a fragment was achieved, the photographical archive was reviewed in search of the specific fragment. This process entailed viewing numerous photographs spanning from the pre-disturbance survey up to the moment the artefact was lifted, to correctly identify its location within the site. As the bow area was investigated in five separate seasons (2010, 2011, 2016, 2018, 2019) it was imperative that all photographs were checked, so as to detect whether the artefact had undergone any displacement prior to its recovery and to ensure that the position used in the plotting procedure was the earliest one recorded.

Plotting process

Once the *in situ* location of an artefact was identified, a segment of the area was cut from the point cloud that depicts it best. This was done using the segmentation tool in the software CloudCompare. The segment was then named after the artefact and saved to be used in the later 3D plotting process. On some occasions, a small artefact might have been exposed during excavation and retrieved before any photographic or photogrammetric documentation

could take place. In such instances, a segment of the specific area was cut from the point cloud closest in time, to the date and dive of the artefact's retrieval. This segment provided the trench (ground) level onto which the artefact was to be plotted.

It is important at this point to discuss a difficulty encountered and how this was overcome. As the mapping method used at Mazotos went through an optimization phase during 2010-2012, certain 2010 and 2011 point clouds inevitably had spatial inaccuracies (Skarlatos et al. 2012: 5; Demesticha et al. 2014: 141-142). This problem needed to be confronted and solved, to ensure the correct geo-referencing of the investigated fragments in the 3DSM. For this reason, three point clouds needed to be readjusted.

Realigning point clouds that share matching points was not an option because of the seabed instability, or the process of the excavation itself that changed the environment with every dive. Instead point clouds were realigned using the geo-referenced artefact CAD models (that populate the 3DSM). Each point cloud was first imported into the 3DSM to assist with identifying visible artefacts and export their corresponding CAD models together as one single file (in .OBJ format; hereafter .OBJ). Then the point cloud in question and the .OBJ were loaded in CloudCompare, where the 'Align (point pairs picking)' tool was used to identify, select and finally align equivalent points between the two entities. The accuracy of this realignment exercise is increased if a large set of equivalent points is used and also by making sure that these equivalent points are distributed evenly over the area that must be realigned. The realigned point cloud is then saved, ready to be used in the plotting process. Three point clouds were realigned in this manner, as they were necessary for plotting some of the sherds related to the twelve Reconstructions (Table 2).

Table 2: Realignment process of the three point clouds at the bow area.

Point cloud	Total artefact CAD models used in the realignment	Total point pairs used in the realignment	Reconstruction involved (Artefact number)
2010-05-09-03-04 	31	101	04 (P0265b)
2010-05-25-06 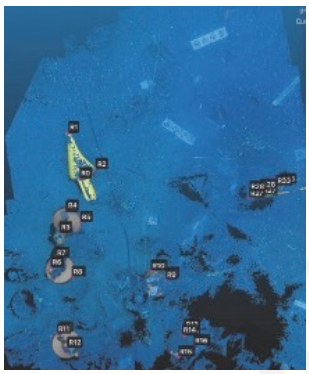	10	33	08 (P0295, P0282a, P0292a-d, P0293a-i) 07 (P0292e-f) 10 (P0362)
2010-06-03-02 	17	42	09 (P0333a-b)

Returning to the subject of plotting the fragments, the next step was to create a digital representation of the artefact in question. As five of the fragments had already been documented through photogrammetry (P0265a-b, P0365a, P0366b and P0362), their digital model was ready for geo-referencing (Fig. 19a). Another five fragments (P0220, P0395b-d and P0911a) were created in Rhinoceros as approximate 3D CAD models, by adjusting already existing theoretical models (Fig. 19b). A vector outline drawing was created for the remaining fragments by tracing their artefact photograph in the software Adobe Illustrator. The scale bar from the photograph was also drawn, so as to assist in correctly scaling the drawing once in the Rhinoceros 3D software (Fig. 19c). The .AI file of the outline drawing was then imported into Rhinoceros and rescaled. The scale bar was removed and the vector outline of the artefact was organized in its own named layer, ready for geo-referencing.

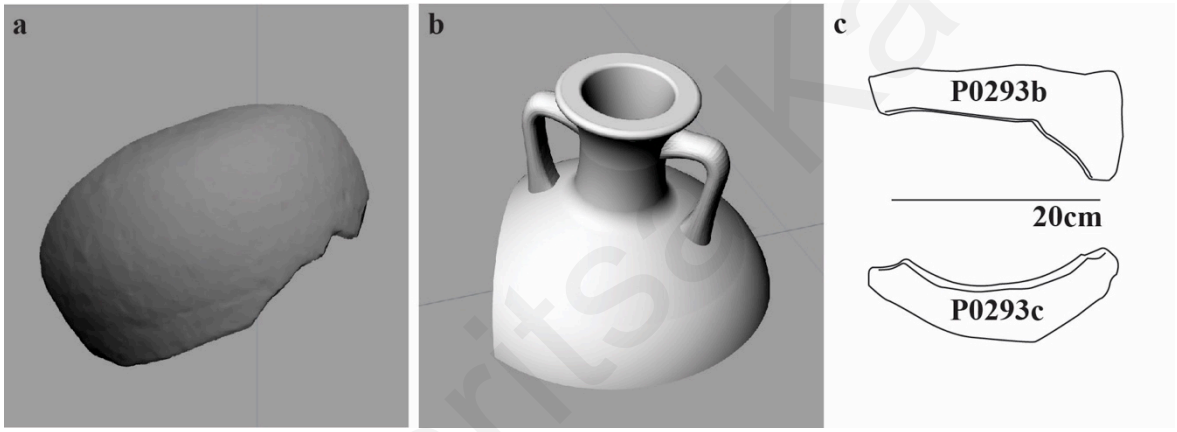

Figure 19: Examples of the three digital representations used: a) the photogrammetric model of P0265a; b) the approximate CAD model of P0220; c) the vector outline drawing of two sherds from lot P0293.

Pottery sherds are found in large quantities at the site and their dimensions are not individually recorded. The vector outline drawing approach provided the quickest and most meaningful representation of the fragments, while offering two additional advantages: a) the outline assists in matching the fragment's shape and size to the visible information in the point cloud segment, as a further check in confirming it has been accurately identified; b) it is also versatile, in that it can be extruded in Rhinoceros 3D (by assigning a thickness) to create an approximate 3D model of the fragment, if required in the future.

The plotting process was completed within Rhinoceros, by geo-referencing the 3D representation of each artefact (either digital model or vector drawing) through alignment to its corresponding point cloud segment.

4.2 Reconstructed finds

The following section presents each of the twelve Reconstructions, by providing relevant information pertaining to all the artefacts involved in each case, as well as the process followed for their mapping inside the 3DSM. The augmented 3DSM was then used to examine and spatially analyse the newly modelled micro-stratigraphic 3D information, in order to determine what insights may be acquired regarding both: the stratigraphy at the micro-level and the dynamics and WSFP present at the site.

A catalogue containing information and photographs of the artefacts involved in the twelve Reconstructions is available at the end of this thesis (Appendix), intended to provide the reader with a quick overview where necessary.

Reconstruction 01: A South - Aegean Amphora (Mushroom Rim - Knob Toe) reconstructed of four pieces P0371 – P0365a – P0366a – P0220

(i) Brief description of the finds involved

During conservation, two large body sherds, one from lot P0365 (named P0365a) and one from P0366 (named P0366a) were joined to the surface find P0371, a lower part of a Mushroom-Rim amphora lifted in 2011 (Fig. 20). Both lots were collective numbers for sherds raised in 2011; P0365 comprised seven fragments and P0366 fifty-six. The conservators additionally identified that the upper part of a Mushroom-Rim amphora (P0220), raised in 2010, also belonged to the artefact in discussion (as P0371, P0365a and P0366a) (Fig. 20).

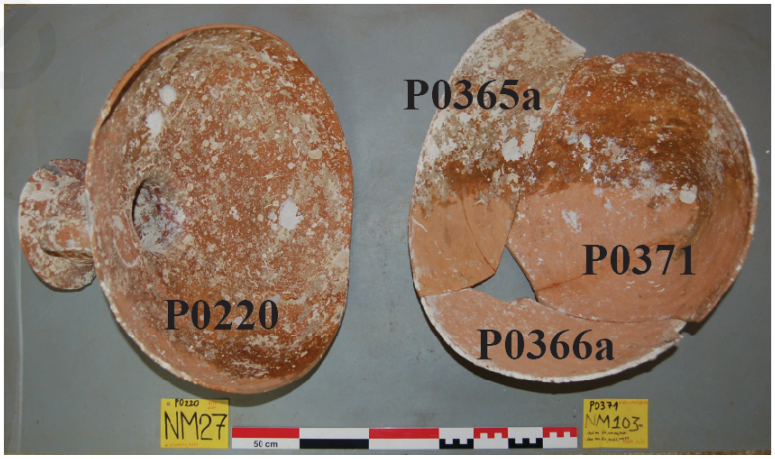

Figure 20: P0371 during its reconstruction (photograph provided courtesy of the Department of Antiquities).

(ii) Stratigraphic/Spatial Interpretation

It seems that the find spot of P0371, P0365a and P0366a in 2011 was different to the one recorded in the pre-disturbance survey in 2007 (Fig. 21). This displacement could perhaps have been caused accidentally by divers whilst setting up the 2010 trench or by marine life activity. P0220 was found approximately 15m away from the main assemblage and out of the established network of photogrammetric control points (Fig. 23).

Figure 21: The earliest recorded location of P0371, P0365a (white dot) and P0366a (black dot) in 2007, in comparison to their retrieval location in 2011.

(iii) Plotting in the 3DSM

The 2007 pre-disturbance locations of P0371, P0365a and P0366a were used for plotting these fragments in the 3DSM (Fig. 22).

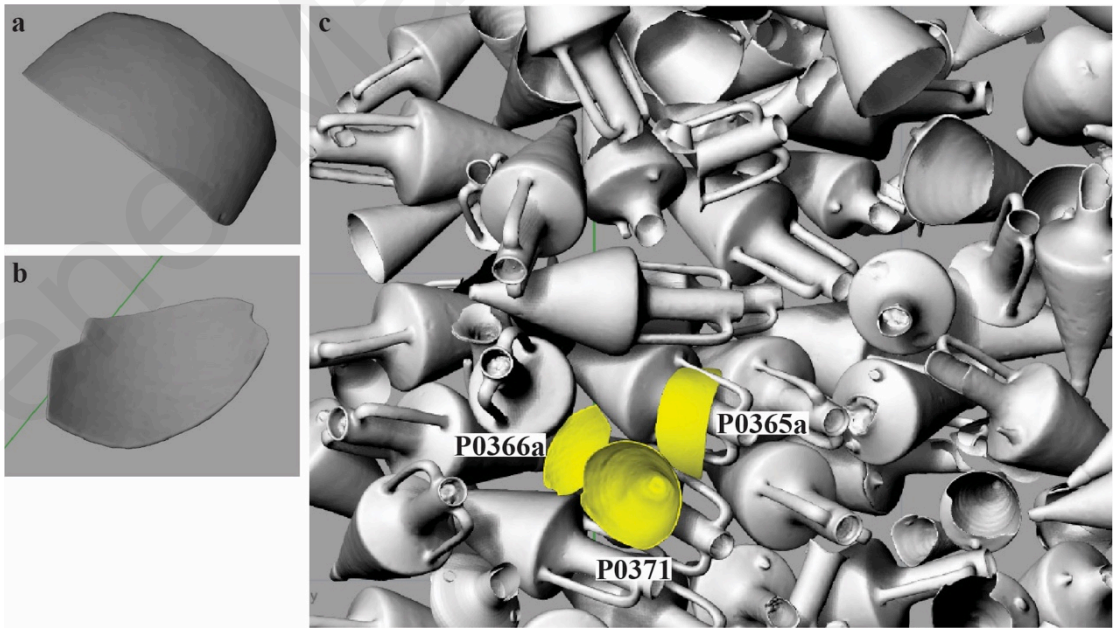

Figure 22: The photogrammetric models of: a) P0365a and b) P0366a, were plotted in c) their earliest recorded location, near P0371.

The approximate retrieval position for P0220 (Fig. 23) was plotted by calculating the distance (15,05m) from B2 (a site-grid fixed point) and the azimuth (130^0) as reported in the database log.

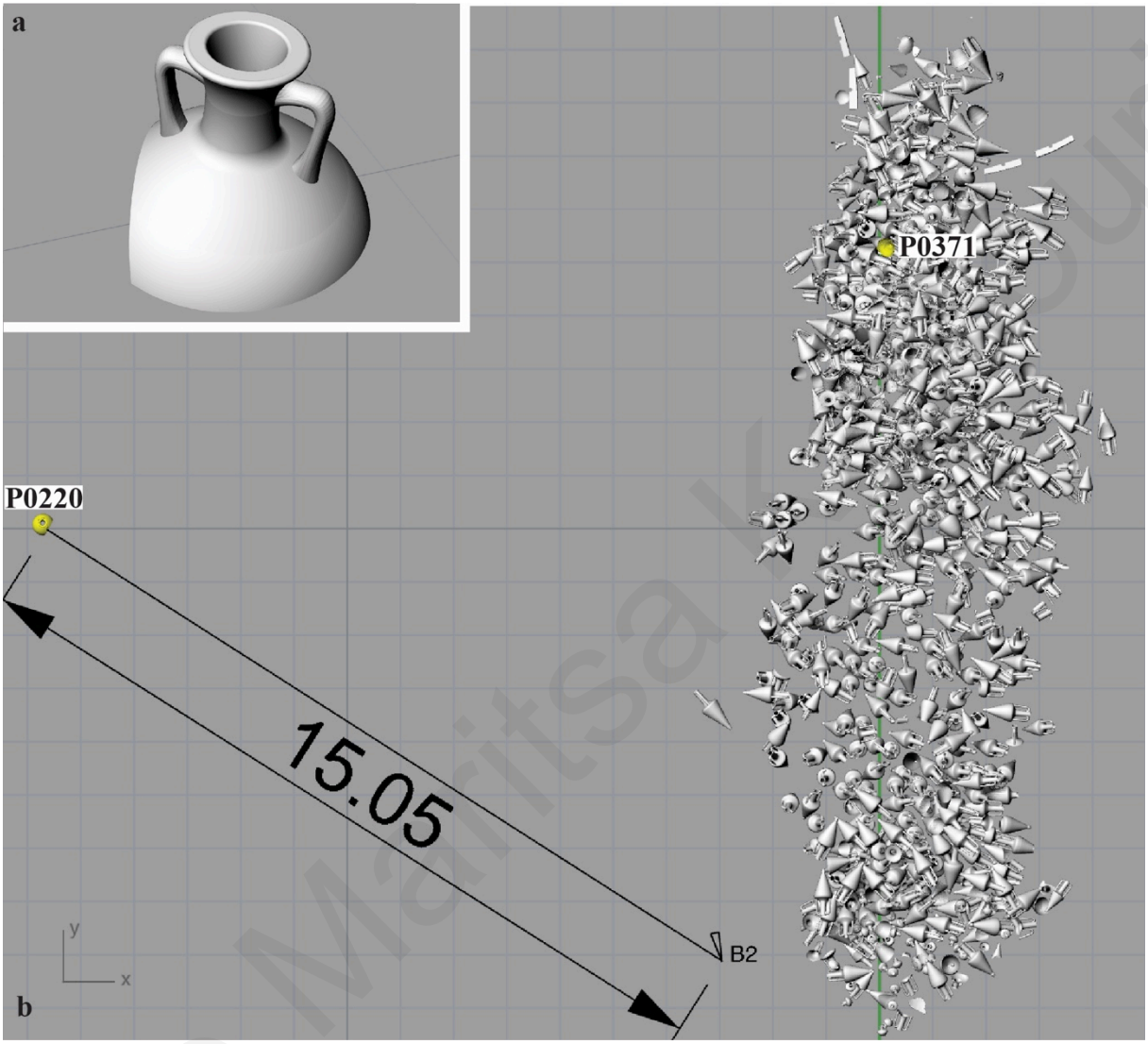

Figure 23: a) The approximate CAD model of P0220 was plotted in the 3DSM, b) according to the database information; P0220 and P0371 inside the 3DSM.

(iv) Spatial Analysis: Cultural transforms

The displacement of P0220, calculated to be 16.82m away from the area of P0371, P0365a and P0366a could be due to cultural transforms, perhaps modern fishing activities using nets (Fig. 24). The fact that P0371, P0365a and P0365a are all surface finds and were found alongside each other inside the assemblage, strongly suggests that P0220's displacement was post-depositional.

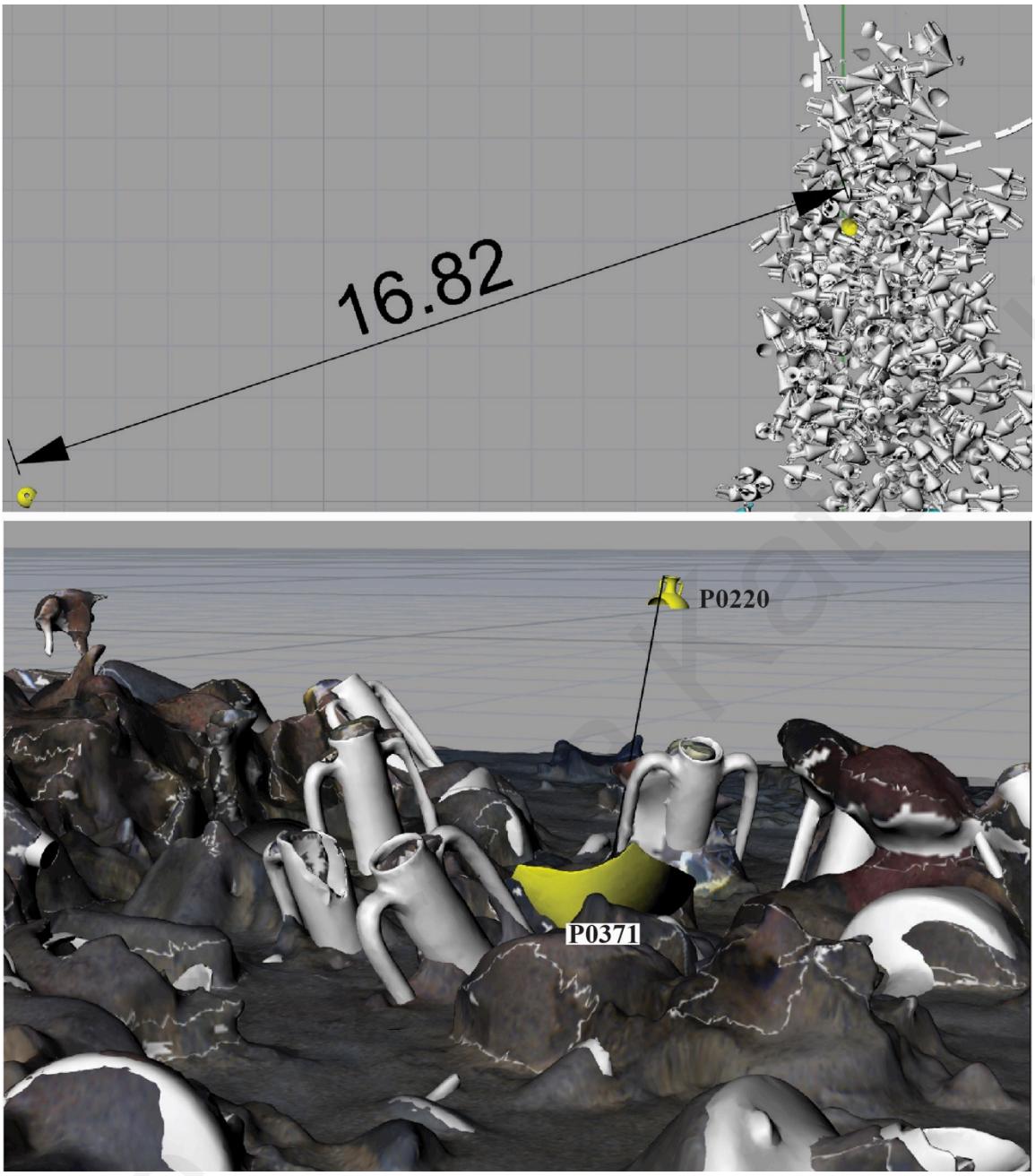

Figure 24: P0220 in relation to P0371 inside the 3DSM (calculated distance between them: 16.82m).

Reconstruction 02: A Chian Amphora reconstructed of two pieces P0018 – P0320a

(i) Brief description of the finds involved

A Chian amphora (P0018) was lifted in 2015 missing its toe. The toe (named P0320a) was found 3.26m away, inside another amphora of the top layer (P0263), excavated in 2010 (Figs. 25 and 26). Apart from the Chian toe fragment (P0320a), lot P0320 contained another thirty-six diagnostic and non-diagnostic fragments, but also three stray tags (see Appendix).

Figure 25: P0018 during its reconstruction (photograph provided courtesy of the Department of Antiquities).

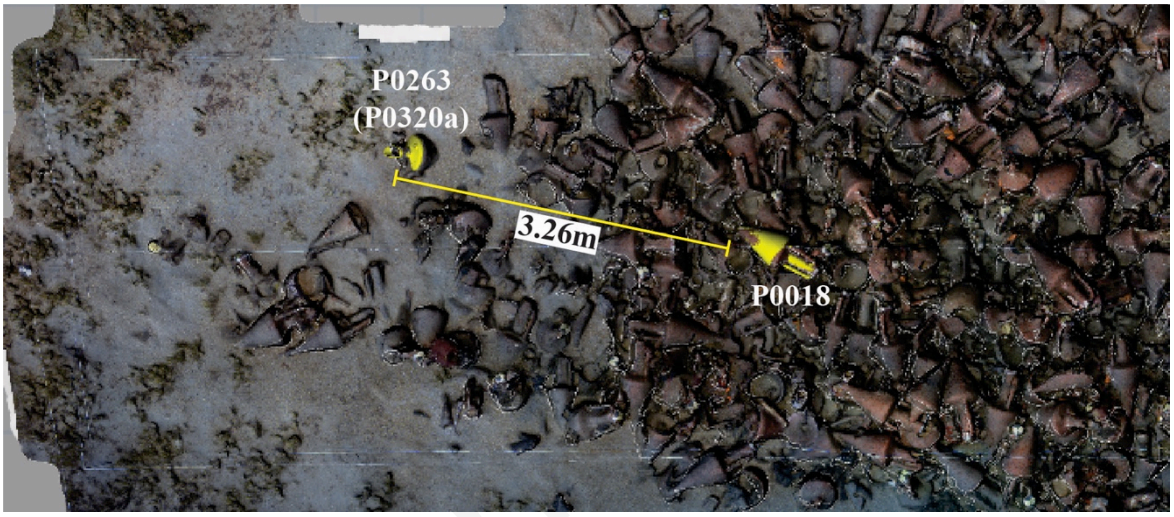

Figure 26: The toe (P0320a) of P0018 was found inside P0263.

(ii) Stratigraphic/Spatial Interpretation

The amount and variety of artefacts comprising lot P0320, have led to the conclusion that P0263 was probably used as a shelter by an octopus, which acted as a scrambling device (for a similar process see Reconstructions 03 and 04). The hypothesis of the octopus' disturbance is further substantiated by photographs from the 2008 field season which indeed show an increased accumulation of sherds around P0263 (Fig. 27b), an area almost empty of finds in 2007 (Fig. 27a). The excavation during the 2008 field season focused on the stern of the ship, so the available photographs were part of the site's photogrammetric documentation. Despite the low number of photographs, at least one sherd from the P0320 lot (recovered from inside amphora P0263) can be positively identified just outside the mouth of P0263, most probably before it was moved inside (Fig. 28). If this is correct, it is reasonable to deduce that more sherds of P0320 were similarly disturbed, resulting in fewer sherds remaining around P0263, as seen in the photograph from 2010 (Fig. 27c).

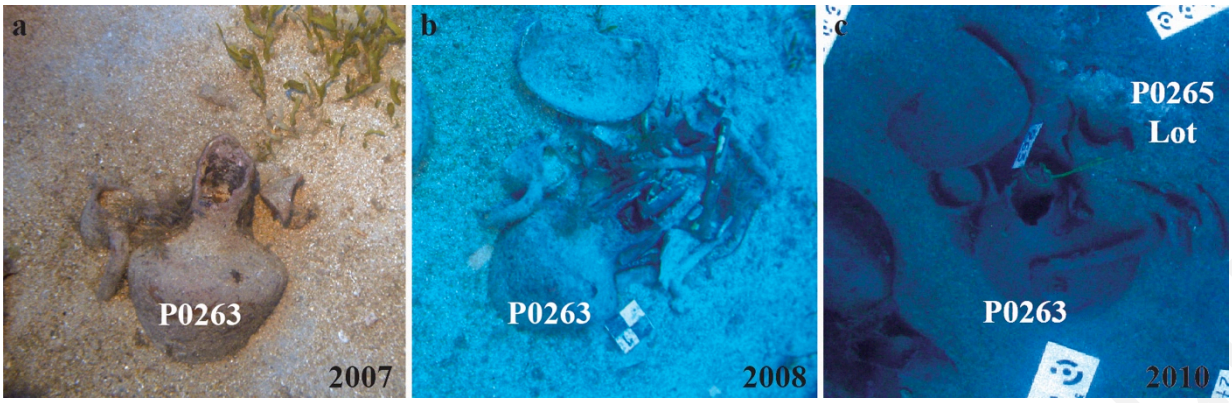

Figure 27: The 2008 photograph showing an increased accumulation of sherds around P0263 (b), an area almost bare in 2007 (a); c) the number of sherds decreases in 2010 (later collected as lot P0265).

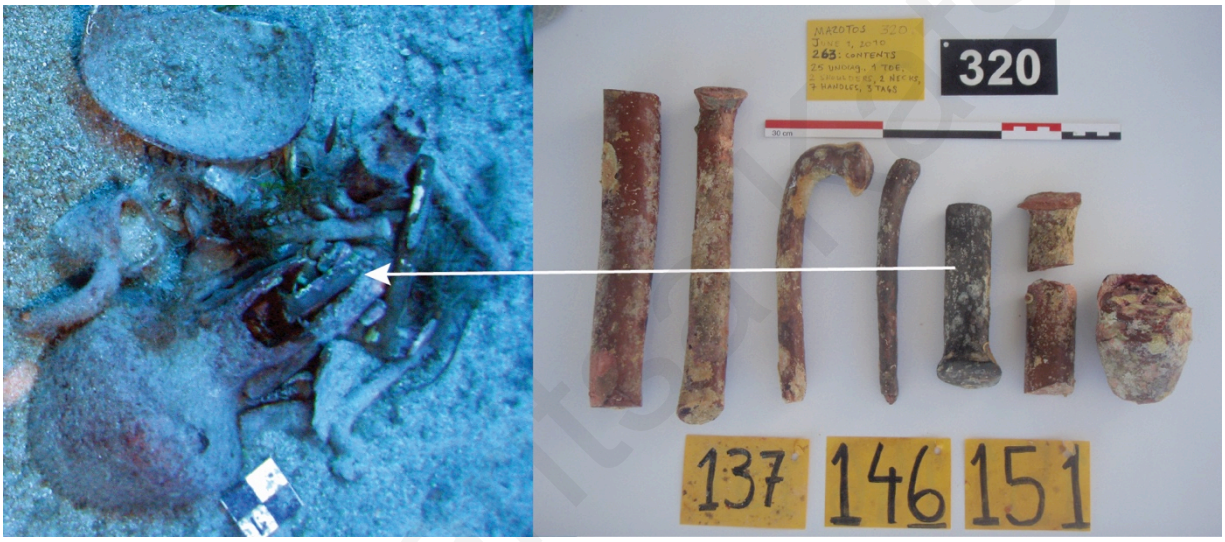

Figure 28: An underwater photograph from 2008, showing one sherd from lot P0320 located at the mouth of amphora P0263.

(iii) Plotting in the 3DSM

A vector outline drawing was created for P0320a, which was later scaled and plotted inside the 3D model of P0263 (Fig. 29).

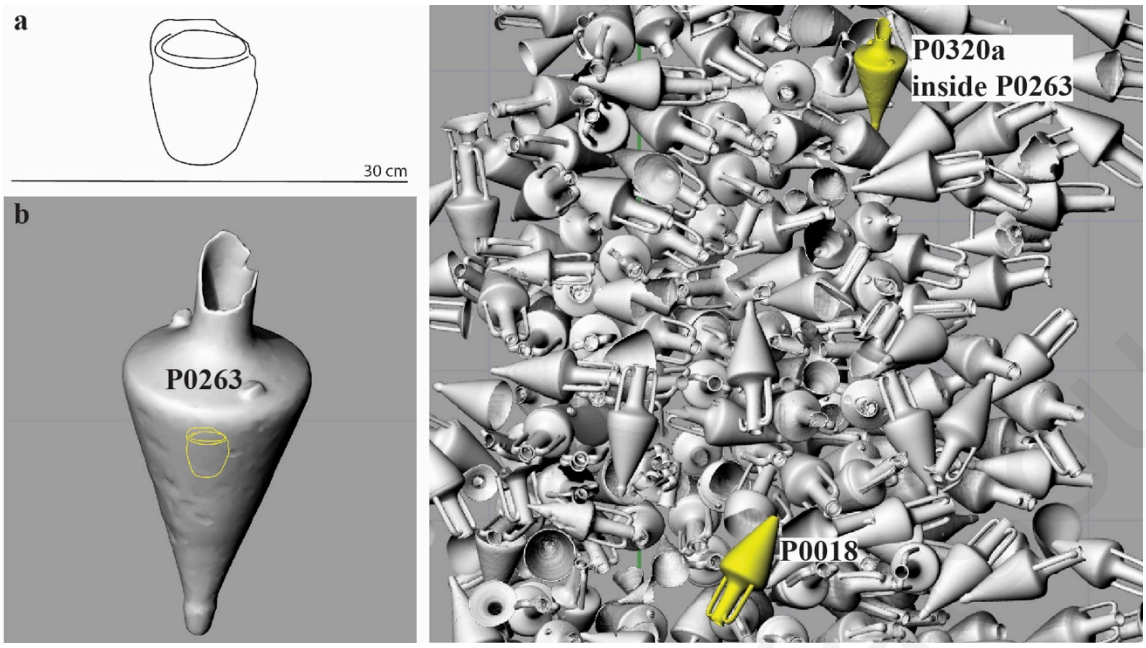

Figure 29: a) The outline drawing of P0320a b) plotted inside the model of P0263 c) Reconstruction 02: P0018 and P0320a inside the 3DSM.

(iv) Spatial Analysis: Scrambling activities of marine life

This Reconstruction is discussed below, alongside others (03-05) showing evidence of scrambling processes.

Reconstruction 03: A South - Aegean Amphora (Mushroom Rim - Knob Toe) reconstructed of two pieces P0141 – P0265a

(i) Brief description of the finds involved

A Mushroom-Rim amphora (P0141) was reconstructed using a large body sherd (named P0265a) from lot P0265 (Fig. 30), collected from around amphora P0263.

Figure 30: P0141 during its reconstruction (photograph provided courtesy of the Department of Antiquities).

(ii) Stratigraphic/Spatial Interpretation

As described in Reconstruction 02, the area surrounding P0263 shows evidence of scrambling processes (Fig. 27). The photographic archive clearly indicates that P0265a was relocated to this secondary/retrieval location (near P0263 as seen in Figure 31b) between the 2008-2010 seasons, from its earliest recorded location, i.e. inside of P0141 (Fig. 31a).

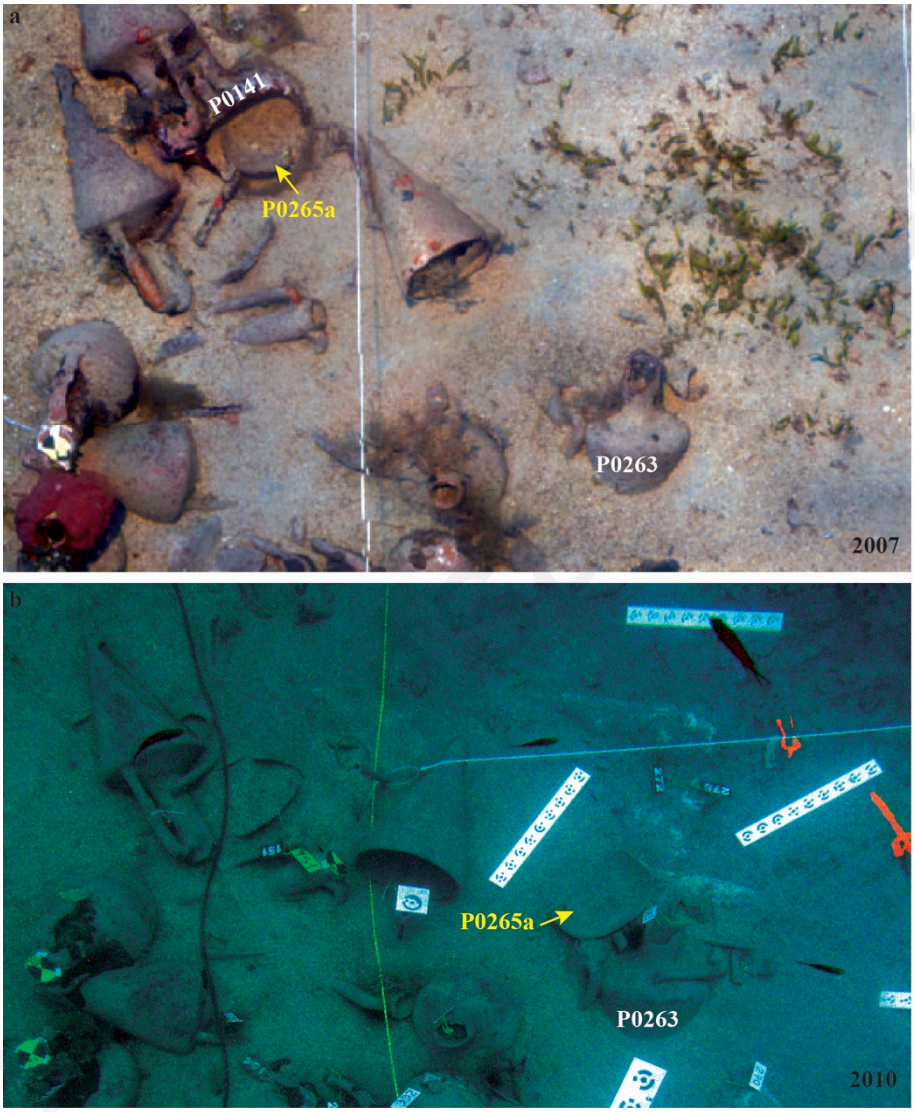

Figure 31: a) The earliest recorded location of P0265a (inside P0141) and b) its retrieval location (close to P0263).

(iii) Plotting in the 3DSM

The existing photogrammetric model of the fragment (P0265a) was plotted inside the model of P0141 (Fig. 32), according to the segment cut from the pre-disturbance point cloud. In this case, having a photogrammetric model proved additionally helpful in verifying that the morphology of the raised sherd matched that of the visible fragment in the segment.

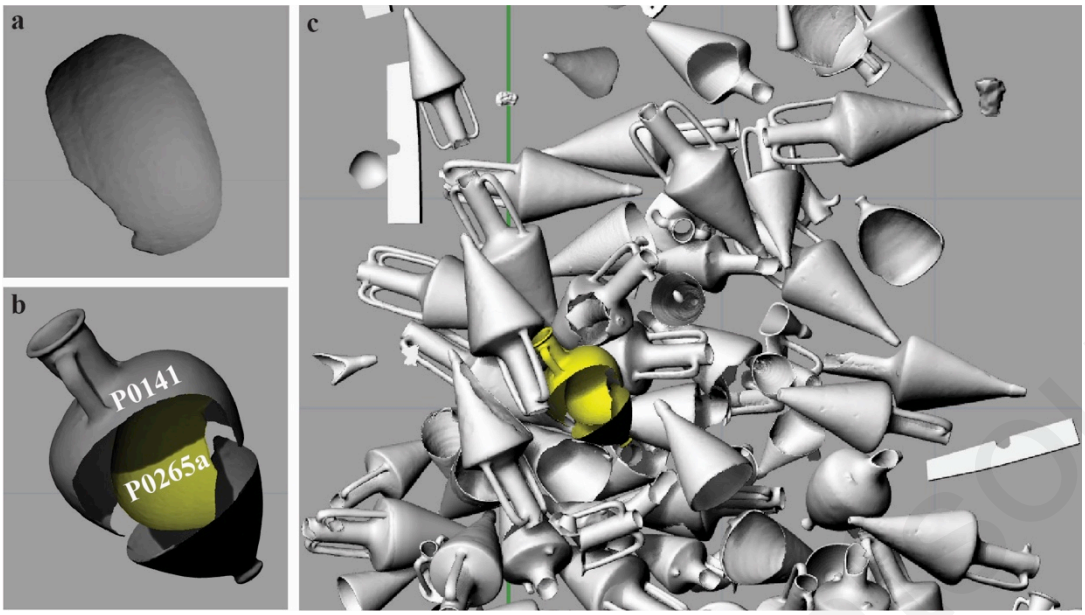

Figure 32: a) The photogrammetric model of P0265a, was plotted in b) its earliest recorded location, inside P0141; c) Reconstruction 03: P0141 and P0265a inside the 3DSM.

(iv) Spatial Analysis: Scrambling activities of marine life

This Reconstruction is discussed below, alongside others (02, 04 and 05) showing evidence of scrambling processes.

Reconstruction 04: A Chian Amphora reconstructed of two pieces P0151 – P0265b

(i) Brief description of the finds involved

Another surface fragment originating from lot P0265 (a shoulder fragment of a Chian amphora, named P0265b) was joined by the conservators to a top half of a Chian amphora (P0151) as seen in Figure 33.

Figure 33: P0151 during its reconstruction (photograph provided courtesy of the Department of Antiquities).

(ii) Stratigraphic/Spatial Interpretation

Similarly to P0265a (Reconstruction 03), P0265b was also displaced to the area near P0263 at some point between 2008 and 2010, due to the scrambling effects of octopus activity (Fig. 34b). No earlier recorded location was identified however for the P0265b sherd.

(iii) Plotting in the 3DSM

The photogrammetric model of this sherd (P0265b) was plotted in its secondary/retrieval location, i.e. near P0263 (Fig. 34).

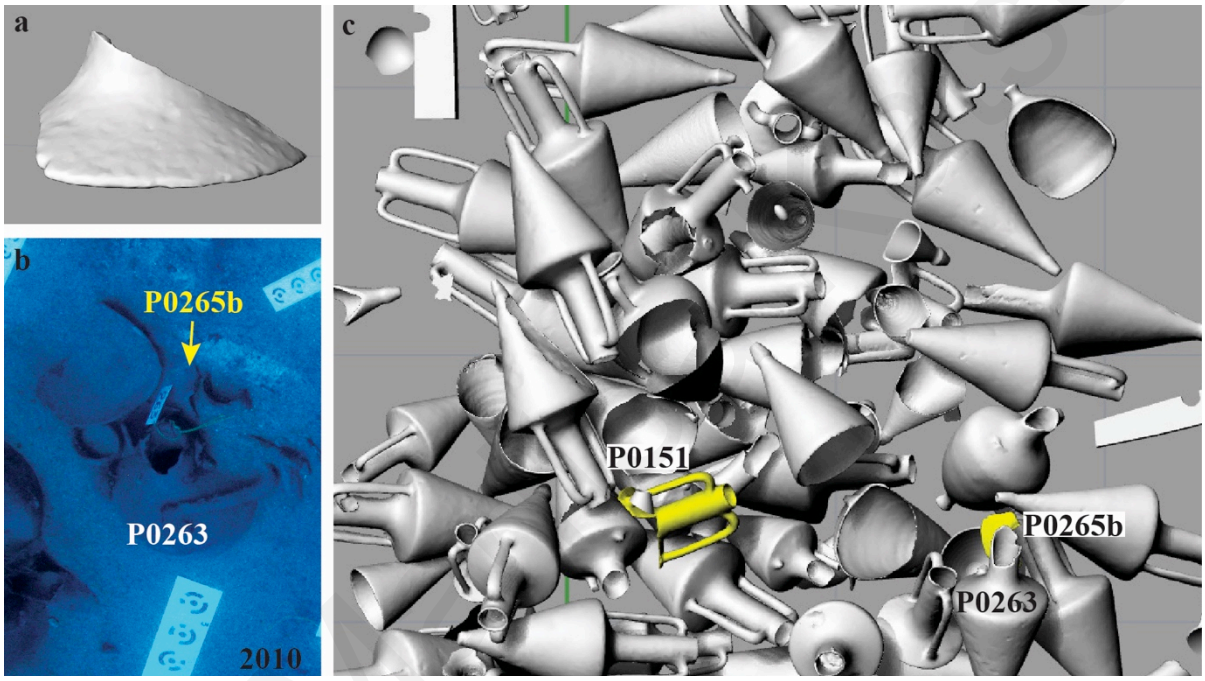

Figure 34: a) The photogrammetric model of P0265b, was plotted in b) its secondary location, near P0263 c) Reconstruction 04: P0151 and P0265b inside the 3DSM.

(iv) Spatial Analysis: Scrambling activities of marine life

This Reconstruction is discussed below, alongside others (02, 03 and 05) showing evidence of scrambling processes.

Reconstruction 05: A Chian Amphora reconstructed of two pieces P0273 - P0342a

(i) Brief description of the finds involved

A Chian amphora handle fragment (named P0342a) was found inside amphora P0273, to which it belonged (Fig. 35).

Figure 35: P0273 during its reconstruction (photograph provided courtesy of the Department of Antiquities).

(ii) Stratigraphic/Spatial Interpretation

This peculiar situation (P0342a found inside the artefact it belongs to, P0273) may again be an indication of octopus activities, as was the case of nearby P0263 (Reconstructions 02-04). Thus the plotted location is again a secondary one, but this time directly associated with the original.

(iii) Plotting in the 3DSM

The vector outline drawing created for P0342a was accordingly plotted inside P0273 (Fig. 36).

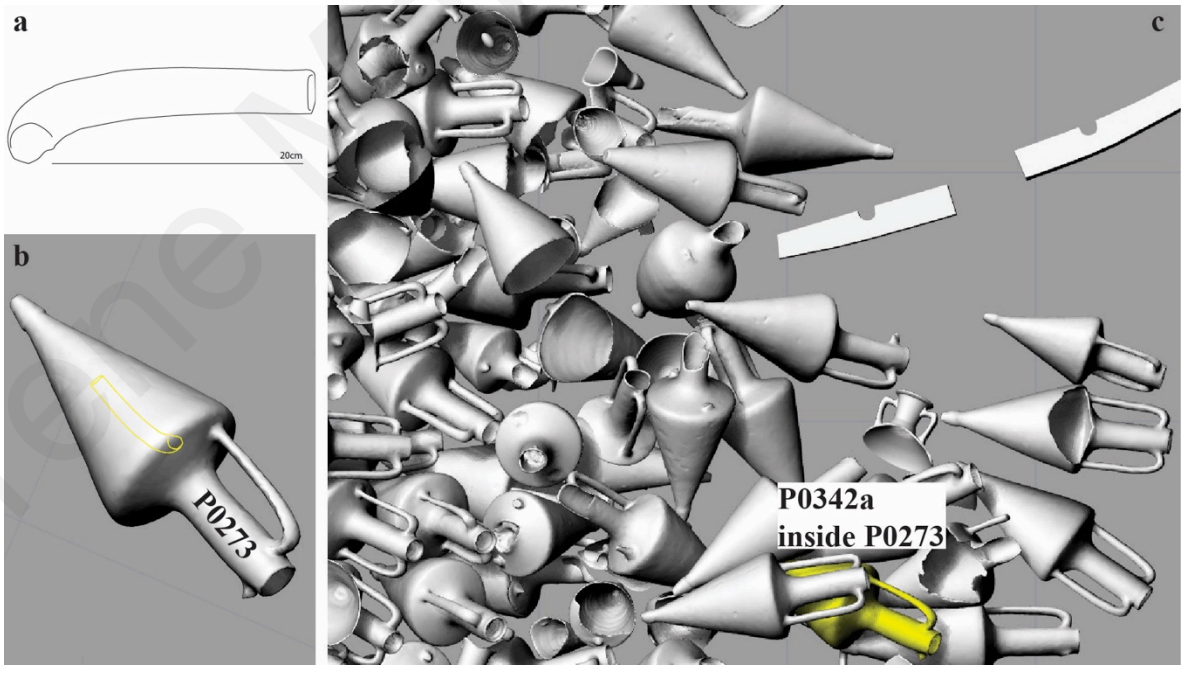

Figure 36: a) The outline drawing of P0342a, b) plotted inside the model of P0273. c) Reconstruction 05: P0273 and P0342a inside the 3DSM.

(iv) Spatial Analysis of Reconstructions 02-05: Scrambling activities of marine life

The displacement and accumulation of surface fragments inside and around P0263 strongly indicates the activities of an octopus. What can also be surmised is that it is a recent event, which seems to have ceased by 2010. A database dive log (05/08/2010) may provide an explanation for this, as it notes that P0263 was the habitat of a moray eel, something that must have kept the octopus away from the area.

Using the 3DSM we can visualize the area in which this post-depositional movement of fragments occurred (Fig. 37). This was achieved by examining the clues derived from Reconstructions 02-04: i) the three stray labels noting numbers P0137, P0146, P0151, retrieved from inside P0263, ii) P0320a which belongs to P0018, iii) P0265a which belongs to P0141, iv) P0265b which was joined to P0151 and lastly v) P0263 itself.

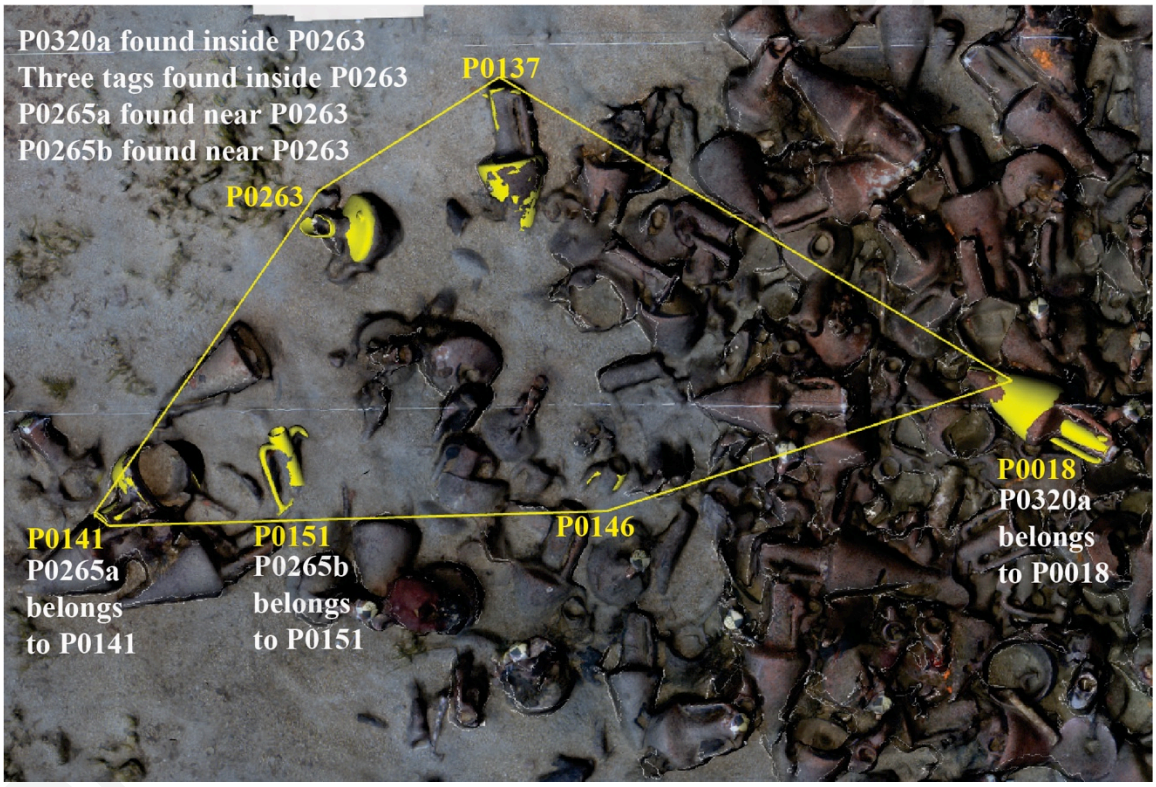

Figure 37: The possible area of movement of the octopus causing the scrambling processes of Reconstructions 02-04.

Although the depositional location of the Chian toe fragment (P0320a) and the shoulder fragment (P0265b) prior to the scrambling event cannot be traced with certainty, there is a strong possibility that like P0265a, these were also surface finds within or close to the demarcated area noted in Figure 37. Even if the depositional location of an artefact is impossible to trace, the fact that a retrieval location has been recognised as a secondary

displacement, is equally as significant for the study of the WSFP.

In contrast to P0263, which was found half exposed, P0273 (of Reconstruction 05) was fully buried (Fig. 38). This signifies that the octopus activity relating to P0273 is not a modern occurrence as in the case of P0263 (which can be placed between the 2008-2010 field seasons). Instead, the displacement of P0342a is more likely to have occurred closer to the wrecking event, in the period between the latest and initial stabilization phases. Indeed, according to the reconstruction of the ancient and the pre-disturbance seabed levels (Secci et al. 2021: 7-8) P0273 has remained half-buried during a long period of time in antiquity (Fig. 39).

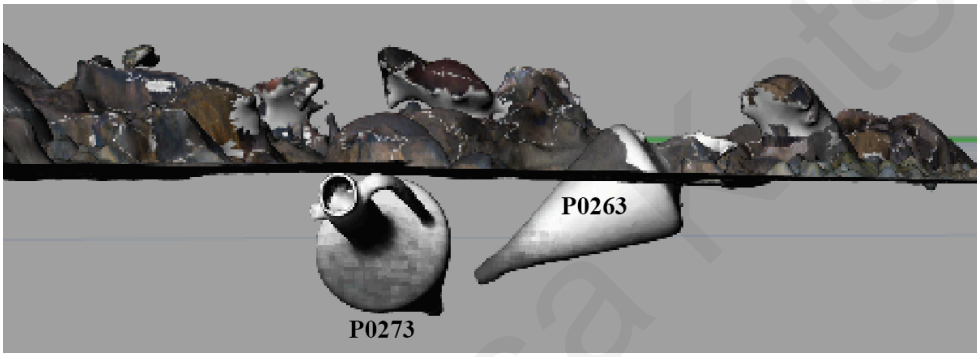

Figure 38: Visualisation of the relative positions of P0263 and P0273 in the 3DSM.

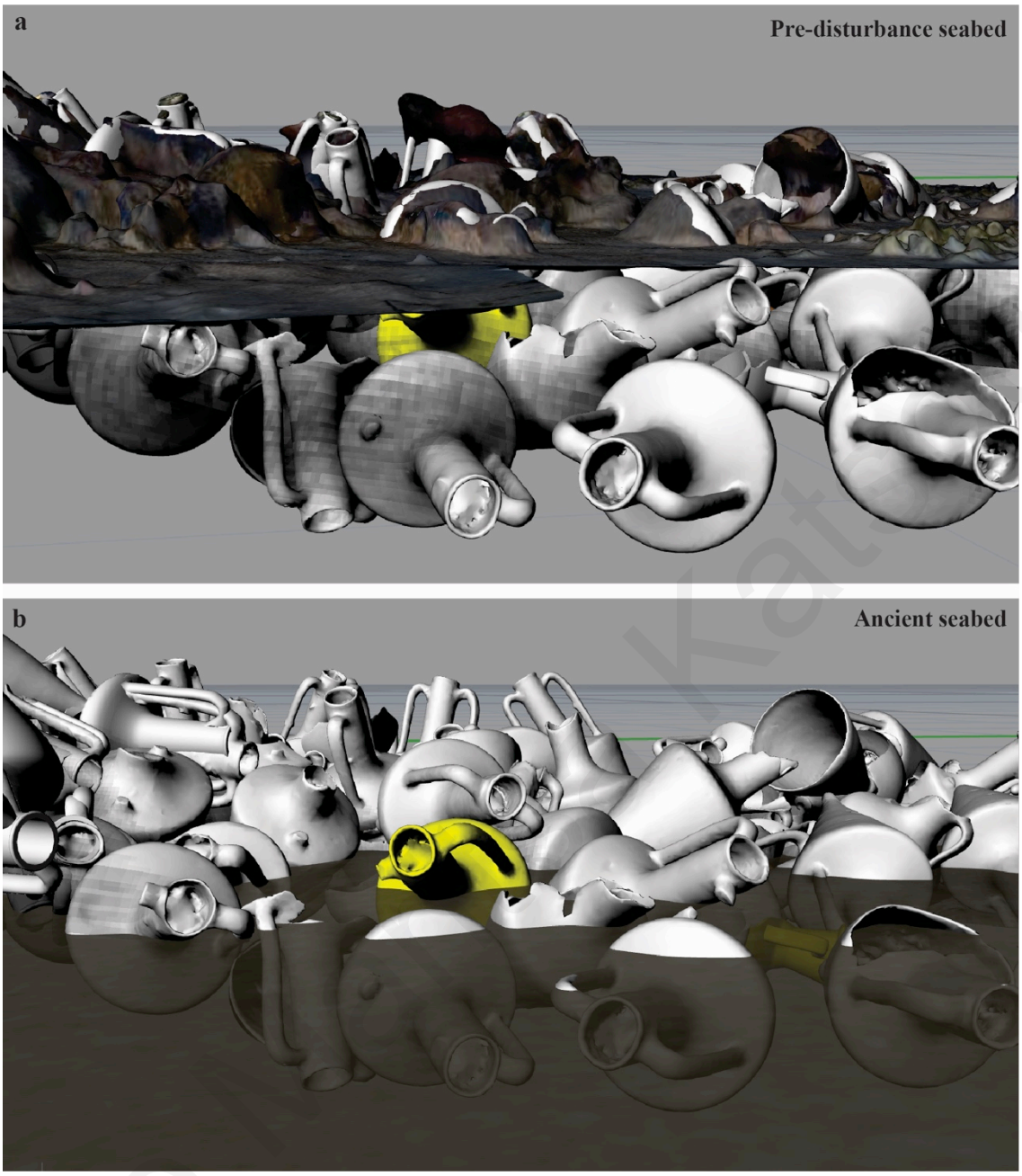

Figure 39: P0273 (in yellow) in relation to the a) latest (pre-disturbance seabed) and b) initial (ancient seabed) stabilization phase as reconstructed by Secci (Secci at al. 2021:7-8).

The displacement of sherds raises important questions regarding the study and plotting of small artefacts which must be taken into account in the interpretation of an artefact's find spot. In the case of both P0263 and P0273, the data clearly indicate the effect of scrambling devices, but their study also highlights the need to thoroughly investigate each retrieval position in order to obtain an accurate and full understanding of the site and its components.

Reconstruction 06: A Chian Amphora reconstructed of two pieces P0357 – P0395a

(i) Brief description of the finds involved

A shoulder fragment (named P0395a) from a lot of 115 sherds (P0395) was found to belong to a Chian amphora (P0357) broken *in situ* and recovered in two parts (Fig. 40).

Figure 40: P0357 during its reconstruction (photograph provided courtesy of the Department of Antiquities).

(ii) Plotting in the 3DSM to enable the Stratigraphic/Spatial Interpretation

A different approach than the one used for the other Reconstructions was necessary to identify the find spot of P0395a. The reasons for this are: a) the large number of fragments comprising lot P0395 and b) that they were retrieved from different locations of the 2011 excavation trench. To avoid plotting this fragment in an approximate location, each 'added event' relating to P0395 was investigated. 'Added events' are registered in the database with every addition of one or more sherds into a lot. P0395 had 20 such events related to different dates and dives.

The excavation areas of each of the added events for lot P0395 were investigated separately, resulting in 20 excavation/block areas being plotted in the 3DSM (Table 3). The volume of each excavation/block area was recreated by combining the point clouds of the top (i.e. ground level prior to excavation) and bottom (i.e. ground level after excavation) of each area into a single model in Rhinoceros 3D. Where point clouds were not available, photographs were used as a reference to model the levels.

Table 3: The plotting of the 20 block areas of lot P0395 (Reconstruction 06).

Block #: Date Dive	Description of event	Information on plotting process	Block inside the 3DSM
Block 1: 09/06/2011 Dive 3	Two sherds were recovered.	3D block based on point clouds: 2011-06-06-07 (top surface) and 2011-06-09-10 (bottom surface).	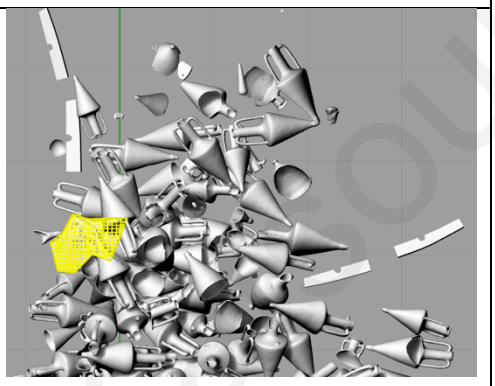
Blocks 2 & 3: 09/06/2011 Dive 5	Four handles and fifteen sherds were recovered. One sherd and one part of a rim were recovered.	3D block based on photographs from 2011-06-09-05 (top surface) and 2011-06-09-10 point cloud (bottom surface).	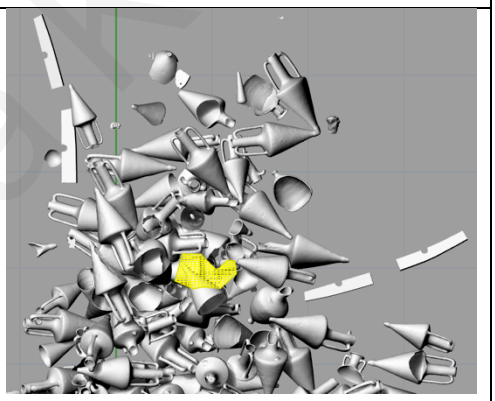
Block 4: 09/06/2011 Dive 6	Two sherds were recovered.	3D block based on point clouds: 2011-06-06-07 (top surface) and 2011-06-09-10 (bottom surface).	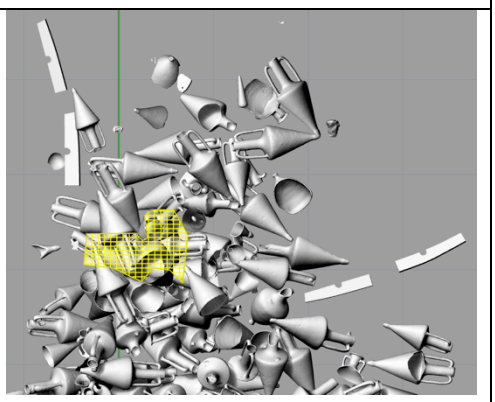

Blocks 5 & 6: 09/06/2011 Dive 7	Seventeen sherds were recovered. One handle and six sherds were recovered.	Corresponds to the same area as Block 4.	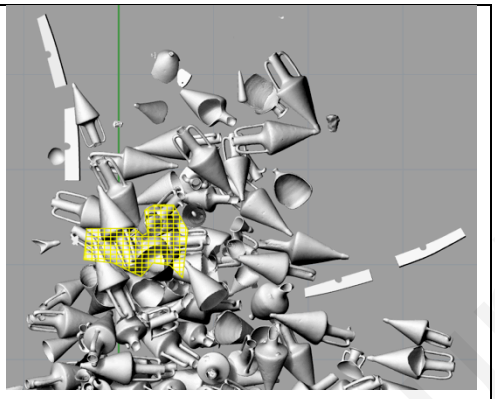
Block 7: 09/06/2011 Dive 9	Seven sherds were recovered.	Corresponds to the same area as Block 4.	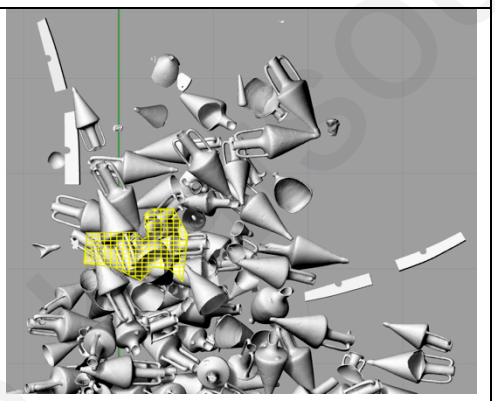
Block 8: 15/06/2011 Dive 1	Eleven sherds, one Chian amphora toe, one neck fragment and one shoulder fragment preserving the genesis of a handle, were recovered.	3D block based on point clouds: 2011-06-09-10 (top surface) and 2011-06-15-08 (bottom surface).	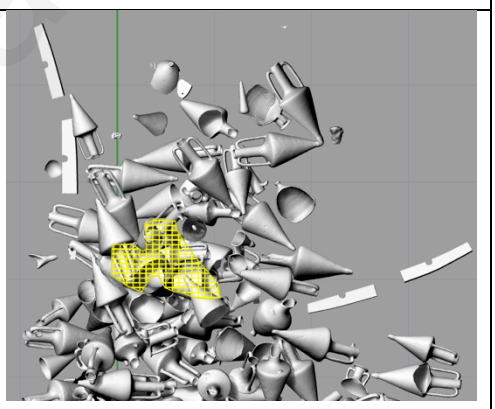
Block 9: 15/06/2011 Dive 3	Three sherds and one handle fragment were recovered.	3D block based on point clouds: 2011-06-09-10 (top surface) and 2011-06-15-08 (bottom surface).	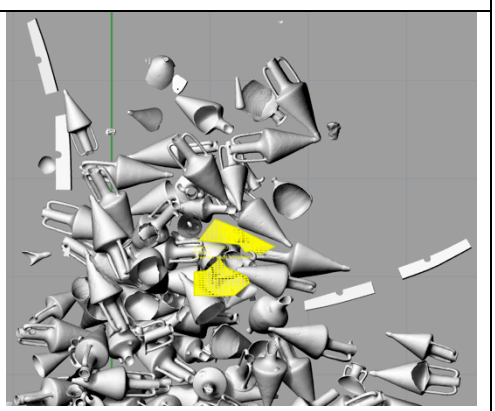

Block 10: 15/06/2011 Dive 4	Two sherds were recovered.	3D block based on point clouds: 2011-06-09-10 (top surface) and 2011-06-15-08 (bottom surface).	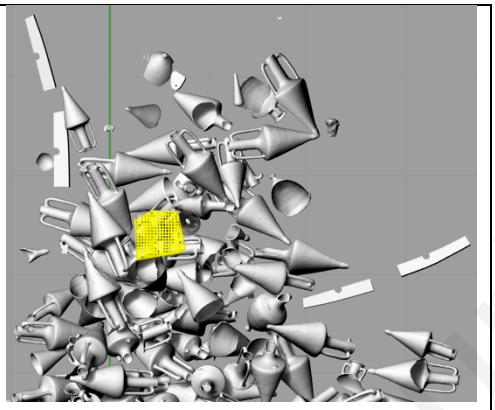
Blocks 11 & 12: 15/06/2011 Dive 7	Three sherds were recovered. Four sherds, *two neck fragments* and one handle fragment were recovered.	3D block based on the point clouds: 2011-06-09-10 (top surface) and 2011-06-15-08 (bottom surface). **Note: The two neck fragments were plotted as an approximate CAD model, after being identified as P0395c-d of Reconstruction 11.**	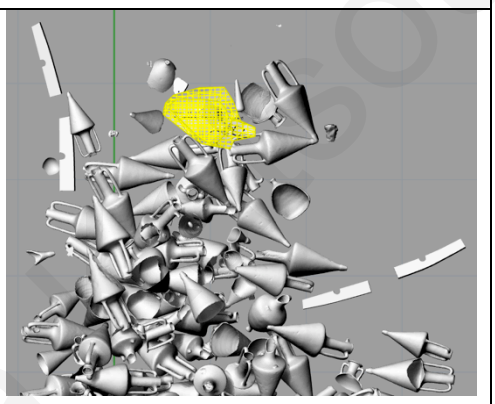
Block 13: 16/06/2011 Dive 4	Seven sherds and two neck fragments were recovered.	3D block based on the point clouds: 2011-06-16-02 (top surface) and 2011-06-17-08 (bottom surface).	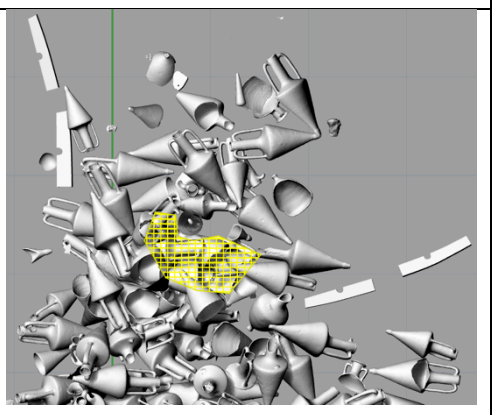

Block 14: 16/06/2011 Dive 9	*One Chian amphora handle* was recovered.	This fragment was plotted as an approximate CAD model. **Note: Fragment was identified as P0395b of Reconstruction 11.**	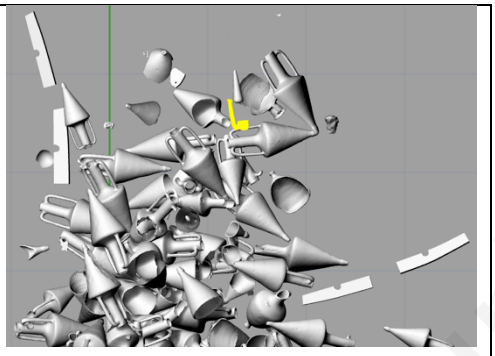
Block 15: 17/06/2011 Dive 3	Five sherds were recovered.	3D block based on point clouds: 2011-06-16-02 (top surface) and 2011-06-17-08 (bottom surface).	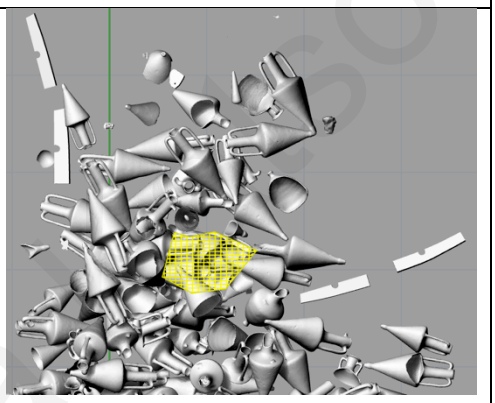
Block 16: 17/06/2011 Dive 4	One sherd was recovered.	3D block based on point clouds: 2011-06-16-02 (top surface) and 2011-06-17-08 (bottom surface).	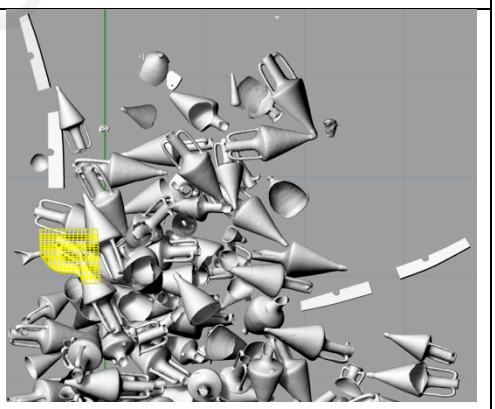
Block 17: 18/06/2011 Dive 2	One sherd was recovered.	3D block based on photographs from dates: 2011-06-17-09 (top surface) and 2011-06-19-01 (bottom surface).	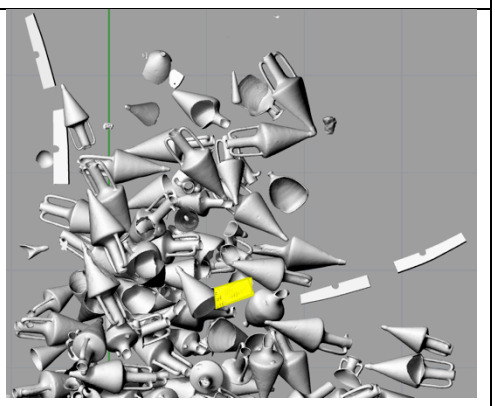

Block 18: 19/06/2011 Dive 4	Two sherds were recovered.	3D block based on point clouds: 2011-06-19-01 (top surface) and 2011-06-21-02 (bottom surface).	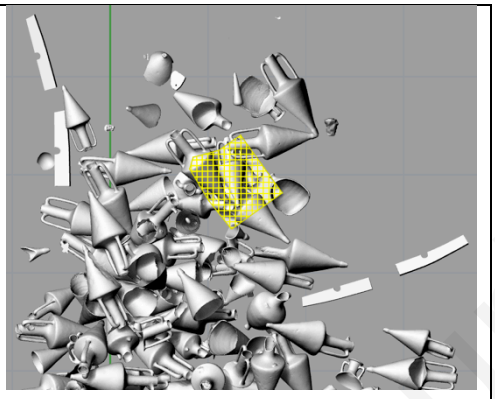
Block 19: 19/06/2011 Dive 8	One handle fragment, one shoulder fragment and three sherds were recovered.	3D block based on point clouds: 2011-06-19-01 (top surface) and 11-06-21-02 (bottom surface).	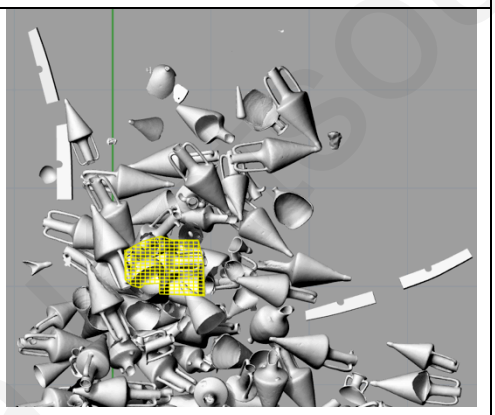
Block 20: 21/06/2011 Dive 3	Five sherds were recovered.	A 3D surface of this block was created based on the point cloud 2011-06-21-02.	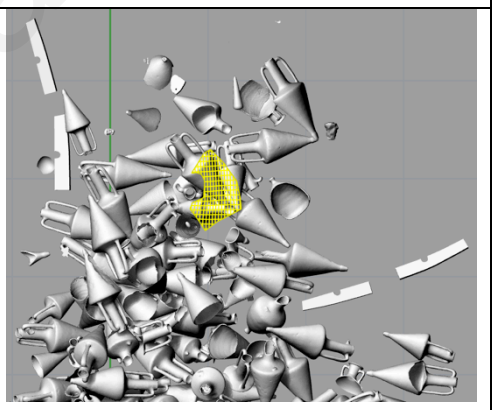

The plotting of the 20 excavation/block areas enabled a more efficient search for P0395a through the project's photographic and video archive. The only information found was in underwater photographs depicting the fragment in question in a displaced location – near the unexcavated area of the trench-grid fixed point T1 (Fig. 41). This displacement was likely caused by divers collecting sherds for recovery. As a result, the accurate plotting of this fragment was not feasible and so it was not added to the 3DSM.

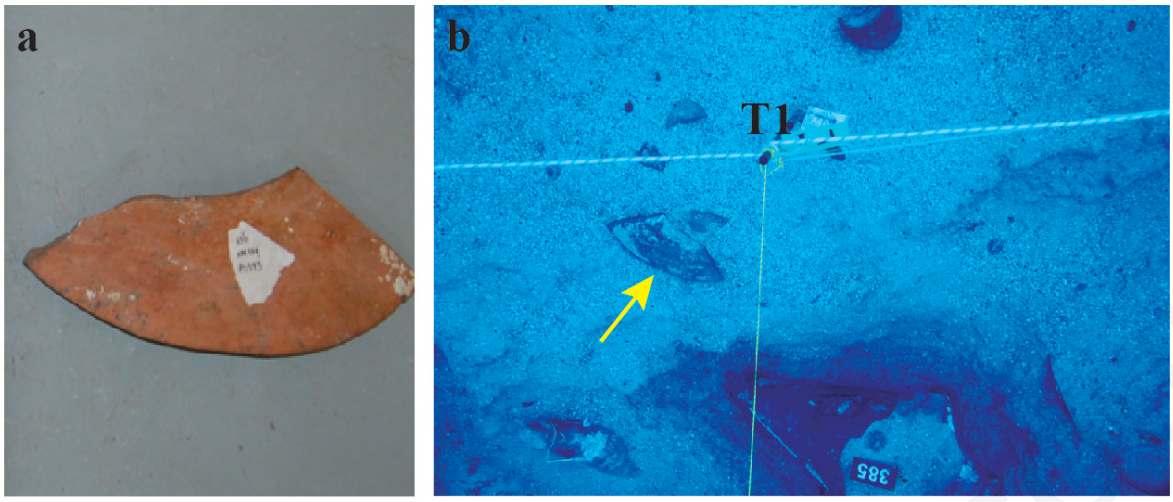

Figure 41: a) P0395a only appears in b) a displaced location in the underwater photographs.

(iii) Spatial Analysis: Detecting Spatial and Temporal Permutations

Even though P0395a was not plotted in the 3DSM because its *in situ* position was not precisely identified, it was possible to identify its location area, close to the artefact it belongs to (P0357). Thirteen of the twenty investigated blocks (blocks: 2-10, 13, 15, 17 and 19) correspond to an area nearby P0357, hence this fragment has a 65% probability of having been deposited near the artefact to which it belongs (Fig. 42).

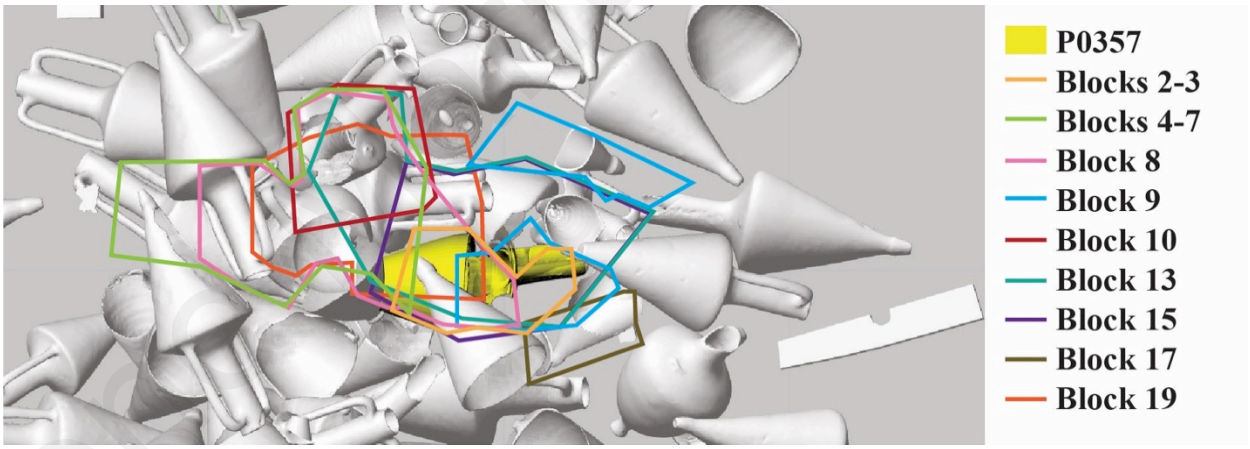

Figure 42: The delineated thirteen blocks and their proximity to P0357.

The only added events that explicitly mention shoulder fragments in their descriptions are: blocks 8 and 19; these blocks correspond to roughly the same excavated area and depth and are in close proximity to P0357 (Fig. 43).

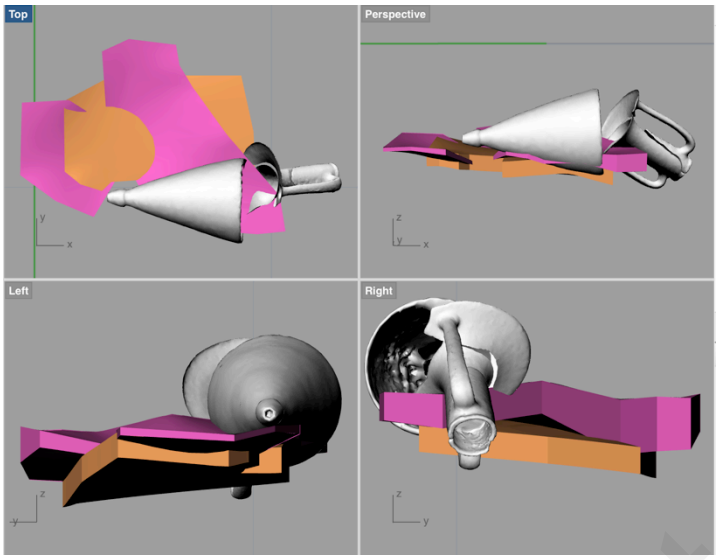

Figure 43: Blocks 8 (pink) and 19 (orange) and their spatial relation to P0357.

P0357's location, along with that of other specific amphorae (Fig. 44), was identified and described by Demesticha et al. (2014: 147), as: "…found broken *in situ* in a disturbed, but not entirely disordered position. The amphorae were found at a distance of 1m west from, and parallel to, the keel. They were broken in half with their lower part still standing *in situ* in an upright position. The amphorae behind this line were lying on their sides, with their neck among the standing lower halves. This situation may be indicative of the wreckage episode or a phase of the deterioration of the ship's hull".

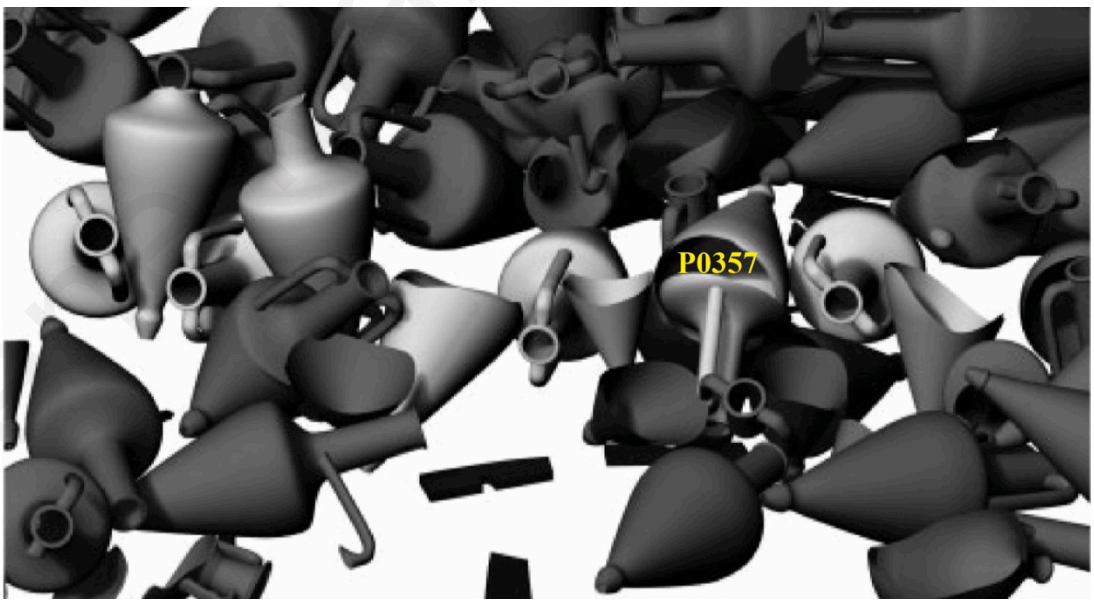

Figure 44: The arrangement of specific amphorae, shown in light gray color, may be indicative of the sudden displacement of the deck after the crash of the bow on the seabed (based on Demesticha et al. 2014, Fig. 12).

It stands to reason that the fragment P0395a was retrieved from one of the aforementioned area blocks, deposited in close proximity to the artefact it belongs to. A more precise pinpointing of this fragment's *in situ* location would assist in determining whether this sherd broke off *before* the remaining artefact (P0357) came to rest in its excavated position or whether it broke off during the same event which caused P0357 to be separated into two parts, i.e. the wrecking event.

Reconstruction 07: A possibly Lycian Amphora reconstructed of three pieces P0314 – P0292e-f

(i) Brief description of the finds involved

Two sherds from lot P0292 (named P0292e-f) recovered in 2010 were joined by the conservators to a lower-body fragment of an amphora tentatively identified as Lycian (P0314) lifted in 2011 (Fig. 45).

Figure 45: P0314 during its reconstruction (photograph provided courtesy of the Department of Antiquities).

(ii) Stratigraphic/Spatial Interpretation

The ten fragments contained in lot P0292 were retrieved north of the anchor core M0309.

(iii) Plotting in the 3DSM

The vector outlines of P0292e and P0292f were plotted in the 3DSM using the CAD realigned 2010-05-25-06 point cloud (Figs. 46, 47 and 48). Although P0292e did not appear fully excavated in any underwater photograph, its mapping was possible by firstly identifying the *in situ* location of P0292f and other sherds from lot P0292.

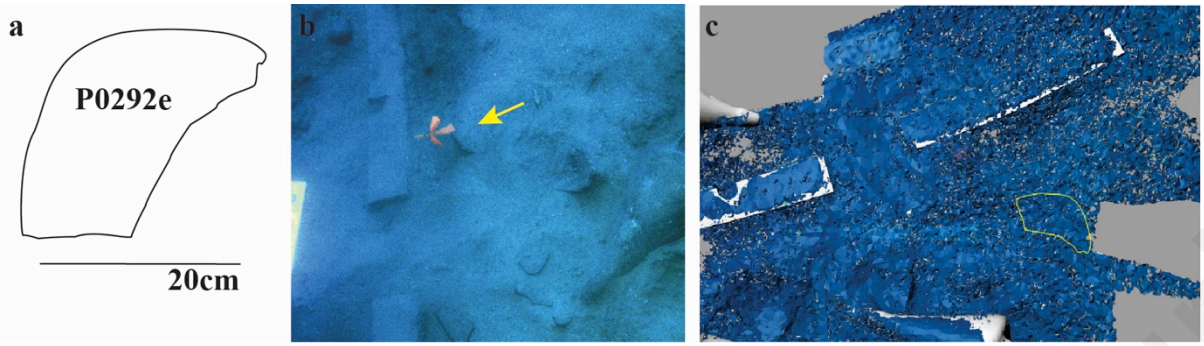

Figure 46: a) The outline drawing of P0292e, b) its suspected *in situ* location and c) subsequent plotting in the 3DSM.

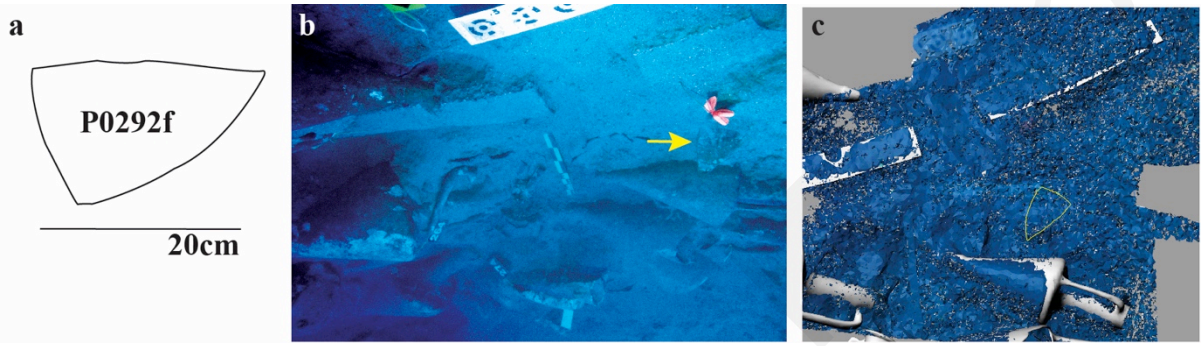

Figure 47: a) The outline drawing of P0292f, b) its *in situ* location and c) subsequent plotting in the 3DSM.

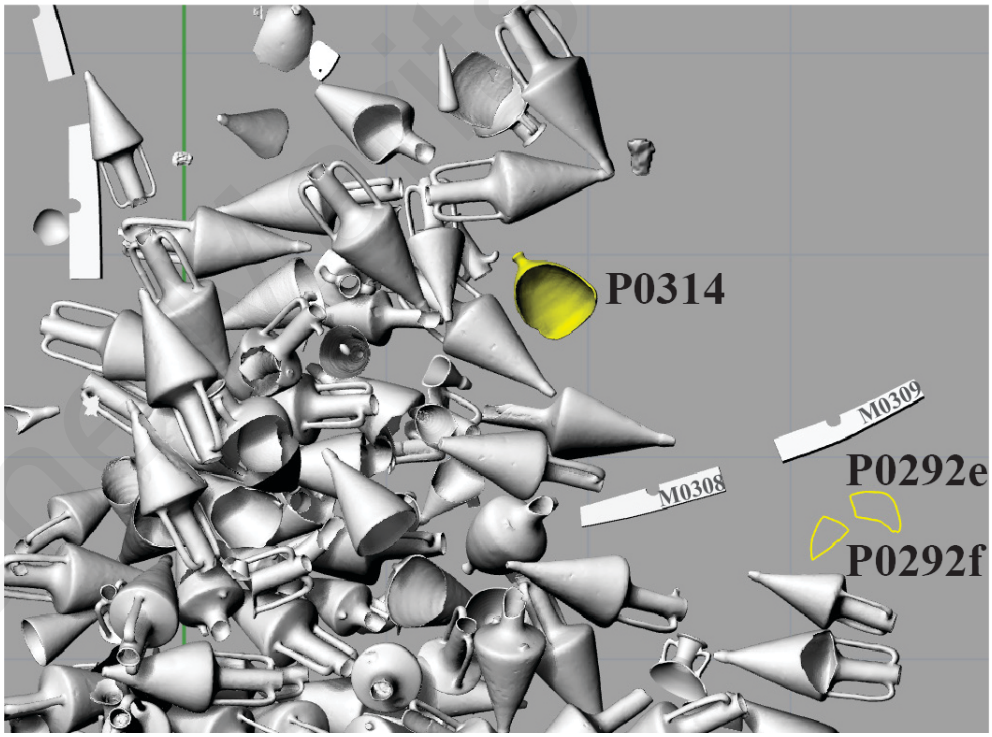

Figure 48: Reconstruction 07: the two fragments that were joined to P0314, inside the 3DSM.

(iv) Spatial Analysis: Detecting Spatial and Temporal Permutations

This Reconstruction is discussed below, alongside Reconstruction 08.

Reconstruction 08: A South - Aegean Amphora (Mushroom Rim - Knob Toe) reconstructed of sixteen pieces P0310 – P0295 – P0282a – P0293a-i – P0292a-d

(i) Brief description of the finds involved

As part of this Reconstruction, the conservators were able to associate fifteen fragments with the same artefact as P0310 – an upper part of a Mushroom-Rim amphora (Fig. 49). Only five (P0295 and P0293e-h) of the aforementioned fifteen fragments were physically joined to P0310 (Fig. 49b). Four sherds (P0293a-c and P0282a) were joined together to form one large amphora body fragment (Fig 49c), whilst another set of five sherds (P0292a-d and P0293d), formed a second large body fragment (Fig. 49d). Lastly, the conservators believe that the toe fragment from lot P0293 (P0293i) also belongs to this Mushroom-Rim amphora (Fig. 49e).

Figure 49: All the fragments involved in Reconstruction 08 and belonging to the same artefact as P0310 (photographs b and d, provided courtesy of the Department of Antiquities).

(ii) Stratigraphic/Spatial Interpretation

P0295 is a sherd broken in two, retrieved south of the anchor cores M0308 and M0309. The twenty-eight fragments comprising lot P0293 were discovered around amphora P0283 and north-east of anchor core M0308, whereas the three fragments of lot P0282 were found just east of M0308. Lastly, the ten sherds of lot P0292 were retrieved north of the anchor core M0309.

(iii) Plotting in the 3DSM

The vector outline drawings for P0295 and P0293e-h, were plotted in the 3DSM using the CAD realigned 2010-05-25-06 point cloud (Figs. 50 and 51). In the case of P0293e-h however, these sherds could not be conclusively identified underwater as no photographs depicted them in a fully excavated state. In order to overcome this obstacle and to ensure the best possible plotting results, other artefacts from lot P0293 were studied and located underwater.

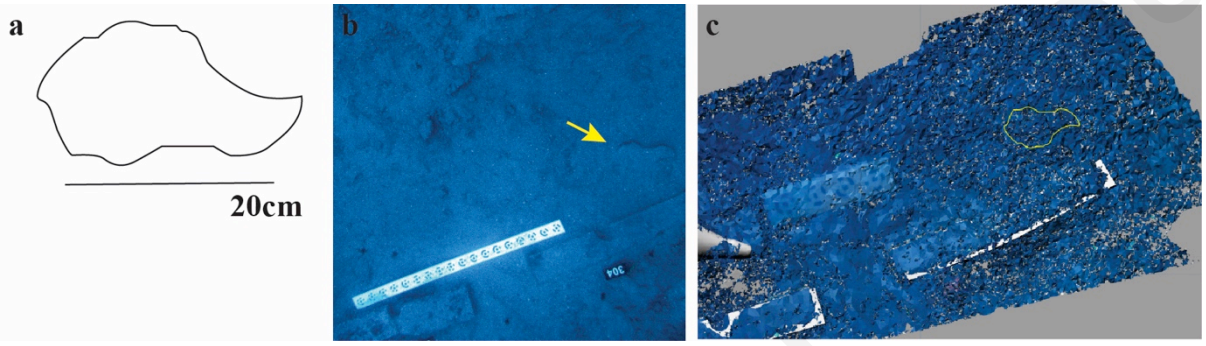

Figure 50: a) The outline drawing of P0295, b) its *in situ* location and c) subsequent plotting in the 3DSM.

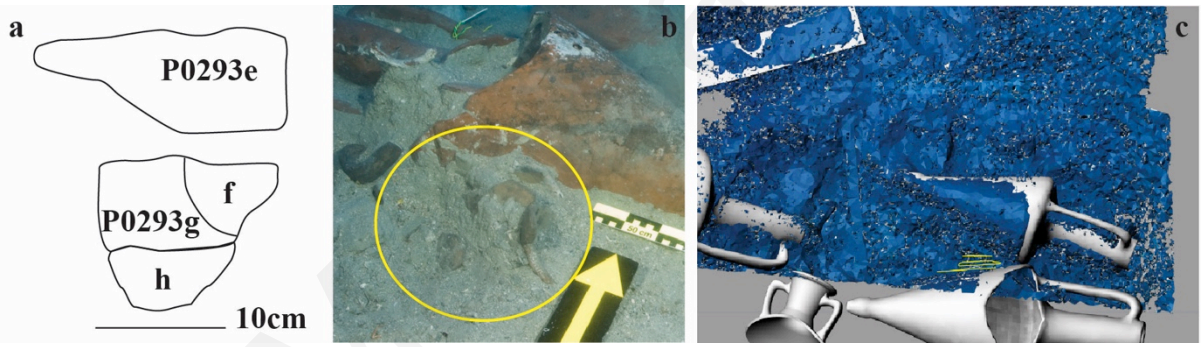

Figure 51: a) The outline drawings of P0293e-h, b) their suspected *in situ* location and c) subsequent plotting in the 3DSM.

The individual vector drawing of each of the four sherds, P0293a-c and P0282a, was plotted in the 3DSM according to the CAD realigned 2010-05-25-06 point cloud and faithful to their database description (Figs. 52, 53 and 54). However, as P0293a and P0282a were not fully visible in the underwater photographs, the *in situ* position of other sherds from their respective lots was traced, to ensure their most accurate mapping.

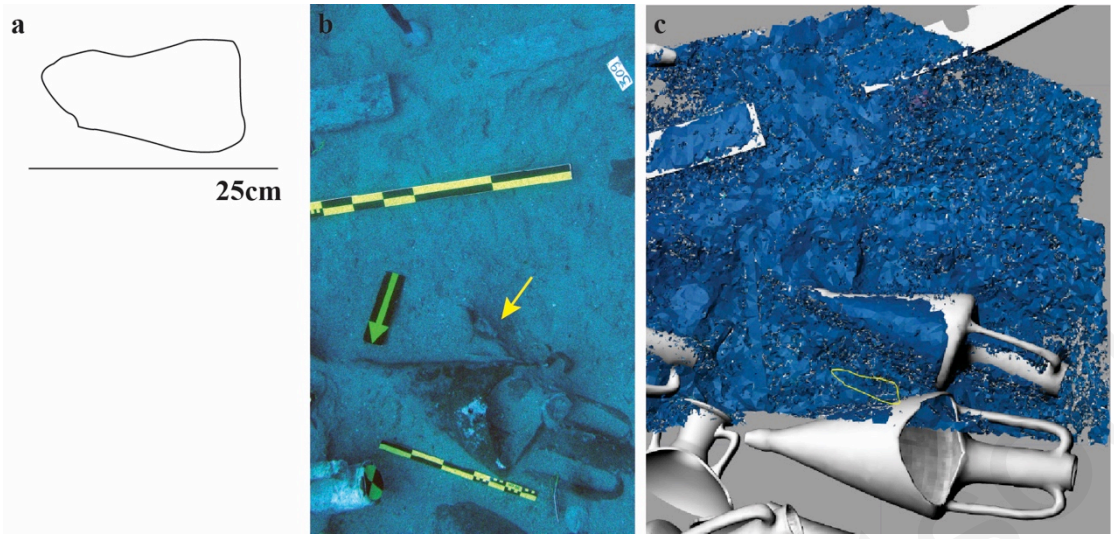

Figure 52: a) The outline drawing of P0293a, b) its suspected *in situ* location and c) subsequent plotting in the 3DSM.

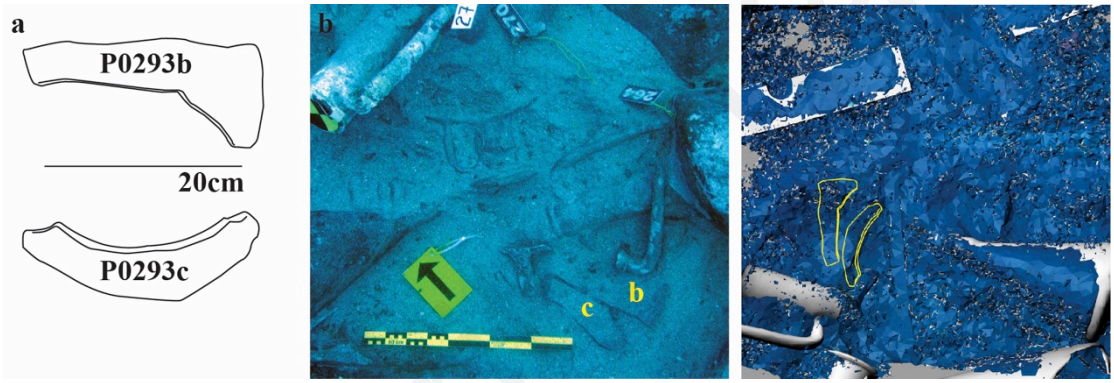

Figure 53: a) The outline drawings of P0293b-c, b) their *in situ* location and c) subsequent plotting in the 3DSM.

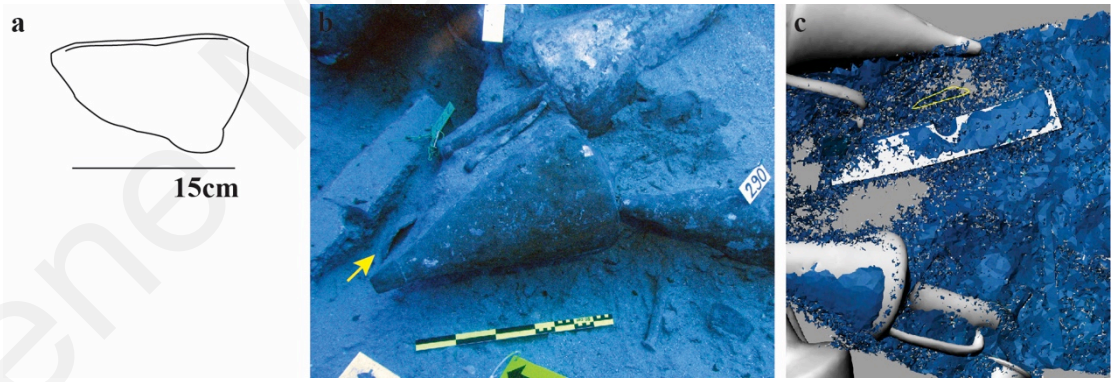

Figure 54: a) The outline drawing of P0282a, b) its suspected *in situ* location and c) subsequent plotting in the 3DSM.

The sherds P0292a-d and P0293d were discovered close to each other in the area north of the anchor stock M0308 and their vector outlines were plotted in the 3DSM according to the CAD realigned 2010-05-25-06 point cloud (Figs. 55 and 56).

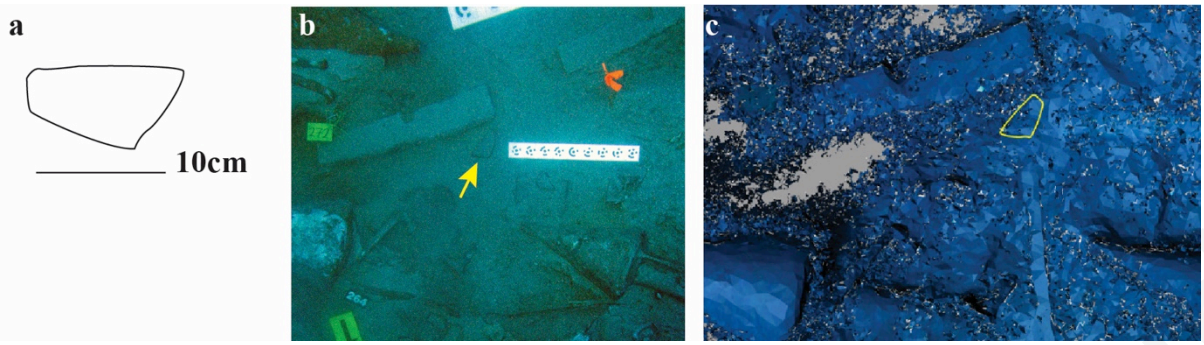

Figure 55: a) The outline drawing of P0293d, b) its *in situ* location and c) subsequent plotting in the 3DSM.

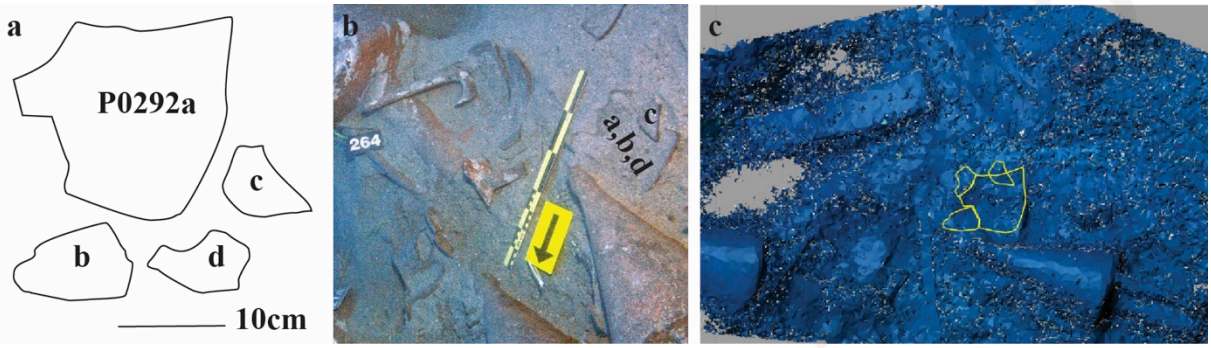

Figure 56: a) The outline drawings of P0292a-d, b) their *in situ* location and c) subsequent plotting in the 3DSM.

The toe fragment (P0293i) was also pinpointed underwater and plotted in the 3DSM using the CAD realigned 2010-05-25-06 point cloud (Fig. 57). Thus all fifteen fragments were plotted in the 3DSM (Fig. 58).

Figure 57: a) The outline drawing of P0293i, b) its *in situ* location and c) subsequent plotting in the 3DSM.

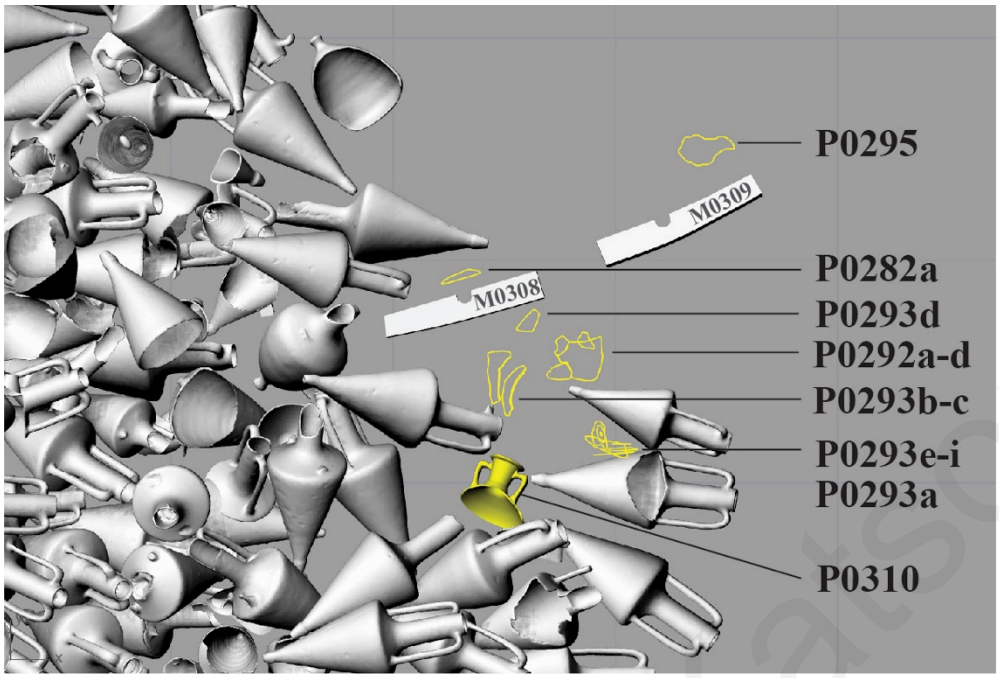

Figure 58: Reconstruction 08: the fifteen fragments that were joined to P0310, inside the 3DSM.

(iv) Spatial Analysis of Reconstructions 07-08: Detecting Spatial and Temporal Permutations

The plotting process of Reconstruction 07 made evident the fact that whilst P0314 was found south of the two anchor stocks (M0308 and M0309), the two sherds (P0292e-f) were recovered from the area north of them (Fig. 59a). Furthermore, plotting the sherds inside the 3DSM, demonstrated that the two sherds were deposited at a similar depth to the anchor stocks M0308 and M0309 (Fig. 59b).

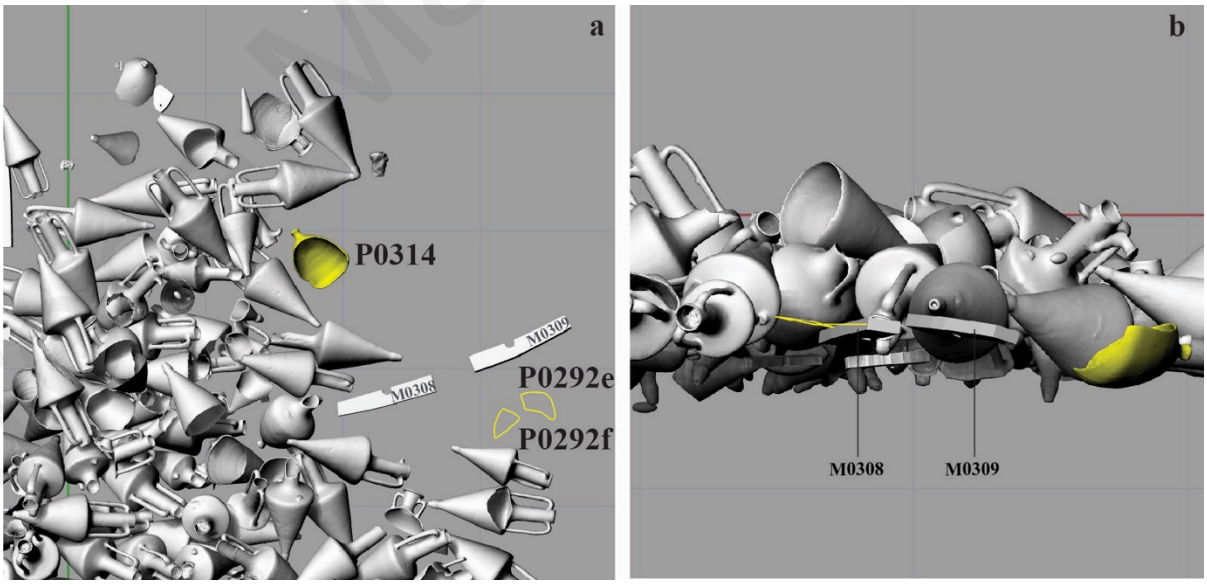

Figure 59: Reconstruction 07: the fragments of P0314, were found at a similar depth to the anchor stocks (M0308 and M0309).

Viewing Reconstruction 08 in the 3DSM, we again see that whilst P0310 and the majority of sherds belonging to it were retrieved north of the anchor stock M0308, this is not the case for P0295 and P0282a; the first found south of the anchor stock M0308 and the other south of M0309 (Fig. 60a). Additionally, similarly to the artefacts involved in Reconstruction 07, the fifteen fragments and P0310 were also deposited at a similar depth to the anchor stocks (Fig. 60b).

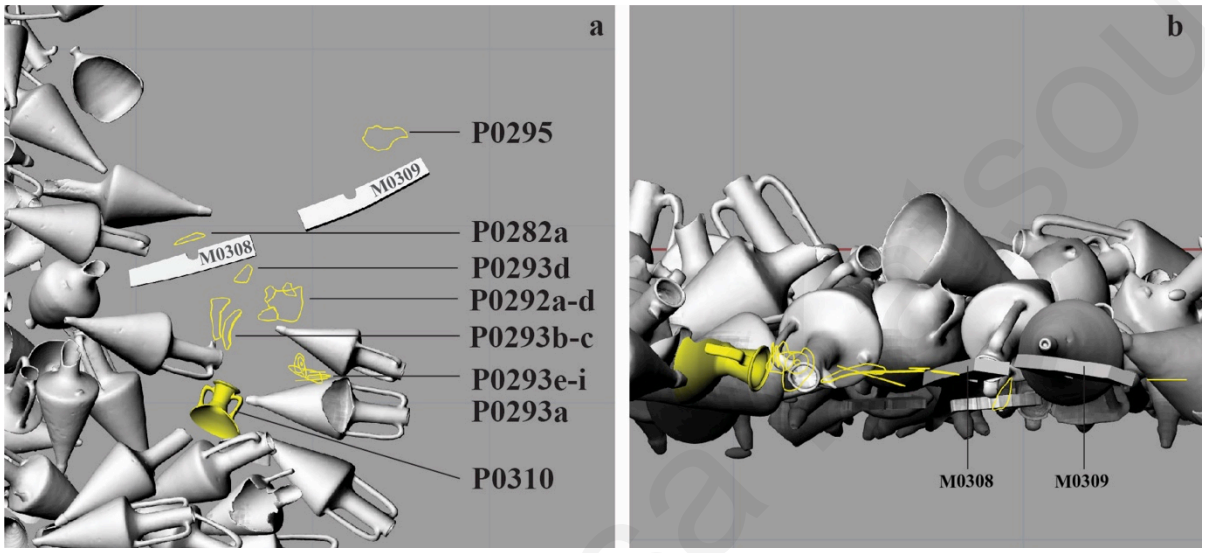

Figure 60: Reconstruction 08: the fragments of P0310, were found at a similar depth to the anchor stocks (M0308 and M0309).

P0310 and P0314 as well as their respective fragments, were retrieved from the starboard side - the side on which the ship tilted - as well as from one of the assemblage extremities. The situation at the most southern end of the assemblage of which P0314 is part, is indicative of a deterioration phase of the vessel's front part; exacerbated by the weight of the two large anchors (one on the port side and the other on the starboard), a section of the bow deteriorated to the point of breaking open and tipping towards the southwest, thus explaining the disordered disposition of a number of finds. In contrast, at the north-western part of the bow, artefacts (including P0310) have spilled off the main assemblage but in a more ordered fashion, after the starboard hull collapsed (Demesticha 2021: 47).

As certain artefacts and sherds from the two aforementioned areas and the anchor stocks area were deposited at a similar depth, the provoking events (i.e. the hull deterioration at the fore of the bow, the starboard hull collapse and the deposition of the starboard large anchor) are perhaps linked and may have happened concurrently or in quick succession. Undoubtedly this is a hypothetical scenario, based on a fraction of the available evidence, hence requiring further scrutiny.

Reconstruction 09: A Chian Amphora reconstructed of three pieces P0263 – P0333a-b

(i) Brief description of the finds involved

Two small neck fragments (named P0333a and P0333b) were reassembled to P0263, a Chian amphora missing most of its neck and both handles (Fig. 61). The two sherds came from lot P0333 (thirty-five sherds retrieved through sieving).

Figure 61: P0263 during its reconstruction (photograph provided courtesy of the Department of Antiquities).

(ii) Stratigraphic/Spatial Interpretation

The sherds comprising lot P0333 were retrieved from the area below a fully buried Chian amphora, P0270.

(iii) Plotting in the 3DSM

The vector drawings of P0333a-b were plotted in the 3DSM, placed between the trench (ground) level closest to their retrieval date (CAD realigned 2010-06-03-02 point cloud) and the photogrammetric model of P0270 (Figs. 62 and 63).

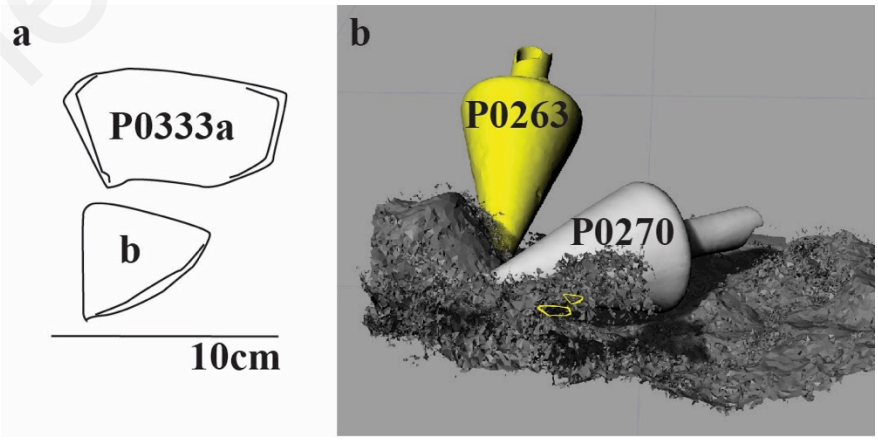

Figure 62: a) The outline drawings of P0333a-b, plotted between P0270 and the trench (ground) level as documented in the CAD realigned 2010-06-03-02 point cloud (b).

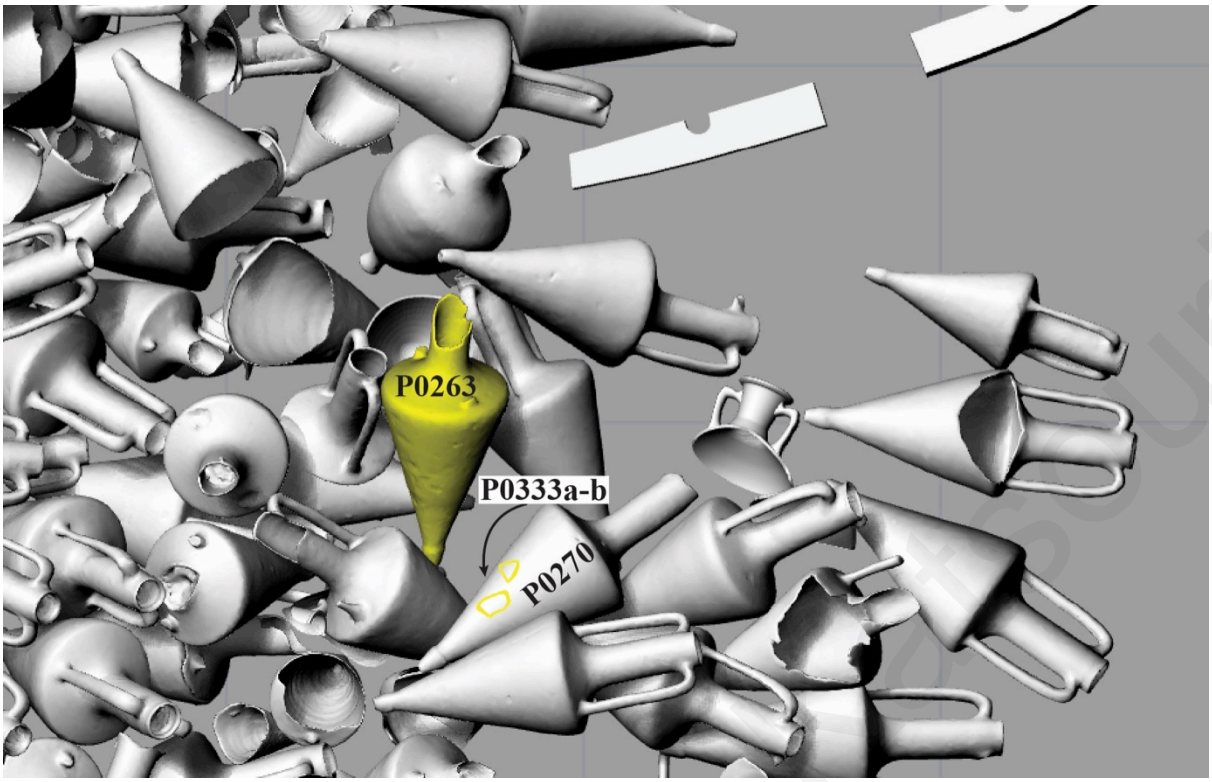

Figure 63: Reconstruction 09: the two fragments that were joined to P0263, in the 3DSM.

(iv) Spatial Analysis: Tracing the sequence of depositions

This Reconstruction is discussed below, alongside Reconstruction 10.

Reconstruction 10: A Chian Amphora reconstructed of two pieces P0290 – P0362

(i) Brief description of the finds involved

The conservators adhered a handle fragment (P0362) to a Chian amphora (P0290), resulting in its complete reconstruction (Fig. 64).

Figure 64: P0290 during its reconstruction (photograph courtesy of the Department of Antiquities).

(ii) Stratigraphic/Spatial Interpretation

The handle fragment (P0362) was found deposited underneath the toe of the Chian amphora, P0312 (Fig. 65b).

(iii) Plotting in the 3DSM

The photogrammetric model of P0362 was plotted in the 3DSM using the CAD realigned 2011-05-26-06 point cloud, underneath the toe of amphora P0312 (Fig. 65).

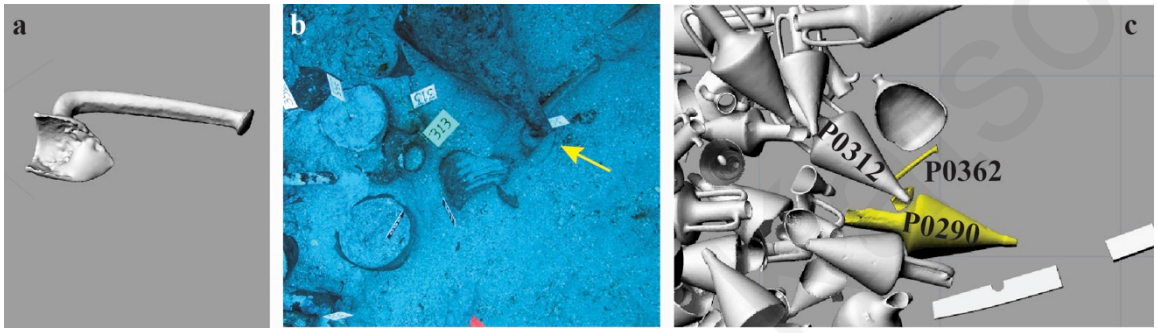

Figure 65: a) The photogrammetric model of P0362, b) its *in situ* location and c) subsequent plotting in the 3DSM near the amphora it belongs to: P0290.

(iv) Spatial Analysis of Reconstructions 09-10: Tracing the sequence of depositions

As part of Reconstruction 09, two small neck fragments (P0333a-b) retrieved from underneath P0270, were attached by the conservators to P0263; all three artefact numbers were found in the north-western part of the bow area (Fig. 66).

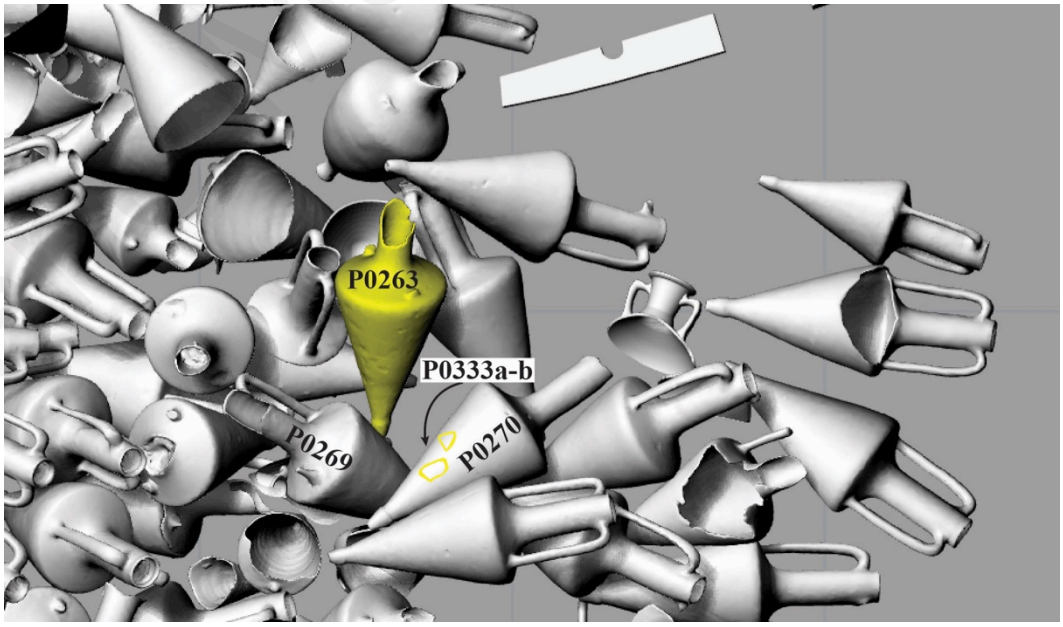

Figure 66: Reconstruction 09: the two small neck fragments (P0333a-b) found underneath P0270, were joined to P0263.

As Demesticha (2021: 45) describes: “The fact that the ship listed to its starboard side after it reached the seafloor is demonstrated by the position of the amphorae on the western (starboard) side; most of them are inclined outwards along the entire assemblage, from bow to stern. Some have been found away from the main concentration lying on their sides, possibly having come from the higher tiers and having fallen on the seabed when the exposed parts of the hull decayed”.

From the 3DSM it was possible to ascertain that the two sherds (P0333a-b) were found approximately 43cm lower and 75cm away from the neck of P0263, to which they were joined during conservation (Fig. 67). In line with the above and from the spatial analysis of this Reconstruction, it can be inferred that the wrecking event and the starboard tilting of the ship, caused P0263 (from a more upright and perhaps northern position) to move and collide with other artefacts, resulting in at least two sherds to break off and fall; P0263 then comes to rest in the position it was found. P0270 (originating perhaps from a more eastern and higher position) also shifts for the same reason and ends up falling on top of the two sherds; P0269 also shifts but in an opposite direction to P0270 (from being more upright in a more western location, to fall towards the east). It might also be the case that either the movement of P0269 or P0270 caused the two fragments (P0333a-b) to break off P0263.

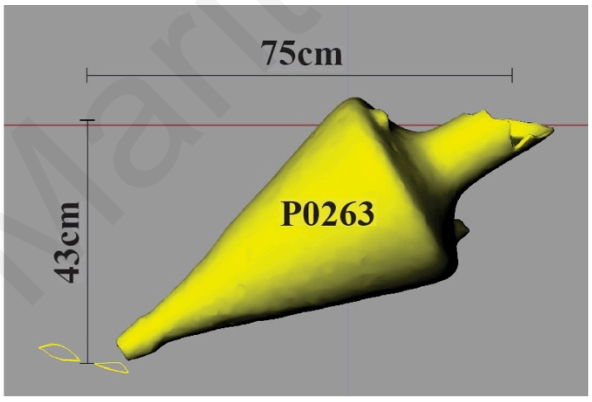

Figure 67: P0333a-b were retrieved approximately 43cm lower and 75cm away from the neck of P0263, to which they belong.

The conservation work relating to Reconstruction 10, resulted in associating the handle fragment (P0362) to the artefact it belongs, i.e. the Chian amphora P0290. The handle was deposited under the toe of P0312, which in turn was deposited below other amphorae: P0277, P0252, P0368 (Fig. 68). This Reconstruction and the spatial proximity between P0290 and its broken handle, essentially add a preceding event to this chain of depositions:

1. The handle (P0362) breaks off P0290, either because the latter hit or was hit by something.

2. As both artefacts were deposited close to each other, their breaking event must have occurred close to the area of their final deposition.

3. Then, the aforementioned sequence of events takes place: P0312 is deposited above P0362 and in turn, the other three artefacts are deposited on top of P0312.

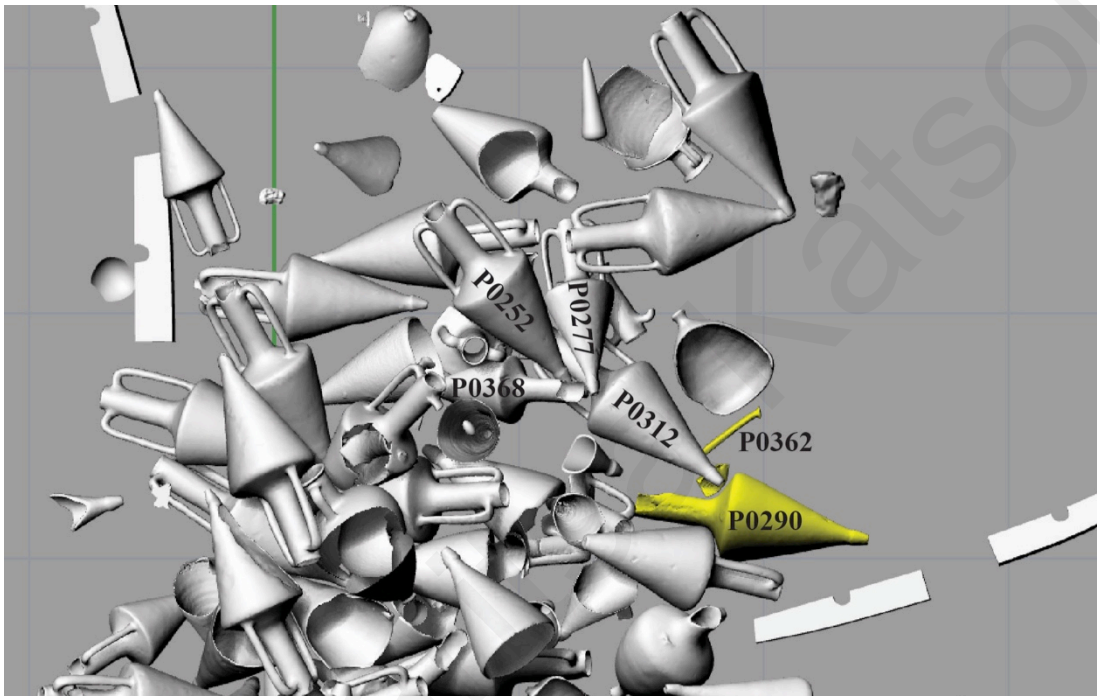

Figure 68: P0362 was joined to P0290 as part of Reconstruction 10. P0362 was deposited underneath the toe of P0312. P0277, P0252 and P0368 are deposited on top of P0312.

If the handle had broken off P0290 after or because it was hit by P0312, then the latter must have rolled over P0290, along with other amphorae that were found next to or over it. This supports Demesticha's view (2020: 45) that the artefacts disorderly deposited at the fore end of the assemblage may have originated from the upper and side layers of the concentration.

Reconstruction 11: A Chian Amphora reconstructed of six pieces P0385 – P0404a – P0395b-d – P0353a

(i) Brief description of the finds involved

During this Reconstruction the conservators identified five fragments as belonging to a broken Chian amphora, P0385 (Fig. 69). These five fragments include: a toe fragment

(named P0404a), a large body fragment (named P0353a) and three fragments (named P0395b-d) from lot P0395.

Figure 69: The five fragments that were joined to P0385 during its reconstruction (photograph courtesy of the Department of Antiquities).

(ii) Stratigraphic/Spatial Interpretation

The P0404 lot of fragments was found inside a lower part of a Chian amphora (P0392). P0353a was lifted along with a Chian amphora lower part (P0353). The process of identifying the three fragments P0395b-d, underwater was facilitated by the block investigation of P0395, detailed in Reconstruction 06. More specifically, P0395b was found in the excavation area of block 14 (Table 3), whereas P0395c-d in blocks 11 and 12 (Table 3).

(iii) Plotting in the 3DSM

The vector outline drawing of P0404a was plotted inside the 3D model of P0392 (Fig. 70).

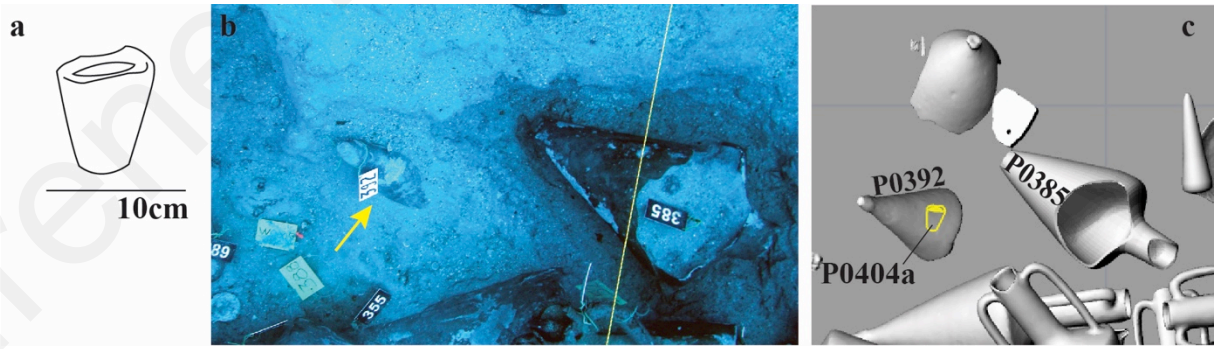

Figure 70: As P0404a was retrieved from inside P0392 (b), the outline drawing of this fragment (a) was plotted inside the 3D model of P0392 (c).

Fragment P0353a was added to the 3DSM, by plotting its outline drawing inside the 3D model of P0353 (Fig. 71).

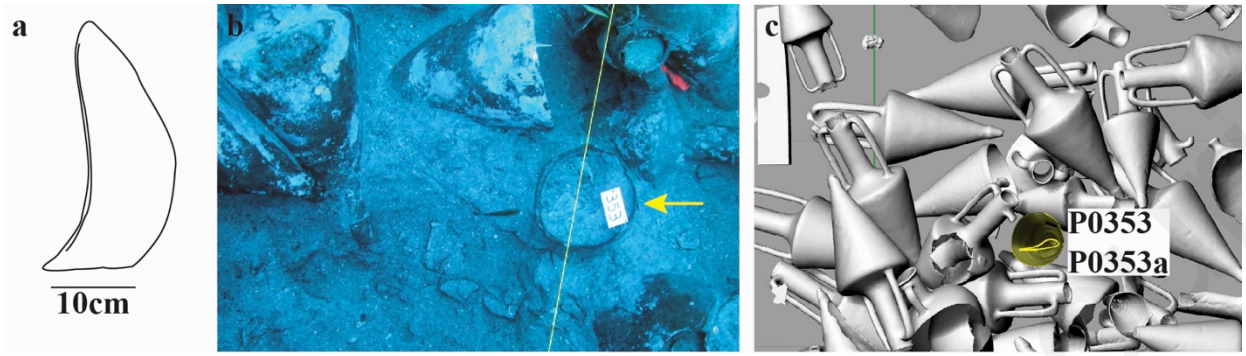

Figure 71: As P0353a was retrieved together with P0353 (b), the outline drawing of this fragment (a) was plotted inside the 3D model of P0353 (c).

Lastly, two approximate CAD models were created - one for P0395b and one for P0395c-d, and used for plotting these fragments next to the artefact they belong to, P0385 (Figs. 72 and 73). Thus all five fragments were plotted inside the 3DSM (Fig. 74).

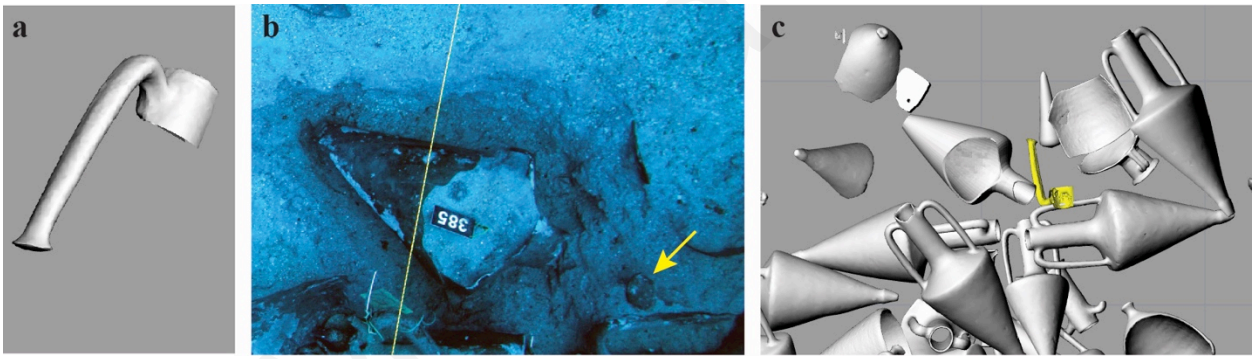

Figure 72: a) The approximate CAD model of P0395b, b) its *in situ* location and c) subsequent plotting in the 3DSM.

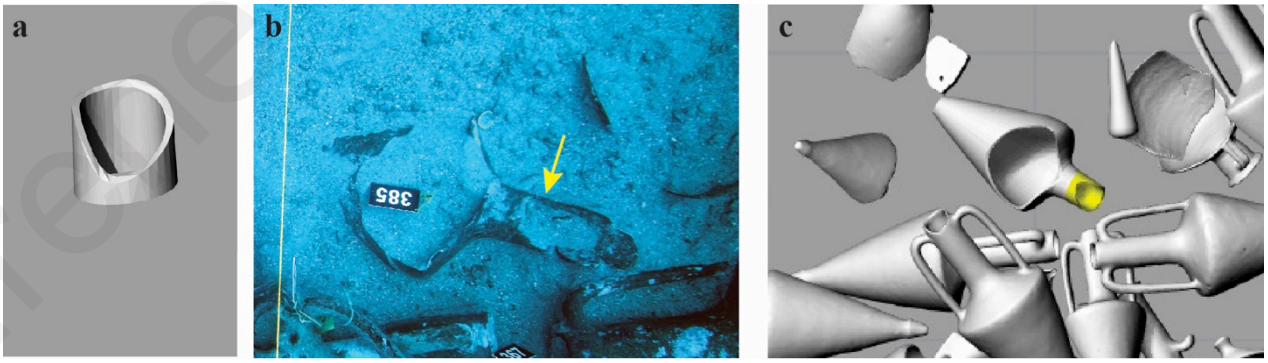

Figure 73: a) The approximate CAD model for P0395c-d, b) its *in situ* location and c) subsequent plotting in the 3DSM.

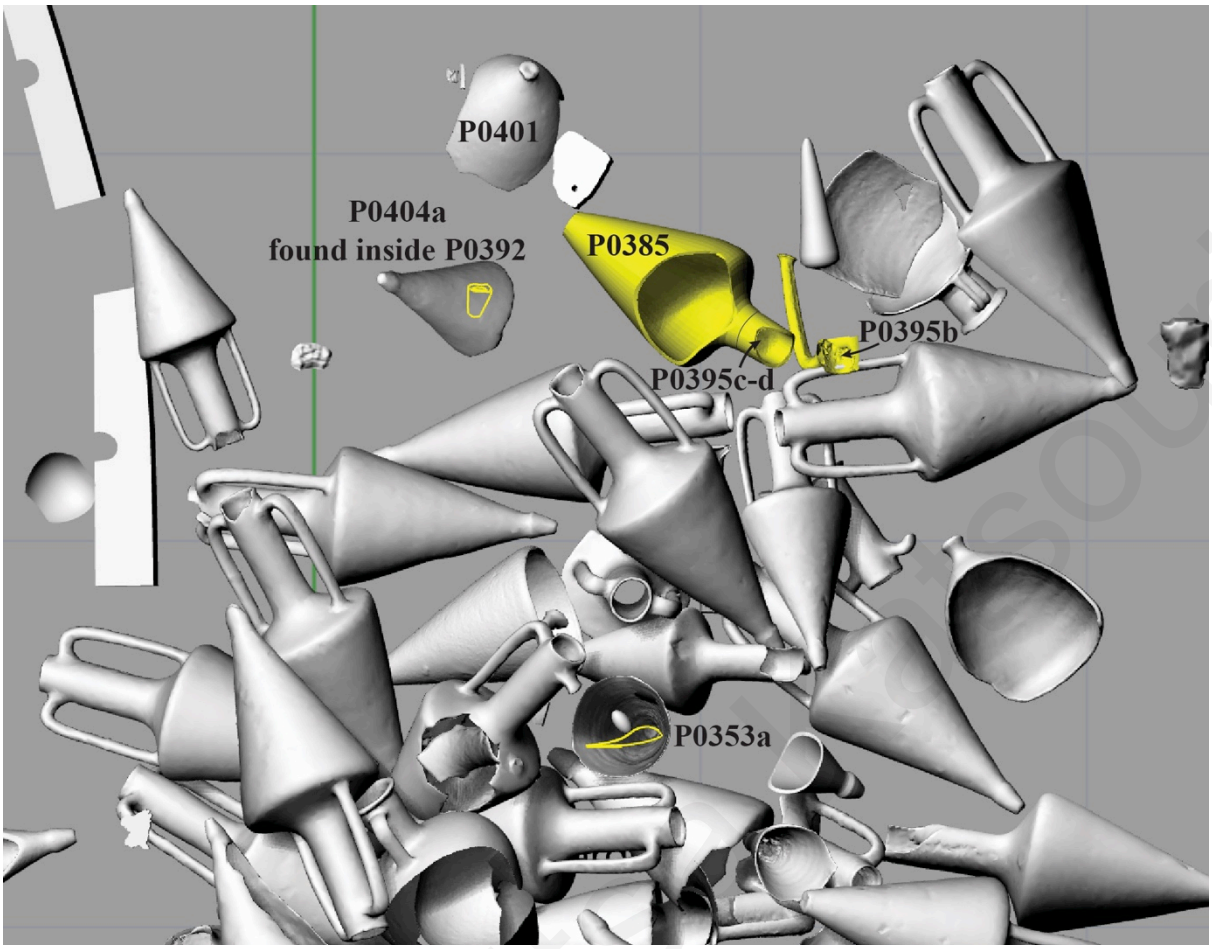

Figure 74: Reconstruction 11: the five fragments that were joined to P0385, in the 3DSM.

(iv) Spatial Analysis: Tracing previous locations

This Reconstruction is discussed below, alongside Reconstruction 12.

Reconstruction 12: A Coan Amphora reconstructed of six pieces P0384 – P0911a – P0844a – P0291a – P0395e-f - (P0401 discussed separately)

(i) Brief description of the finds involved

This Reconstruction resulted in five fragments being joined to P0384, a Coan amphora consisting of two large pieces and two sherds (Fig. 75). The five fragments include: a large body sherd (named P0911a), a body fragment (named P0844a), a fragment (named P0291a) from lot P0291 and two fragments (named P0395e-f) from lot P0395.

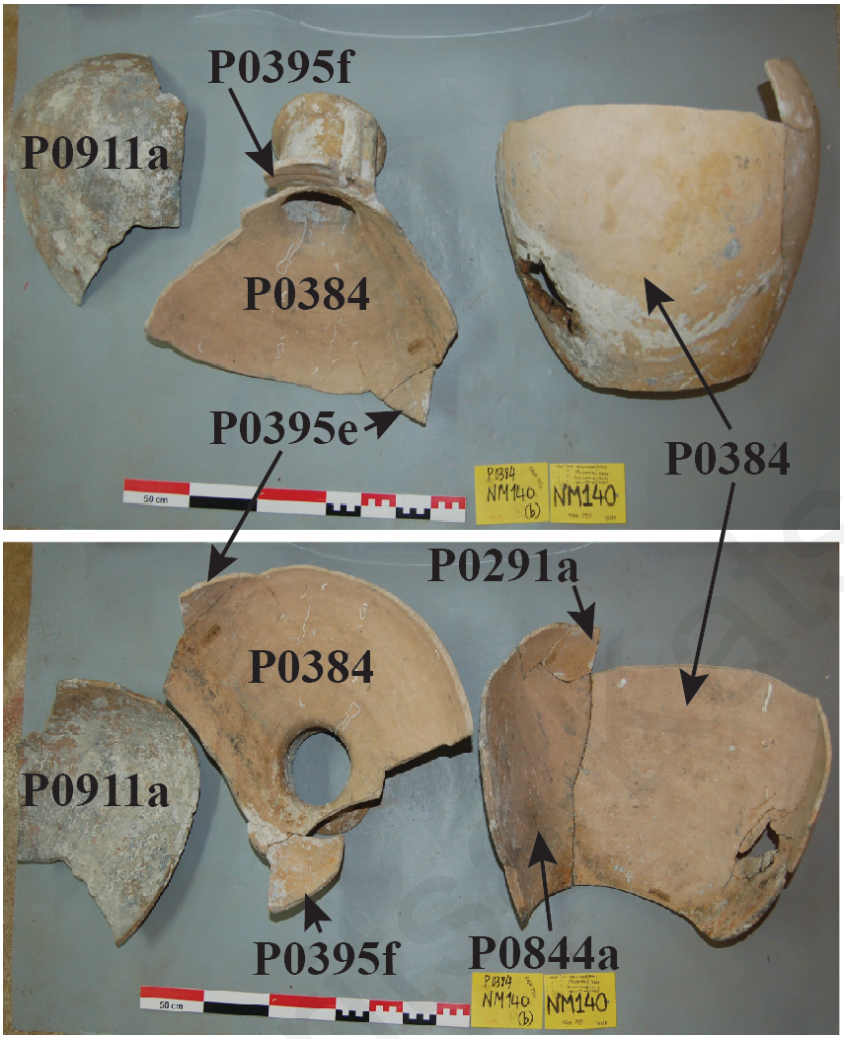

Figure 75: P0384 during its reconstruction (photographs courtesy of the Department of Antiquities).

(ii) Stratigraphic/Spatial Interpretation

P0911a was retrieved near the anchor stock M0004 (belonging to the port side anchor). P0844a was lifted in 2016 but had not been documented *in situ* either through photographs nor photogrammetry. Instead its *in situ* location was traced by reviewing underwater video footage, in which P0844a distinctive shape appears faintly distinguishable near the anchor stock M0004 (Fig. 77b). The third fragment (P0291a) was collected when a broken Chian amphora (P0291) was recovered. Lastly, the two fragments (P0395e-f) from lot P0395 were lifted from the 2011 excavation trench.

(iii) Plotting in the 3DSM

The first of these five fragments, P0911a was added to the 3DSM by plotting its approximate 3D model in its *in situ* location: close to the anchor stock M0004 (Fig. 76).

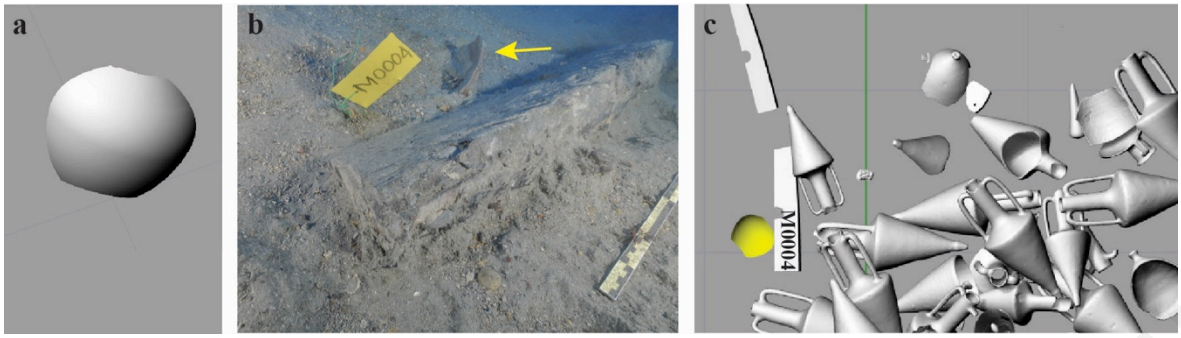

Figure 76: a) The approximate CAD model of P0911a, b) in its *in situ* location, close to M0004 and c) subsequent plotting in the 3DSM.

The vector drawing for the P0844a fragment was plotted, in its *in situ* location as seen in the video footage: close to the anchor stock M0004 (Fig. 77).

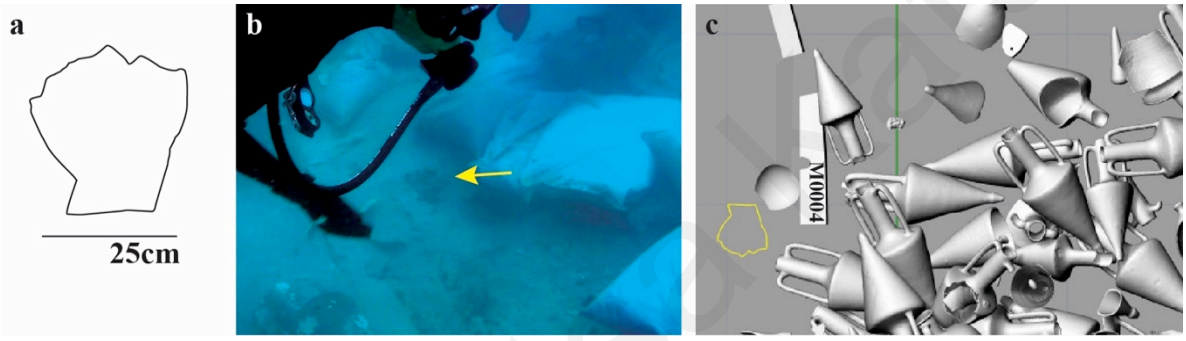

Figure 77: a) The outline drawing of P0844a, b) in its *in situ* location near M0004, according to video footage and (c) subsequent plotting in the 3DSM.

The outline drawing of P0291a was plotted in an approximate location, underneath the 3D model of P0291 (Fig. 78).

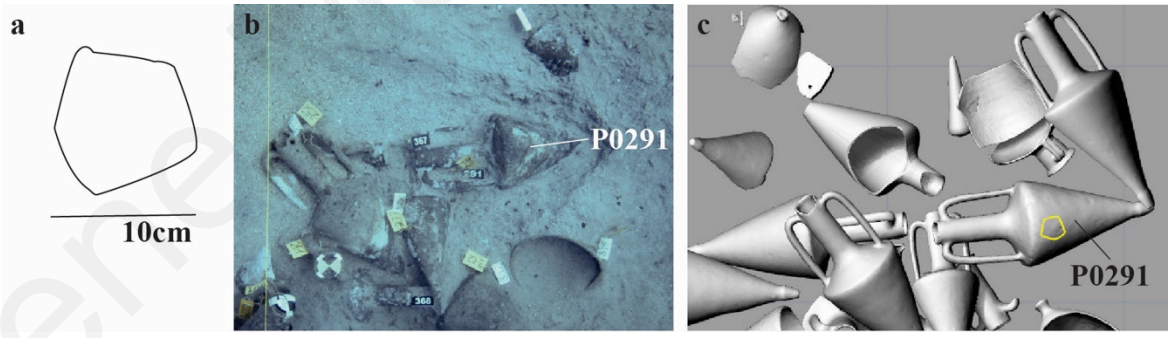

Figure 78: a) The outline drawing of P0291a, was plotted in the 3DSM underneath P0291 (c) from where it was retrieved (b).

The *in situ* location of P0395e was identified in underwater photographs and its outline drawing was plotted accordingly in the 3DSM (Fig. 79) Unfortunately P0395f could not be identified underwater and was thus excluded from the 3DSM and this analysis.

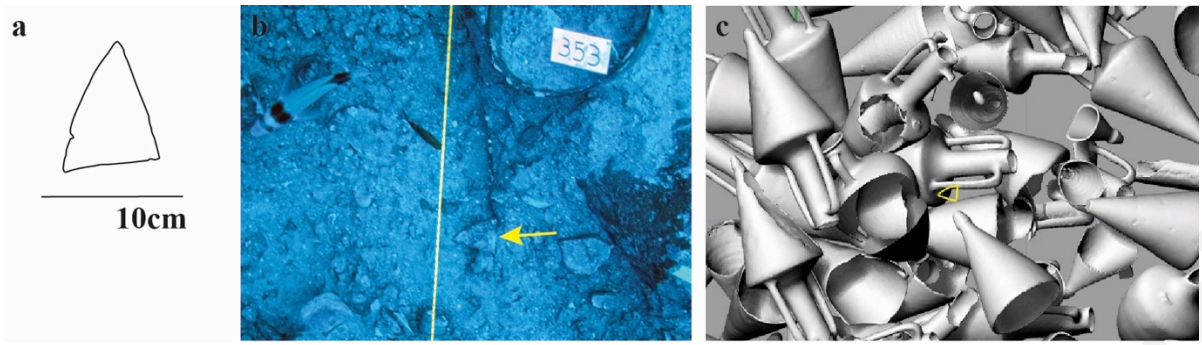

Figure 79: a) The outline drawing of P0395e, b) its *in situ* location and c) subsequent plotting in the 3DSM.

(iv) The case of P0401

The five fragments identified by the conservators (i.e. P0911a, P0844a, P0291a, P0395e-f) as belonging to P0384, were joined together to recreate a large part of this Coan amphora – but it was still missing its base (Fig. 75). By reviewing the 3DSM and the area around P0384, an amphora base (P0401), appeared to be a likely candidate.

An attempt was made by the author to digitally reassemble P0401 to P0384 using their respective photogrammetric models and indeed the three fragments (P0401 and P0384 in two parts) seemed to connect to each other (Fig. 80). Following this 'digital reassembly', the conservators were advised and after inspecting the physical fragments it was verified that P0401 in fact belongs to P0384. For this reason P0401 was also included in the discussion of Reconstruction 12 (Fig. 81).

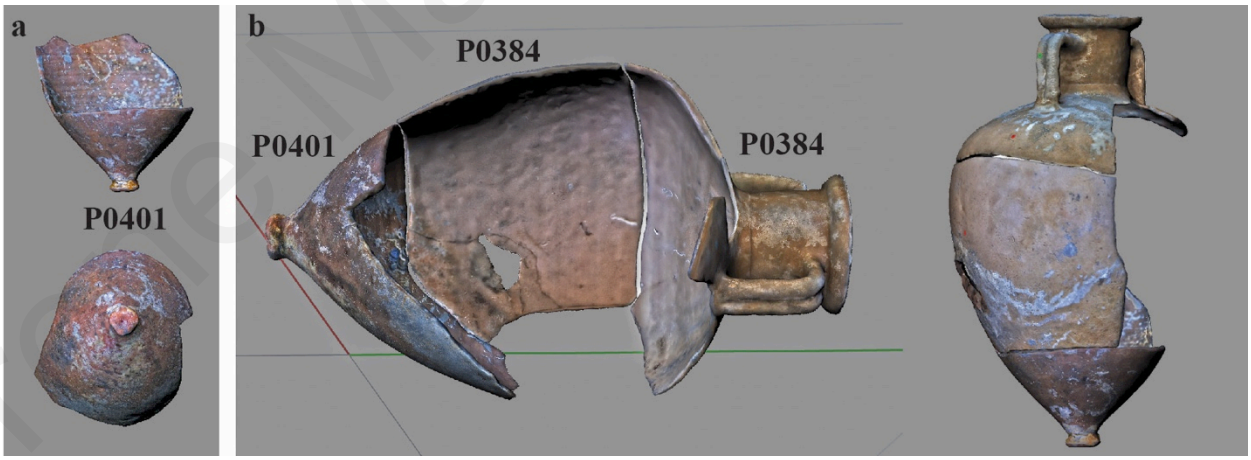

Figure 80: a) The photogrammetric model of P0401, b) was used in conjunction to the photogrammetric models of the two parts of P0384, to investigate whether it belonged to the same artefact.

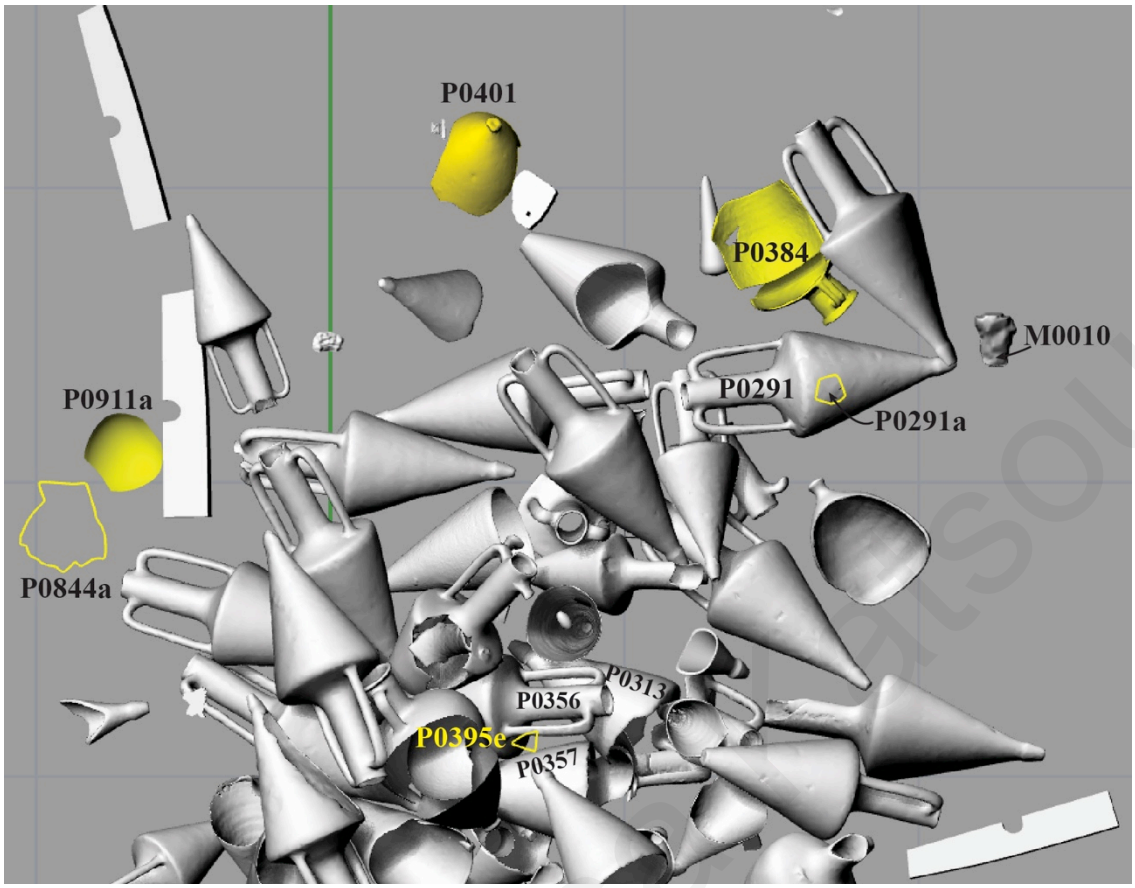

Figure 81: Reconstruction 12: five of the six fragments (P0395f was not plotted) that belong to P0384, in the 3DSM.

(v) Spatial Analysis of Reconstructions 11-12: Tracing previous locations

In the southern most area of the assemblage, where P0385 (Reconstruction 11) and P0384 (Reconstruction 12) were found (Fig. 82), artefacts are deposited in a disorderly manner, with certain amphorae found broken and turned upside down. As Demesticha (2021: 45) describes, the dislocation of artefacts in this area is mainly caused by site-formation processes: firstly "when the ship listed as it settled on the seafloor, and then later as they lost their support-surface as the wooden hull gradually disintegrated". Perhaps burdened by the weight of the two larger anchors, part of the bow broke away falling forward (southwards), causing certain artefacts to roll and relocate and finally to be deposited in the manner they were found. Demesticha (2021: 45, 47) suggests that these artefacts mostly came from the upper and side layers of the assemblage and points out that the deposited larger anchors "must have created a barrier that prevented the collapsed amphorae from spilling farther off the concentration".

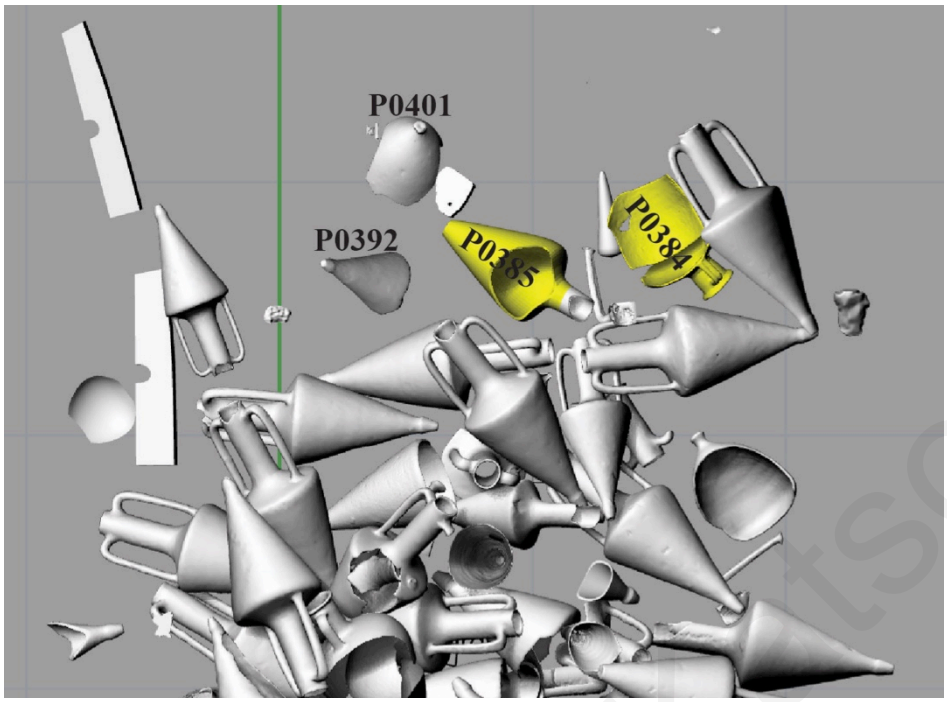

Figure 82: P0384 and P0385 were deposited in the southernmost area of the assemblage, where certain amphorae were found broken and turned upside down (P0392 and P0401).

As part of Reconstruction 11, the conservators were able to join five fragments (P0404a, P0395b-d and P0353a) to the Chian amphora P0385 and their addition to the 3DSM (Fig. 83) resulted in discerning the information that follows.

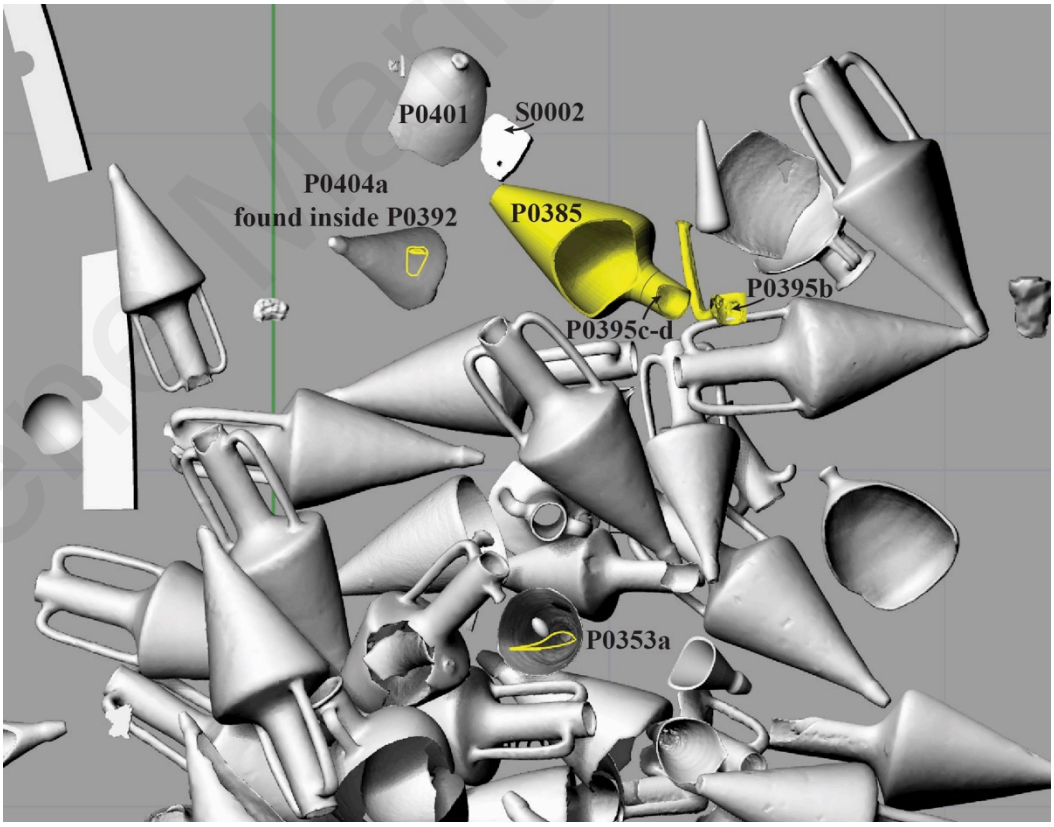

Figure 83: Reconstruction 11: the six fragments that were joined to P0385, in the 3DSM.

Firstly, fragments P0395b-d were discovered next to the amphora they belong to (P0385), in a manner that would imply that their breaking occurred after P0385 had already reached its final position; perhaps they broke off because P0385 was struck by artefacts shifting and being deposited nearby. These three fragments however, were separated upon recovery and placed under a different numbered group, because their association was not made underwater.

The position of P0404a inside another amphora (P0392), could be interpreted in two ways: either the toe fragment was already on the seafloor when P0392 landed on top of it, or that the toe fragment was already inside P0392 when the latter came to rest in its discovered location. The first seems more likely, considering also P0404a's depositional proximity to P0385. If this is indeed the case, then we can additionally hypothesize that one of the artefacts deposited nearby (P0401, P0392, S0002 – a stone weight) could have been the reason for the toe breaking off P0385 (Fig. 83).

The retrieval location of P0353a is most intriguing, as this is the only fragment belonging to P0385 that was found away from it and within an area that is less disordered. P0353a can perhaps provide an indication as to where P0385 was situated prior to the hull disintegration and fore deck collapse, from which its original stowage location may be more easily extrapolated.

By visualizing the corresponding fragments in the 3DSM, it became apparent that the Coan amphora (P0384) involved in Reconstruction 12, was broken into many pieces, which scattered and were deposited in four different areas (Fig. 84). Perhaps this can be explained with two different scenarios: i) that the amphora broke as it moved away from its original stowage position; ii) or more likely, that it broke first into many pieces and these were then displaced to different locations, by scrambling devices (e.g. the disintegration of the ship's structure).

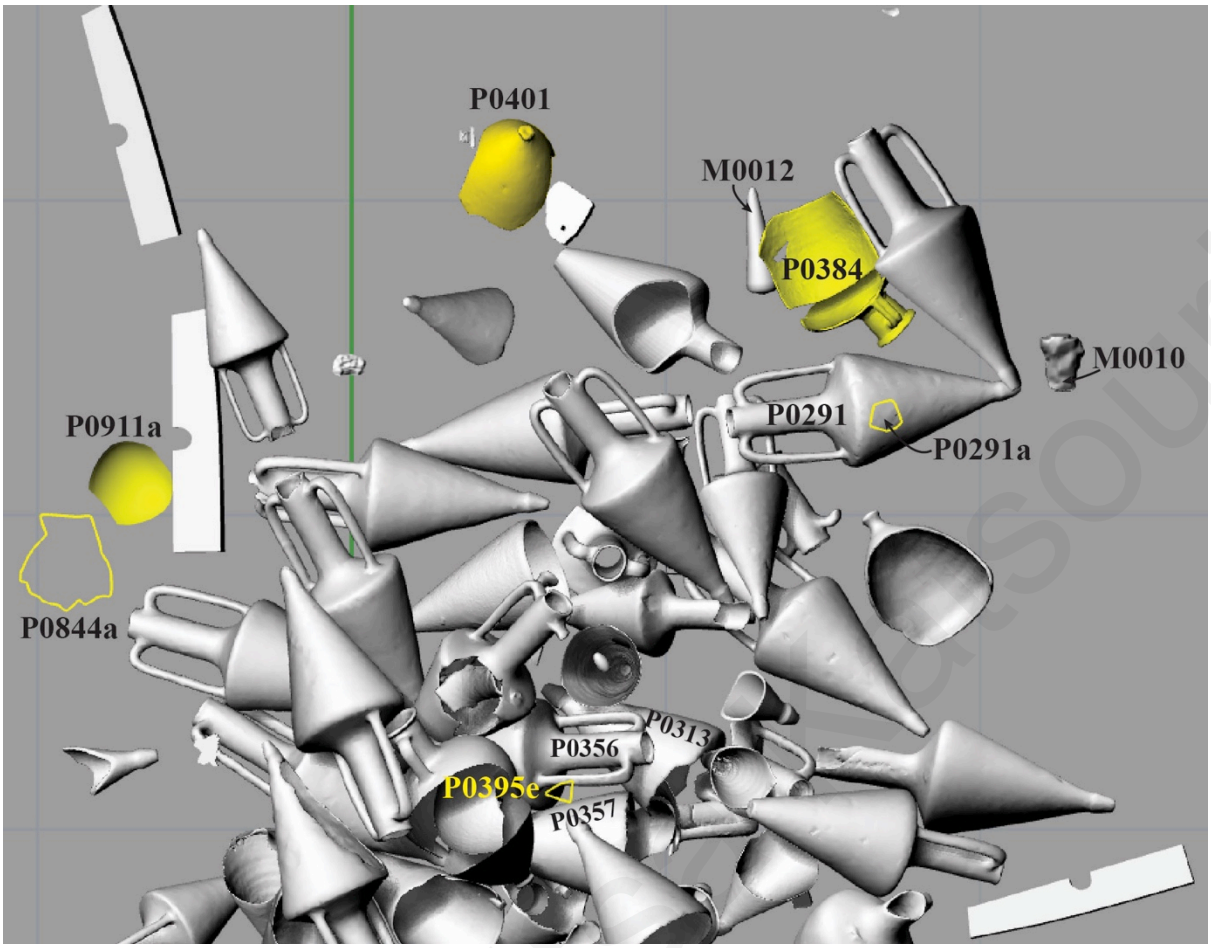

Figure 84: Reconstruction 12: the scattered fragments of the Coan amphora P0384; P0384 and P0291a deposited in the south-western extremity whereas P0911a and P0844a on the south-eastern; P0401 deposited at the southernmost point and lastly, P0395e deposited underneath the Chian amphora P0356, in a more central location of the bow.

The retrieval location of P0395e, which in a way is reminiscent of that of P0353a (seen in Reconstruction 11), makes it the only fragment belonging to P0384 not found in the extremities of the assemblage. More specifically, this fragment was found at approximately the level of the surviving bow starboard planking – in the space between P0357, P0356 and P0313 (Fig. 84). For one sherd of this Coan amphora to de deposited at this location, in an area where the distribution of artefacts is more dense and one would assume less affected by post-wreckage formation processes, could perhaps give information as to where P0384 was situated prior to the hull disintegration and fore-deck collapse events.

The three fragments (the two parts under the label P0384 and P0291a) deposited in the south-western extremity of the assemblage, were likely affected by the disintegration of the wooden elements of the large, starboard bower, as attested by its two iron arm tips (M0010 and M0012) which were also retrieved from this area (Fig. 84). That P0384 is associated with the

iron arm tip M0012 was clear from the excavation. As seen in Figure 75, P0291a was part of the body of the Coan amphora. The aforementioned information may infer the following sequence of events:

1. P0384 arrives in the area of its final deposition, with P0291a still attached.
2. Perhaps due to the aforementioned anchor disintegration, artefacts are displaced, and P0291a breaks off P0384.
3. P0291a is then deposited on the seafloor, followed by P0291 falling on top of it.

5. Discussion

The results presented in Section 4.2 will be used as the starting point for the following discussion, firstly, on the applied methodological approach for mapping micro-stratigraphic evidence, and secondly, on the potential of this approach for the study of shipwreck stratigraphy and site formation processes.

5.1 Evaluation of the methodological approach

The methodology applied for the plotting and visualization of fragments and small finds at the Mazotos shipwreck site, mirrors the methodology already implemented in the project, for plotting larger artefacts. Taking into account the excavation constraints, the method necessitates and presupposes the use of a virtual 3D environment, as well as the detailed documentation of the site through the use of photogrammetry. In contrast to 2D recording and representation techniques, 3D recording methods and modelling enable the full investigation, analysis and understanding of a site's three-dimensionality (i.e. stratigraphy) and context.

The Mazotos 3DSM, which already included the larger artefacts from the site, was augmented with the newly mapped fragments, thus enabling the correlation of both large-scale and small-scale evidence and leading to the accurate spatial contextualization and meaningful analysis of the fragments. In comparison to 2D representations, the 3D site model strengthens the ability to visualize, interrogate and understand how the artefacts relate to one another, how they relate to the hull remains and how they relate to the overall context. Moreover, the 3DSM-based visualization provides an effective means of data navigation, since any contained model can be viewed with the same level of detail, from different perspectives. Further manipulation of data is also possible, as they can be updated and transformed easily. Most importantly, the use of the 3D environment and the capability of visualizing and overlaying different data simultaneously enabled the formulation and investigation of hypotheses and facilitated the perception of initially unanticipated phenomena, such as the visualisation of the area of octopus activity, discerned from Reconstructions 02-04, or the sequence of natural formation processes, such as the two different phases of scrambling activities exemplified by Reconstructions 02-04 and 05.

The use of 3D models and the 3DSM can facilitate the study of the site in an additional and unexpected manner. Determined during the process of the spatial analysis of Reconstruction 12, an additional fragment (P0401 - which was not part of the conservation report) was

studied in 3D and associated with P0384. This leads to the conclusion that, as the conservation work has informed the 3DSM, the reverse also holds true; the 3D work can inform the conservation work. Therefore it can be suggested that both the digital and conservation work, would benefit by engaging in a bi-directional process; such a method could expedite results, as well as the stream of information regarding both the site and its contents.

The novel aspect of the present study lies in the fact that micro-stratigraphic evidence was modelled, mapped and incorporated into the site's 3DSM, which precipitated their spatial analysis and investigation. As made evident from the digital site plans presented in Section 2.3, such information from shipwreck sites is rarely visualized and examined in 3D, thus their potential contribution with both spatial and temporal information, has not been fully explored so far. The only other example of modelling and plotting individual fragments in 3D, comes from the use of the ARPENTEUR application and the published information of its implementation for the reconstructions of the Grand Ribaud F (Drap et al. 2003) and Cala Rossa (Seinturier et al. 2004) sites. It remains unclear however, how said application accomplishes the 3D modelling of non-diagnostic sherds; presumably the contour of such fragments can be more difficult to match, 'fit' and extract with certainty from the corresponding theoretical amphora models. In this respect, the approach of creating the vector outline drawings of fragments (which can be transformed into full 3D objects at a later stage) provides more flexibility, as it is not reliant upon defining the semantic data of a fragment (i.e. identifying the potential amphora type or to which part of an amphora the fragment may belong). ARPENTEUR offers other advantages, for instance it eliminates the requirement of segmenting point clouds for the purpose of plotting artefacts in the digital site model; however, even though this tool has become open source, to the best of the author's knowledge, it has not seen widespread use in the 3D reconstruction and study of shipwreck sites.

From a total of thirty-eight fragments that were to be plotted as part of this thesis, only two were not added to the 3DSM: P0395a (of Reconstruction 06) and P0395f (of Reconstruction 12). Both fragments belong to a lot that contained 115 sherds (P0395) deriving from 20 added events (specifically investigated in Reconstruction 06). Even when a small artefact is lifted prior to documenting its *in situ* position, the photogrammetric recording, photographic archive and database information can be used to identify its retrieval location. As the photogrammetric documentation of the excavation progress provides an almost daily

recording of the state of the working trench, the excavated areas of each of the 20 added events pertaining to P0395 could and were accurately modelled. P0395a's location was tracked down to two possible blocks of roughly the same area, a fact which enabled its subsequent analysis. Instead it was not possible to connect P0395f to a specific excavation /block area – but its investigation was not exhaustive. What can be suggested is that all remaining fragments from lot P0395 be examined and retraced to their *in situ* positions and corresponding blocks; this would perhaps assist in identifying to which block P0395f belongs. This approach however was unfeasible within the scope of this study, due to the numerous fragments and information that would need to be reviewed.

It is important at this point to discuss certain constraints that can impact the 3D mapping process. The 3D plotting of micro-stratigraphic evidence is a lengthy process requiring focused study and data review, in order to ensure accurate results. As smaller or loose artefacts are seldomly labeled underwater due to the excavation constraints, their retrieval location is more laborious to trace in the photogrammetric data (when they are depicted) and instead, needs to be firstly traced through the photographic archive and the database information. When lots contain fewer sherds, the process of associating each sherd with its respective retrieval date and event through the database information and the photographic archive, is relatively easy to achieve. On the contrary as lots become larger and especially when they include a large number of non-diagnostic sherds, the same process becomes more time consuming and difficult. Even though the research potential of the spatial analysis of micro-stratigraphy has been demonstrated through the present study, it is undoubtedly a process entailing significant time and effort, amplified by the amount of such evidence present at shipwreck sites. For the bow area of the Mazotos shipwreck alone (corresponding to seasons 2010, 2011 and 2016), the total number of pottery fragment lots amounts to 67, or approximately 941 individual pieces.

Even though the 3DSM was augmented with information from just twelve Reconstructions, this was sufficient to highlight two important issues: the practical scalability and legibility of mapping such information and their associations for the entire site. The proposed methodology and subsequent spatial analysis would benefit from having the 3D models connected and juxtaposed to relevant textual information. This would facilitate the correlation of data deriving from different sources (from the excavation, the conservation, the spatial and temporal data resulting from analysis) but also the management, easy identification and querying of data.

5.2 Evaluation of the 3D spatial analysis of micro-stratigraphic evidence

The process of associating fragments and reconstructing artefacts through the conservation work was imperative for the spatial analysis conducted in this research. By 3D plotting the thirty-eight fragments and visualizing both their depositional location and their spatial relationship to the artefacts they belong to, it was possible to ascertain that the mapping of micro-scale evidence can provide both spatial and temporal information. The results of the present study indicate that micro-stratigraphic evidence can significantly contribute in the study and understanding of the stratigraphy and the formation processes of a shipwreck site, in a number of ways.

It has been demonstrated that the 3D plotting and the ability to analyse micro-stratigraphic evidence spatially, can provide clues regarding natural and cultural processes that have affected the site. Retracing of the mechanisms of destruction, dispersal, decay and stabilization of artefacts becomes possible by: a) deciphering the cause of fractured artefacts, b) tracing events such as artefact displacements as well as movements and furthermore, c) understanding the sequence of such events.

The correlation of the information from the conservation work and the 3D spatial analysis, served in recognizing and determining that a surface artefact (P0220) was most likely displaced due to post-depositional cultural transforms, perhaps modern fishing activities using nets. Although the fact that this fragment was retrieved away from the main assemblage may also be interpreted as having occurred prior or during the sinking event, this scenario is now considered less probable based on the aforementioned information.

It was also possible to identify that certain fragments were reallocated due to the post-depositional, scrambling effects of marine life present at the site. The photographic and photogrammetric documentation permitted the detection of such displacements, some of which taking place in the interim of field seasons. Such disturbances highlight the importance of thoroughly investigating each fragment's retrieval position, as smaller artefacts are more susceptible to displacements. The ability however, to recognise that an artefact has been displaced is significant in that it can inform the analysis and interpretation process of less reliable evidence.

The 3D plotting facilitates the positioning in space and by implication in time, of an artefact or context with respect to another. This is achieved by first determining the sequence of depositions, to which the study of fragments can again, offer insights. The plotting of

fragments has demonstrably offered clues pertaining to the movement and breaking of amphorae, which when investigated in reverse order can also prove useful in relocating their original stowage positions and by extension the ships' original spatial arrangement. Undoubtedly, the same clues (i.e. the movement and breaking of artefacts as well as the sequence of depositions) can also provide information on the dynamic processes that have affected and transformed the shipwreck site, post-depositionally. The temporal associations that can be construed through the 3D spatial analysis of both large-scale and small-scale artefacts concurrently can contribute towards visualizing and understanding the ship's structural deterioration/disintegration episodes, as well as their consequences in relation to the dispersal and reordering of artefacts associated to each episode.

The fragments that were used in the twelve Reconstructions, were already associated to the artefacts they belonged to through the conservation work. Nonetheless, the process of 3D mapping on a micro-scale can progress independently and be connected to information attained through the conservation work, as this becomes available. Indeed the mapping of such evidence (even before being associated to the artefacts they belong) would assist in visualizing concentrations and distribution patterns within the site, but also in explaining certain areas in the 3DSM that now appear to be empty of artefacts. For instance, Demesticha (2021: 49-51) notes that a large gap was left at the starboard side, when attempting to reconstruct the bow's stowage arrangement based on the find-spots of each amphora (Fig. 85).

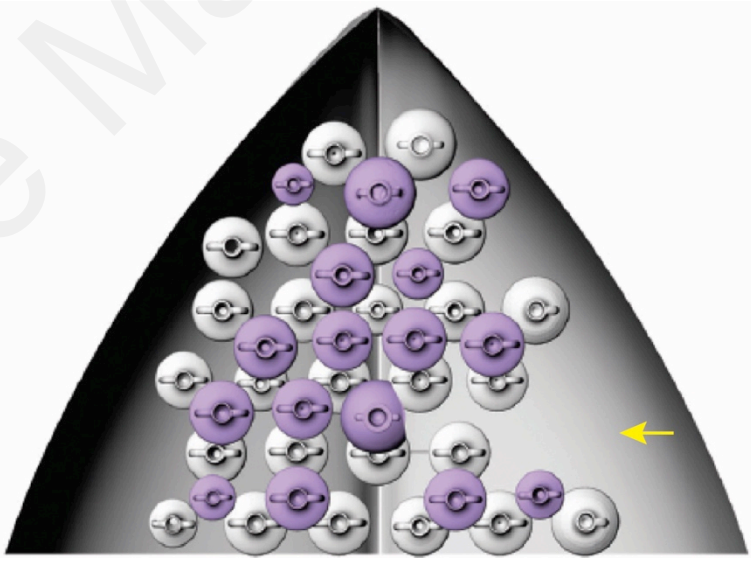

Figure 85: A large gap at the starboard side was noticed in the suggested stowage reconstruction where the amphorae find-spots were taken into account. This may represent a true gap, where organic material (nets or rope, now destroyed) was stored (based on Demesticha 2021:50, Fig 13a).

It is hypothesized that this is either a true gap, indicating an area where perishable organic material might have been stored (perhaps ropes or nets) or that this gap resulted from the deck collapse. In the case where micro-stratigraphic evidence were deposited in this area, their examination and plotting would serve to both further our understanding of the processes that have affected the site but also in reconstructing the original ship's spatial arrangement more conclusively and in more detail.

6. Conclusions

The aim of this thesis was to investigate the potential of plotting pottery fragments in a 3D environment and by extension the use of 3D applications, in the stratigraphic analysis of shipwreck sites and the study of their formation processes. As demonstrated in the preceding chapters, the acquired documentation and excavation data from the Mazotos site have enabled the accurate plotting of such information, post-fieldwork. As affirmed by the spatial analysis employed in this research, the plotting of micro-scale evidence can provide spatial and temporal information that can significantly contribute in the study and understanding of the site. Valuable insight can be gained from observing the spatial disposition of sherds in a 3D environment; through the process of tracing where each artefact's fragments are deposited, one can more fully understand, how and why an artefact broke, how it was displaced and came to rest in its depositional location. Gaining a better understanding of an artefact's process of deposition contributes in decoding the phases and events of the post-depositional site formation processes. The 3D spatial analysis of fragments can also add to the study of the amphora stowage system, which has already begun (Demesticha 2021). Undoubtedly however, until the excavation and conservation work is fully completed, new information and clues will continue to come to light, which will necessitate the revision and revaluation of previous interpretations.

Furthermore, as the use of a 3DSM is already part of the excavation documentation methodology of the Mazotos project, the proposed and applied method could be used to 3D plot other artefacts found during excavation, the sieving process or inside amphorae, such as: organic finds, stones, wooden and metal fragments.

In conclusion, digital photogrammetry and 3D computer graphics have become indispensible tools in shipwreck archaeological research, providing and permitting new ways of acquiring, analyzing and interpreting the evidence of the past. The implementation of 3D digital mapping and visualization enables the spatial examination of elements such as micro-stratigraphy, which can demonstrably contribute significantly to the identification, understanding and reconstruction of both the depositional and site formation processes, aiding in attaining a more complete interpretation of the archaeological record.

Appendix

Catalogue of the artefacts involved in the twelve Reconstructions.

Artefact	Description	Photograph (© MARELab unless otherwise indicated)
P0018	A Chian amphora missing its toe. Lifted in 2015. Reconstruction 02	
P0141	A South-Aegean amphora (Mushroom Rim - Knob Toe) in two parts. Lifted in 2008. Reconstruction 03	
P0151	An upper part of a Chian amphora. Lifted in 2011. Reconstruction 04	

P0220	An upper part of a South-Aegean amphora (Mushroom Rim - Knob Toe). Lifted in 2010. Found 15m from the main assemblage. Joined to P0371 (Reconstruction 01).	
P0263	A Chian amphora missing most of its neck and both handles. Lifted in 2010. Reconstruction 09	
P0265	Nine sherds. Lifted in 2010, from the area of P0263. **P0265a:** A body sherd joined to P0141 (Reconstruction 03). **P0265b:** A shoulder sherd joined to P0151 (Reconstruction 04).	
P0273	A Chian amphora missing most of one handle. Lifted in 2010. Reconstruction 05	

P0282	Two sherds and a Chian handle fragment. Lifted in 2010. **P0282a:** One sherd likely to belong to P0310 (Reconstruction 08).	
P0290	A Chian amphora missing one handle, as well as part of its rim, and neck. Lifted in 2010. Reconstruction 10	
P0291	A Chian amphora retrieved in two large parts. Plus 25 sherds. Lifted in 2011. **P0291a:** One sherd joined with P0384 (Reconstruction 12).	
P0292	Ten sherds. Lifted in 2010, from the area north of the anchor core M0309. **P0292a-d:** Four sherds joined with P0293d and likely to belong to P0310 (Reconstruction 08). **P0292e-f:** Two body sherds joined to P0314 (Reconstruction 07).	

P0293	Twenty-eight fragments. Lifted on many dates in 2010, from the area around amphora P0283 and from northeast of anchor core M0308. **P0293a-c:** Three sherds joined with P0282a and likely to belong to P0310 (Reconstruction 08). **P0293d:** One sherd joined with P0292a-d and likely to belong to P0310 (Reconstruction 08). **P0293e-h:** Four sherds joined to P0310 (Reconstruction 08). **P0293i:** A toe fragment likely to belong to P0310 (Reconstruction 08).	 
P0295	One sherd broken in two. Lifted in 2010, from the area south of the anchor cores M0308 and M0309. Joined to P0310 (Reconstruction 08).	 (Photograph provided courtesy of the Department of Antiquities)
P0310	An upper part of a South-Aegean amphora (Mushroom Rim - Knob Toe) broken into three pieces. Lifted in 2010. Reconstruction 08	 (Photograph provided courtesy of the Department of Antiquities)

P0314	A lower part of a possibly Lycian amphora. Lifted in 2011. Reconstruction 07	
P0320	Contents of amphora P0263. Lifted in 2010. **P0320a:** Toe fragment joined to P0018 (Reconstruction 02).	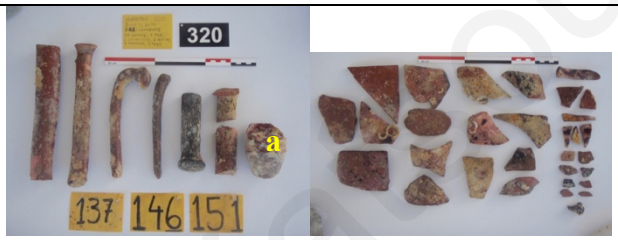
P0333	Thirty-five sherds retrieved through sieving. Lifted in 2010, from the area underneath P0270. **P0333a-b:** Two neck sherds joined to P0263 (Reconstruction 09).	
P0342	Contents of P0273: Four fragments. Lifted in 2010. **P0342a:** A handle fragment joined to P0273 (Reconstruction 05).	 (Photograph provided courtesy of the Department of Antiquities)

P0353	A lower part of a Chian amphora, plus twelve sherds. Lifted in 2011. **P0353a:** A large body fragment joined to P0385 (Reconstruction 11).	 (Composite of two photographs provided courtesy of the Department of Antiquities)
P0357	A Chian amphora broken *in situ* and recovered as three parts. Lifted in 2011. Reconstruction 06	
P0362	A Chian amphora handle preserving its genesis as well as part of the neck and rim. Lifted in 2011. Joined to P0290 (Reconstruction 10).	
P0365	Seven sherds. Lifted in 2011. **P0365a:** A large body sherd joined to P0371 (Reconstruction 01).	

P0366	Fifty-six sherds. Lifted in 2011. **P0366a:** A large body sherd joined to P0371 (Reconstruction 01).	 
P0371	A lower part of a South-Aegean amphora (Mushroom Rim - Knob Toe). Lifted in 2011. Reconstruction 01	
P0384	A Coan amphora broken into two large parts. Plus two sherds. Conglomerated on one of the parts, was the anchor tip concretion, M0012. Lifted in 2011. Reconstruction 12	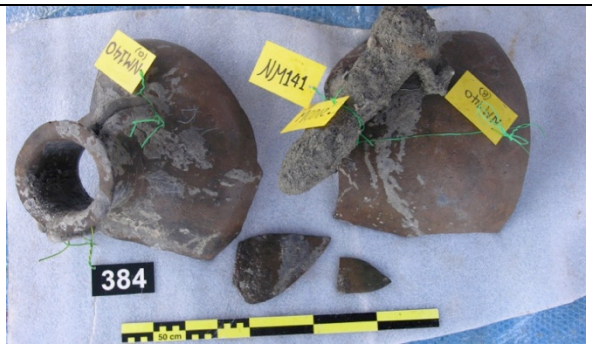

P0385	A Chian amphora broken during excavation. Plus 14 sherds. Lifted in 2011. Reconstruction 11	
P0395	One hundred and fifteen sherds. Lifted in 2011. **P0395a:** A shoulder fragment joined to P0357 (Reconstruction 06). **P0395b:** A Chian amphora handle fragment joined to P0385 (Reconstruction 11). **P0395c-d:** Two neck fragments joined to P0385 (Reconstruction 11). **P0395e-f:** Two sherds joined to P0384 (Reconstruction 12).	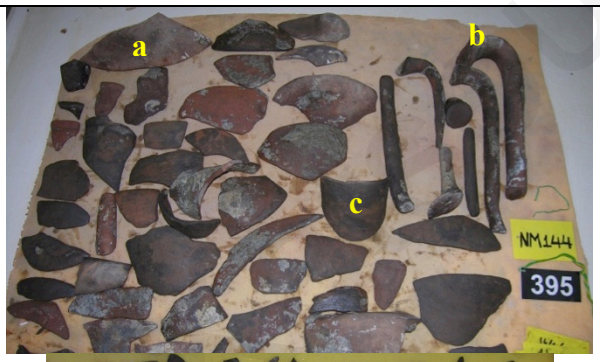 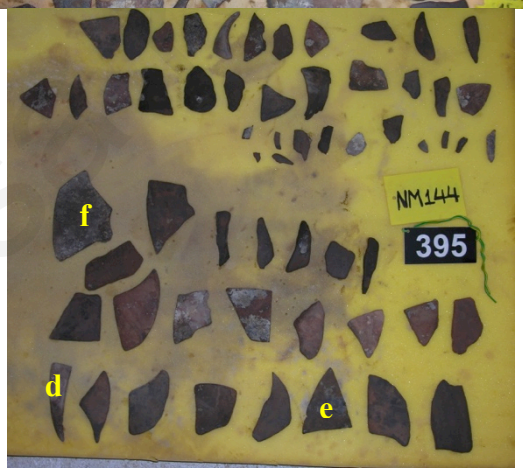
P0401	A lower part of a South-Aegean amphora (Mushroom Rim - Knob Toe). Lifted in 2018. Verified of belonging to the same artefact as P0384 (Reconstruction 12).	

P0404	Contents of P0392: A Chian amphora toe fragment and four sherds. Lifted in 2011. **P0404a:** A toe fragment joined to P0385 (Reconstruction 11).	
P0844	Nineteen fragments. Lifted in 2016. **P0844a:** A large body fragment joined to P0384 (Reconstruction 12).	
P0911	Four fragments. Lifted in 2016, from the area of the anchor stock M0004. **P0911a:** A large body fragments joined to P0384 (Reconstruction 12).	

Bibliography

Adams, J. (2013). *A Maritime Archaeology of Ships: Innovation and Social Change in Medieval and Early Modern Europe*. Oxford: Oxbow Books.

Adams, J.R., Antoniadou, A., Hunt, C.O., Bennett, P., Croudace, I.W., Taylor, R.N., Pearce, R.B., Earl, G.P., Flemming, N.C., Moggeridge, J., Whiteside, T., Oliver, K. and Parker, A.J. (2013). The Belgammel Ram, a Hellenistic‐Roman Bronze Proembolion Found off the Coast of Libya: Test Analysis of Function, Date and Metallurgy, with a Digital Reference Archive. *International Journal of Nautical Archaeology*, 42(1), pp. 60-75.

Bahn, P. (ed.). (2001). *The New Penguin Dictionary of Archaeology*. London: Penguin Books.

Ballard, R., Hiebert, F., Coleman, D., Ward, C., Smith, J., Willis, K., Foley, B., Croff, K., Major, C. and Torre, F. (2001). Deepwater Archaeology of the Black Sea: The 2000 Season at Sinop, Turkey. *American Journal of Archaeology*, 105, pp. 607-623.

Barker, P. (1993). *Techniques of Archaeological Excavation*. 3rd ed. London: B. T. Batsford.

Bartoli, D., Capulli, M. and Holt, P. (2012). Creating a GIS for the Underwater Research Project ANAXUM: the Stella 1 Shipwreck. In: Fozzati, L. and Roberto, V. (eds.), *Proceedings of the 2nd Workshop on The New Technologies for Aquileia*. Aquileia (2012), E1-E9.

Bass, G. F. (1966). *Archaeology Under Water*. London: Thames and Hudson.

Bass, G. F. and van Doorninck, F. H. (1982). *Yassi Ada I, a Seventh-Century Byzantine Shipwreck*. College Station: Texas A & M University Press.

Bastida, R., Elkin, D. and Grosso, M. (2010). *Enfoques Interdisciplinarios Para el Estudio de Procesos Naturales de Formación de Sitios Arqueológicos Subacuáticos: Investigaciones en el Marco del Proyecto Swift (Provincia de Santa Cruz, Argentina)*. In: F. Oliva, F., de Grandis, N. and Rodríguez, J. (eds.), Arqueología Argentina en los Inicios de un Nuevo Siglo, Tomo III, Rosario: Laborde Editor, pp. 269-283.

Beltrame, C. (1998). *Processi Formativi del Relitto in Ambiente Marino Mediterraneo*. In: Volpe, G. (ed.), Archeologia Subacquea. Come Opera L' Archeologo Sott' Acqua. Storie Dalle Acquae (VIII Ciclo di Lezioni sulla Ricerca Applicata in Archeologia. Certosa di Pontignano SI, 1996). Firenze: Edizioni all' insegna del Giglio, pp. 141–166.

Beltrame, C. and Manfio, S. (2014). Alcune Proposte Metodologiche per l'Impiego di un GIS Intra-Site nella Documentazione di un Relitto: L'Applicazione sul Brick Mercurio (Punta Tagliamento, Italia). *Archeologia e Calcolatori*, 25, pp. 113 - 129.

Beltrame, C. and Costa, E. (2018). 3D Survey and Modelling of Shipwrecks in Different Underwater Environments. *Journal of Cultural Heritage*, 29, pp. 82–88.

Boetto, G. and Poveda, P. (2018). Napoli A, Un Voilier Abandonné dans le Port de Neapolis à la Fin du Ier Siècle: Architecture, Fonction, Restitution et Espace de Navigation. In: G. Boetto, G. and Rieth, E. (eds.), *De re Navali: Pérégrinations Nautiques Entre Méditerranée et Océan Indien. Mélanges en l'Honneur de Patrice Pomey*, Paris: Archaeonautica (20), pp. 19-56.

Bowens, A. (ed.). (2009). *Underwater Archaeology: The NAS Guide to Principles and Practice.* Second Edition. Oxford: The Nautical Archaeology Society.

Carlson, D. N. and Aylward. W. (2010). The Kızılburun Shipwreck and the Temple of Apollo at Claros. *American Journal of Archaeology*, 114, pp. 145-59.

Casabán, J., Radic Rossi, I., Yamafune, K. and Castro, F. (2013). *Underwater Photogrammetry Applications: The Gnalic Shipwreck, 2013 (Croatia)*. [online] ResearchGate. Available at: https://www.researchgate.net/publication/287986452_Underwater_Photogrammetry_Applications_The_Gnalic_Shipwreck_2013_Croatia [Accessed 20 Apr. 2021].

Castro, F. and Capulli, M. (2016). A Preliminary Report of Recording the Stella 1 Roman River Barge, Italy. *International Journal of Nautical Archaeology*, 45(1), pp. 29-41.

Catsambis, A. (2007). Three-dimensional Underwater Mapping: The Kizilburun Excavation. In: Clark, J.T. and Hagemeister, E.M. (eds.), *Digital Discovery. Exploring New Frontiers in Human Heritage. Proceedings of Computer Applications and Quantitative Methods in Archaeology.* Fargo (2006). Budapest: Archaeolingua, pp. CD-ROM 611-615.

Cibecchini, F., Rico, C. and Poveda, P. (2018). Capo Sagro 2: Une Epave Romaine à Chargement de Lingots d'étain à 500 mètres de Profondeur. In: G. Boetto, G. and Rieth, E. (eds.), *De re Navali: Pérégrinations Nautiques Entre Méditerranée et Océan Indien. Mélanges en l'Honneur de Patrice Pomey*, Paris: Archaeonautica (20), pp. 67-87.

Clarke, D. (1973). Archaeology: The Loss of Innocence. *Antiquity*, 47, pp. 6–18.

Cook, C. (2011). *A Parametric Model of the Portuguese Nau.* Master's Thesis. Texas A&M University.

Daly, P. and Evans, T. (2006). *Introduction: Archaeological Theory and Digital Pasts*. In: Evans, T. L. and Daly, P. (eds.), Digital Archaeology. Bridging Method and Theory. Abingdon: Routledge, pp. 2-7.

de Juan Fuertes, C., Cibecchini, F. and Vento, E. (2012). El Pecio Altoimperial de Bou Ferrer. (La Vila Joiosa, Alicante). Estado Actual de la Investigación. *Actas de las Jornadas de ARQUA 2011.* Madrid: Ministerio de Educación, Cultura y Deporte, pp. 109-116.

Delgado, J.P. (1997). *Maritime Archaeology.* In: Delgado, J. P. (ed.), Encyclopaedia of Underwater and Maritime Archaeology. London: The British Museum Press, pp. 259-260.

Demesticha, S. (2009). Questions on Trade; The Case of the Mazotos Shipwreck. *Cahiers de Centre Etude Chypriotes*, 39, pp. 1-16.

Demesticha S. (2010). The 4th-century Mazotos Shipwreck, Cyprus: A Preliminary Report. *International Journal of Nautical Archaeology*, 40(1), pp. 39-59.

Demesticha, S. (2011). *Press Release: Underwater Archaeological Research at Mazotos Shipwreck 2011 Field Season*. [online] Department of Antiquities. Available at: http://www.mcw.gov.cy/mcw/DA/DA.nsf/All/E7FA95DF40DFCFAE422577B200386256/$file/PIO%20Mazotos%20Shipwreck%202011%20engl.pdf [Accessed 20 Apr. 2021].

Demesticha, S., Skarlatos, D. and Neophytou, A. (2014). The 4th-century B.C. Shipwreck at Mazotos, Cyprus: New Techniques and Methodologies in the 3D Mapping of Shipwreck Excavations. *Journal of Field Archaeology,* (39), pp. 134-150.

Demesticha, S. (2017). *'...when the ship sank with the loss of all its cargo...' The Underwater Archaeological Investigation of the Mazotos Shipwreck*. In: Papadimitriou, N. and Tolis, M. (eds.), Ancient Cyprus. Recent developments in the archaeology of the Eastern Mediterranean. Athens: Museum of Cycladic Art, pp. 285 – 300 (in Greek).

Demesticha, S. (2019). *The 2019 Excavation Season at the Mazotos Shipwreck.* [online] Honor Frost Foundation. Available at: https://honorfrostfoundation.org/grants-awarded/small-grants/cyprus/marelab/the-mazotos-shipwreck-project/ [Accessed 20 Apr. 2021].

Demesticha, S. (2021). *The Mazotos Shipwreck, Cyprus: A Preliminary Analysis of the Amphora Stowage System*. In: Demesticha, S. and Blue, L. (eds.), Under the Mediterranean I, Studies in Maritime Archaeology. Leiden: Sidestone Press, pp. 43-58.

De Reu, J., Plets, G., Verhoeven, G., De Smedt, P., Bats, M., Cherretté, B., De Maeyer, W., Deconynck, J., Herremans, D., Laloo, P., Van Meirvenne, M. and De Clercq, W. (2013). Towards a Three-dimensional Cost-effective Registration of the Archaeological Heritage. *Journal of Archaeological Science,* 40, pp. 1108-1121.

Diamanti, E. and Vlachaki, F. (2015). 3D Recording of Underwater Antiquities in the South Euboean Gulf. *ISPRS - International Archives of the Photogrammetry, Remote Sensing and Spatial Information Sciences*, 40(5/W5), pp. 93-98.

Drap, P., Seinturier, J. and Long, L. (2003). Archaeological 3D Modelling Using Digital Photogrammetry and Expert System. The Case Study of Etruscan Amphorae. In: Plemenos, D. (ed.), *Proceedings of the VIth Infographie Interactive et Intelligence Artificielle International Conference.* Limoges (2003), pp. 177-188.

Drap, P. (2012). *Underwater Photogrammetry for Archaeology*. In: Carneiro da Silva, D. (ed.), Special Applications of Photogrammetry. Rijeka: IntechOpen, pp.111-136.

Drap, P., Merad, D., Mahiddine, A., Seinturier, J., Peloso, D., Boï, J.-M., Chemisky, B. and Long, L. (2013). Underwater Photogrammetry for Archaeology. What Will Be the Next Step? *International Journal of Heritage in the Digital Era*, 2, pp. 375-394.

Drap, P., Merad, D., Hijazi, B., Gaoua, L., Nawaf, M., Saccone, M., Chemisky, B., Seinturier, J., Sourisseau, J.-C., Gambin, T. and F. Castro, F. (2015). Underwater Photogrammetry and Object Modelling: A Case Study of Xlendi Wreck in Malta. *Sensors*, 15(12), pp. 30351-30384.

Dumas, F. (1962). *Deep-water archaeology*. Translated by H. Frost. London: Routledge and Kegan Paul.

Easton, N. A. (1997). *Benthic Bioturbation.* In: Delgado, J. P. (ed.), Encyclopaedia of Underwater and Maritime Archaeology. London: The British Museum Press, p. 60.

Ellefi, B. M., Drap, P., Papini, O., Merad, D., Boï, J.-M., Royer, J.-P., Pasquet, J., Sourisseau, J.-C., Castro, F. and Nawaf, M. (2018). Cultural Heritage Resources Profiling: Ontology-based Approach. In: *27th International World Wide Web Conference (WWW)*. Lyon (2018), pp. 1489-1496.

Ferrari, B. (1995). *Physical, Biological and Cultural Factors Influencing the Formation, Stabilisation and Protection of Archaeological Deposits in U.K. Coastal Waters*. Doctoral Thesis. University of St. Andrews.

Ford, B., Sowden, C., Farnsworth, K. and Scott Harris, M. (2016). Coastal and Inland Geologic and Geomorphic Processes. In: Keith, M. E. (ed.), Site Formation Processes of Submerged Shipwrecks. Gainesville: University Press of Florida, pp. 17-43.

Fulton, C., Viduka, A., Hutchinson, A., Hollick, J., Woods, A., Sewell, D. and Manning, S. (2016). Use of Photogrammetry for Non-Disturbance Underwater Survey: An Analysis of In Situ Stone Anchors. *Advances in Archaeological Practice*, 4(1), pp. 17–30.

Gambin, T., Drap, P., Cheminsky, B., Hyttinen, K. and Kozak, G. (2018). Exploring the Phoenician Shipwreck off Xlendi Bay, Gozo. A Report on Methodologies Used for the Study of a Deep-water Site. *Underwater Technology*, 35(3), pp. 71–86.

Gibbins, D. (1990). Analytical approaches in maritime archaeology: a Mediterranean perspective. *Antiquity*, 64, pp. 376-389.

Gibbins, D. and Adams, J. (2001). Shipwrecks and Maritime Archaeology. *World Archaeology*, 32(3), pp. 279-291.

Gibbs, M. (2006). Cultural Site Formation Processes in Maritime Archaeology: Disaster Response, Salvage and Muckelroy 30 Years On. *International Journal of Nautical Archaeology*, 35, pp. 4–19.

Gould, R. A. (1997). *Contextual Relationships*. In: Delgado, J. P. (ed.), Encyclopaedia of Underwater and Maritime Archaeology. London: The British Museum Press, pp. 108-110.

Gould, R. A. (2011). *Archaeology and the Social History of Ships*. 2nd. ed. Cambridge: University Press.

Green, J.N., Baker, P. E., Richards, B. and Squire. D. M. (1971). Simple Underwater Photogrammetric Techniques. *Archaeometry*, 13, pp. 221–232.

Green, J., Matthews, S. and Turlani, T. (2002). Underwater Archaeological Surveying Using PhotoModeler, VirtualMapper: Different Applications for Different Problems. *International Journal of Nautical Archaeology*, 31(2), pp. 283-292.

Green, J. and Gainsford, M. (2003). Evaluation of Underwater Surveying Techniques. *International Journal of Nautical Archaeology,* 32, pp. 252-261.

Green, J. (2004). *Maritime Archaeology: A Technical Handbook*. San Diego: Elsevier Academic Press.

Gregory, D. J. (1995). Experiments into the Deterioration Characteristics of Material on the Duart Point Wreck Site: An Interim Report. *International Journal of Nautical Archa*eology, 24(1), pp. 61–65.

Gregory, D. J. (1996). *Formation Processes in Marine Archaeology, A Study of Chemical and Biological Deterioration.* Doctoral Thesis. University of Leicester.

Hadjivasili, C. (2018). *Final Report on the Conservation of Ceramics Finds from Underwater Sites – Contract for Provision of Services for the Department of Antiquities, Cyprus.* [online] Honor Frost Foundation. Available at: https://honorfrostfoundation.org/wp-content/uploads/2019/09/DoA-Conservation-of-Ceramics-Report-2017-18.pdf [Accessed 20 Apr. 2021].

Harpster, M. (2009). Keith Muckelroy: Methods, Ideas and Maritime Archaeology. *Journal of Maritime Archaeology*, 4, pp. 67-82.

Harris, E. (1989). *Principles of Archaeological Stratigraphy.* 2nd ed. London: Academic Press.

Hazlett, A. D. (2003). *The Nau of the Livro Nautico: Reconstructing a Sixteenth-Century Indiaman from Texts*. Doctoral Thesis. Texas A&M University.

Hein, A. and Kilikoglou, V. (2020). Digital Modelling of Function and Performance of Transport Amphorae. *International Journal of Ceramic Engineering & Science*, 2(4), pp. 187– 200.

Higgins, C. R. (2012). *The Venetian Galley of Flanders: From Medieval (2-Dimensional) Treatises to 21st Century (3-Dimensional) Model*. Master's Thesis. Texas A&M University.

Hill, R. (1994). A Dynamic Context Recording and Modelling System for Archaeology. *International Journal of Nautical Archaeology*, 23(2), pp. 141-145.

Holtorf, C. (2014). *Preservation Paradigm in Heritage Management*. In: Smith, C. (ed.), The Encyclopedia of Global Archaeology. New York: Springer, pp. 6128–6131.

Jézégou, M.-P., Paul, F. and Gassend, J.-M. (2020). L'Utilisation des Images 3D Comme Outil de Compréhension et de Médiation pour l'Etude des Epaves de l'Antiquité Romaine, à Partir de Trois Exemples: Mandirac 1, Laurons 2, et Port-Vendres 1. *Patrimoines du Sud*, [online] Volume 12, pp. 1-26. Available at: https://journals.openedition.org/pds/4456 [Accessed 20 Apr. 2021].

Jones, T. (2009). Three-Dimensional Recording and Digital Modelling of the Newport Medieval Ship. In: Laanela, E. and Moore, J. (eds.), *ACUA Underwater Archaeology Proceedings*. Toronto (2009), pp. 111-116.

Jones, T., Nayling, N. and Tanner, P. (2013). Digitally Reconstructing the Newport Medieval Ship: 3D Designs and Dynamic Visualisations for Recreating the Original Hull Form, Loading Factors, Displacement, and Sailing Characteristics. In: Breen, C. and Forsythe, W. (eds.), *ACUA Underwater Archaeology Proceedings.* Leicester (2013), pp. 123-130.

Knapp, A. B. and Demesticha, S. (2016). *Appendix*. In: Knapp, A. B. and Demesticha, S. Mediterranean Connections: Maritime Transport Containers and Seaborne Trade in the Bronze and Early Iron Ages. London: Taylor & Francis, pp. 172-184.

Konecny, G. (2014). *Geoinformation: Remote Sensing, Photogrammetry and Geographic Information Systems*. 2nd. ed. London: Taylor & Francis.

Krajl, V. Z., Beltrame, C., Miholjek, I. and Ferri, M. (2016). A Byzantine Shipwreck from Cape Stoba, Mljet, Croatia: An Interim Report. *International Journal of Nautical Archaeology*, 45(1), pp. 42–58.

Leino, M., Ruuskanen, A.T., Flinkman, J., Kaasinen, J., Klemelä, U.E., Hietala, R. and Nappu, N. (2011). The Natural Environment of the Shipwreck Vrouw Maria (1771) in the Northern Baltic Sea: An Assessment of her State of Preservation. *International Journal of Nautical Archaeology*, 40, pp. 133–150.

Lin, S.-H. S. (2003). *Lading of the Late Bronze Age Ship at Uluburun*. Master's thesis. Texas A&M University.

Littlefield, J. (2012). *The Hull Remains of the Late Hellenistic Shipwreck at Kızılburun, Turkey*. Master's thesis. Texas A&M University.

Lock, G. (2003). *Using Computers in Archaeology: Towards Virtual Pasts*. London: Routledge.

Loizides, E. (2011). Conservation of Maritime Antiquities by the Department of Antiquities. *To Chroniko*, (194), pp. 16-18 (in Greek).

Loizides, E. (2017). *Conservation Activities of the Department of Antiquities, Cyprus. Progress Report.* [online] Honor Frost Foundation. Available at: https://honorfrostfoundation.org/wp-content/uploads/2019/09/DoA-Conservation-Activities-Report-2017.pdf [Accessed 20 Apr. 2021].

MacLeod, I. D. (1995). In Situ Corrosion Studies on the Duart Point Wreck, 1994. *International Journal of Nautical Archaeology*, 24(1), pp. 53–59.

Martin, C. (2011). *Wreck-Site Formation Processes*. In: A. Catsambis, A., Ford, B. and Hamilton, D. L. (eds.), The Oxford Handbook of Maritime Archaeology. Oxford: Oxford University Press, pp. 47–89.

Martin, K. and McCarthy, J. K. (2019). Virtual Reality for Maritime Archaeology in 2.5D: A Virtual Dive on a Flute Wreck of 1659 in Iceland. In: *2019 23rd International Conference in Information Visualization – Part II.* Adelaide (2019), IEEE, pp. 104-109.

McCarthy, M. (2001). *Iron and Steamship Archaeology: Success and Failure on the SS 'Xantho'*. New York: Kluwer Academic Publishers.

McCarthy, J. and Benjamin, J. (2014). Multi-image Photogrammetry for Underwater Archaeological Site Recording: An Accessible, Diver-Based Approach. *Journal of Maritime Archaeology*, 9, pp. 95-114.

McGlone, J. C., Mikhail, E. M., Bethel, J. S. and Mullen. R. (2004). *Manual of Photogrammetry*. Bethesda: American Society for Photogrammetry and Remote Sensing.

Muckelroy, K. (1975). A Systematic Approach to the Investigation of Scattered Wreck Sites. *International Journal of Nautical Archaeology and Underwater Exploration*, 4(2), pp. 173–190.

Muckelroy, K. (1978). *Maritime Archaeology. New Studies in Archaeology*. Cambridge: Cambridge University Press.

Murphy, L.E. (1997). *Site Formation Processes.* In: Delgado, J. P. (ed.), Encyclopaedia of Underwater and Maritime Archaeology. London: The British Museum Press, pp. 386-388.

Murray, W. M. (2020). *The Ship Class of the Egadi Rams and Polybius' Account of the First Punic War. The Site of the Battle of the Aegates Islands at the End of the First Punic War*. In:

Royal, J. G. and Tusa, S. (eds.), The Site of the Battle of the Aegates Islands at the End of the First Punic War: Fieldwork, Analyses and Perspectives, 2005-2015. Rome: L'ERMA di Bretschneider, pp. 27-38.

Olson, B. R., Placchetti, R. A., Quartermaine, J. and Killebrew. A. E. (2013). The Tel Akko Total Archaeology Project (Akko, Israel): Assessing the Suitability of Multiscale 3D Field Recording in Archaeology. *Journal of Field Archaeology,* (38), pp. 244–262.

O'Shea, J. (2002). The Archaeology of Scattered Wreck-Site: Formation Processes and Shallow Water Archaeology in Western Lake Huron. *International Journal of Nautical Archaeology,* 31, pp. 211–227.

Oxley, I. and Keith, M. E. (2016). *Introduction: Site formation processes of submerged shipwrecks.* In: Keith, M. E. (ed.), Site Formation Processes of Submerged Shipwrecks. Gainesville: University Press of Florida, pp. 1-14.

Parizzi, S. and Beltrame, C. (2020). Calculating the Tonnage and the Dimension of the Cargoes of Marble of Roman Period. *Digital Applications in Archaeology and Cultural Heritage,* 18, e00153. https://doi.org/10.1016/j.daach.2020.e00153.

Pasquet, J., Demesticha, S., Skarlatos, D., Merad, D. and Drap, P. (2017). Amphora Detection Based on a Gradient Weighted Error in a Convolution Neuronal Network. In: *IMEKO International Conference on Metrology for Archaeology and Cultural Heritage*. Lecce (2017), pp. 23-25.

Piccoli, C. (2018). *Visualizing Cityscapes of Classical Antiquity: From Early Modern Reconstruction Drawings to Digital 3D Models, with a Case Study from the Ancient Town of Koroneia in Boeotia, Greece*. Oxford: Archaeopress.

Polakowski, M. (2016). *Warships of the First Punic War: An Archaeological Investigation and Contributory Reconstruction of the Egadi 10 Warship from the Battle of the Egadi Islands (241 B.C.).* Master Thesis. East Carolina University.

Poveda, P. (2017). Les Modèles Tridimensionnels de l'Epave Dramont E. Hydrostatique et Réalité Virtuelle au Service de la Restitution en Archéologie Navale. *Archaeonautica*, (19), pp. 27–40.

Quinn, R. (2006). The Role of Scour in Shipwreck Site Formation Processes and the Preservation of Wreck-Associated Scour Signatures in the Sedimentary Record: Evidence from the Seabed and Sub-surface Data. *Journal of Archaeological Sciences,* 33, pp. 1419–1432.

Radic Rossi, I. (2005). The Amphora's Toe: Its Origin and Function. *Skyllis*, 7(1–2), pp. 160–170.

Radić Rossi, I., Casabán, J., Yamafune, K., Torres, R. and Batur, K. (2019). *Systematic*

Photogrammetric Recording of the Gnalić Shipwreck Hull Remains and Artefacts. In: McCarthy, J., Benjamin, J., Winton, T. and van Duivenvoorde, W. (eds.), 3D Recording and Interpretation for Maritime Archaeology. Cham: Springer, pp. 45-65.

Ravn, M., Bischoff, V., Englert, A. and Nielsen. S. (2011). *Recent Advanced in Post-Excavation Documentation, Reconstruction, and Experimental Maritime Archaeology.* In: A. Catsambis, A., Ford, B. and Hamilton, D. L. (eds.), The Oxford Handbook of Maritime Archaeology. Oxford: Oxford University Press, pp. 232-249.

Rodríguez Iborra, J. (2012). *La Carta Arqueológica Subacuática del Litoral de la Región de Murcia: Actualización Metodológica y Documental*. Master's thesis. Universidad de Murcia.

Rose, K. J. (2014). *The Naval Architecture of Vasa, a 17th-Century Swedish Warship.* Doctoral Thesis. Texas A & M University.

Royal, J. (2018). *The Illyrian Coastal Exploration Program (2010-14): The Roman and Late-Roman Finds.* Raleigh: Independently Published.

Secci, M., Beltrame, C., Manfio, S. and Guerra, F. (2019). Virtual Reality in Maritime Archaeology Legacy Data for a Virtual Diving on the Shipwreck of the Mercurio (1812). *Journal of Cultural Heritage*, 40, pp.169-176.

Secci, M., Demesticha, S., Jimenez, C., Papadopoulou, C. and Katsouri, I. (2021). A LIVING SHIPWRECK: An Integrated Three-dimensional Analysis for the Understanding of Site Formation Processes in Archaeological Shipwreck Sites. *Journal of Archaeological Science: Reports,* 35, 102731.

Sedlazeck, A., Köser, K., and Koch, R. (2010). Supporting Underwater Archaeology by 3D Reconstruction from Underwater Images. *Skyllis,* 10, pp. 179-186.

Seinturier, J., Drap, P., Vincent, N., Cibecchini, F., Papini O. and Grussenmeyer, P. (2004). Orthophoto Imaging and GIS for Seabed Visualization and Underwater Archaeology. In: Niccolucci, F. and Hermon, S. (eds.), *Beyond the Artifact. Digital Interpretation of the Past. Proceedings of Computer Applications and Quantitative Methods in Archaeology.* Prato (2004), Budapest: Archaeolingua, pp. 1-6.

Schiffer, M. B. (1976). *Behavioral Archeology*. New York: Academic Press.

Schiffer, M. B. (1987). *Formation Processes of the Archaeological Record*. Albuquerque: University of New Mexico Press.

Schiffer, M. B. (1996). *Formation Processes of the Archaeological Record*. 2nd. ed. Salt Lake City: University of Utah Press.

Skarlatos, D. (2011). Photogrammetric Documentation of the Wreck. *To Chroniko*, (194), p. 14 (in Greek).

Skarlatos, D., Demesticha, S. and Kiparissi. S. (2012). An 'Open' Method for 3D Modelling and Mapping in Underwater Archaeological Sites. *International Journal of Heritage in the Digital Era,* 1, pp. 1–23.

Spooner, S. Q. (2004). *Shipwreck Taphonomy. A Study of Historic Wreck Formation Processes on the North Coast of the Dominican Republic from 1690 to 1829*. Doctoral Thesis. University of Bristol.

Stewart, D. (1999). Formation Processes Affecting Submerged Archaeological Sites: An Overview. *Geoarchaeology: An International Journal,* 14, pp. 565–587.

Tanner, P. (2013). 3D laser scanning for the digital reconstruction and analysis of a 16th-century clinker built sailing vessel. In: Breen, C. and Forsythe, W. (eds.), *ACUA Underwater Archaeology Proceedings.* Leicester (2013), pp. 137-149.

Throckmorton, P. (1965). *The Lost Ships: An Adventure in Undersea Archaeology*. 1st ed. London: J. Cape.

Tsiafki, D. and Michailidou, N. (2015). Benefits and Problems through the Application of 3D Technologies in Archaeology: Recording, Visualization, Representation and Reconstruction. *Scientific Culture*, 1(3), pp. 37-45.

Verhoeven, G. (2011). Taking Computer Vision Aloft – Archaeological Three-dimensional Teconstructions from Aerial Photographs with PhotoScan. *Archaeological Prospection*, 18, pp. 67–73.

Vlachaki, F., Diamanti, E., Farazis, G. and Agouridis, C. (2020). *Towards Spatio-Temporal 3D Visualization of an Underwater Archaeological Excavation: The Case of the Late Bronze Age Shipwreck of Modi.* [online] Honor Frost Foundation. Available at: https://honorfrostfoundation.org/wp-content/uploads/2020/03/HFF_UTM_SR_Vlachaki_figures.pdf [Accessed 20 Apr. 2021].

Ward, A. K., Larcombe, P. and Veth, P. (1999). A New Process-Based Model for Wreck Site Formation. *Journal of Archaeological Science,* 26, pp. 561–570.

Ware, C. (2004). *Information Visualization: Perception for Design*. 2nd. ed. San Francisco: Morgan Kaufmann.

Wells, A. E. (2008). *Virtual Reconstruction of a Seventeenth-Century Portuguese Nau*. Master's Thesis. Texas A&M University.

Yamafune, K., Torres, R. and Castro, F. (2016). Multi-Image Photogrammetry to Record and Reconstruct Underwater Shipwreck Sites. *Journal of Archaeological Method and Theory*, 24, pp. 703-725.

Zubrow, E. B. (2006). *Digital Archaeology. A Historical Context.* In: Evans, T. L. and Daly, P. (eds.), Digital Archaeology. Bridging Method and Theory. Abingdon: Routledge, pp. 8-27.

Πανεπιστήμιο Κύπρου

ΠΡΟΣ
Τμήμα Αρχαιοτήτων
Λεωφόρος Μουσείου 1, 1097, Λευκωσία
antiquitiesdept@da.mcw.gov.cy

Λευκωσία, 21/05/2021

Αίτηση για χορήγηση άδειας για τη χρήση και δημοσίευση φωτογραφιών

Σε συνέχεια της από 12 Μαΐου 2021 επιστολής σας, επανυποβάλλω το αίτημα για χορήγηση άδειας για τη δημοσίευση φωτογραφιών ευρημάτων από την ανασκαφή ναυαγίου Μαζωτού, τα οποία έχουν συγκολληθεί από την ομάδα συντηρητών του Τμήματος Αρχαιοτήτων (βλ. συνημμένο κατάλογο). Η μελέτη έγινε στο πλαίσιο εκπόνησης της μεταπτυχιακής μου διατριβής για το πρόγραμμα μάστερ Field Archaeology on Land and under the Sea του Πανεπιστημίου Κύπρου, υπό την επίβλεψη της Δρ. Στέλλας Δεμέστιχα.

Επισυνάπτω τη γραπτή άδεια μελέτης των ερυημάτων του καταλόγου από τη διευθύντρια της ανασκαφής του ναυαγίου του Μαζωτού, Δρ. Στέλλα Δεμέστιχα.

Παραμένω στη διάθεσή σας για περαιτέρω πληροφορίες ή διευκρινίσεις.

Με εκτίμηση,

Ειρήνη Κατσούρη

Μεταπτυχιακή Φοιτήτρια
Πρόγραμμα Field Archaeology on Land and under the Sea
Πανεπιστήμιο Κύπρου
ikatso01@ucy.ac.cy

Κατάλογος ευρημάτων και φωτογραφιών από το αρχείο του Εργαστηρίου Συντήρησης Εναλίων Ευρημάτων του Τμήματος Αρχαιοτήτων.

	DSC_4921.JPG Εύρημα: P0385		DSC_6506.JPG Εύρημα: P0273
	DSC_4968.JPG Εύρημα: P0353		DSC_5213.JPG Εύρημα: P0357
	DSC_6509.JPG Εύρημα: P0342		DSC_5240.JPG Εύρημα: P0314
	DSC_5216.JPG Εύρημα: P0310		DSC_6903.JPG Ευρήματα: P0310, P0295
	P4089700.JPG Εύρημα: P0295		DSC_6856.JPG Εύρημα: P0292
	DSC_5244.JPG Ευρήματα: P0220, P0371		DSC_6160.JPG Εύρημα: P0263
	DSC_6865.JPG Εύρημα: P0018		DSC_5271.JPG Ευρήματα: P0290, P0362
	DSC_5279.JPG Εύρημα: P0141		DSC_6610.JPG Εύρημα: P0385
	DSC_5282.JPG Εύρημα: P0151		DSC_6887.JPG Εύρημα: P0384
	DSC_6886.JPG Εύρημα: P0384		

2

Πανεπιστήμιο Κύπρου
Ερευνητική Μονάδα Αρχαιολογίας

Τ.Θ. 20537, Λευκωσία 1678, Κύπρος
Τηλ.: +357 22893560
Τηλεομοιότυπο:: + 357 22895057
Ηλ. Διεύθυνση: archlgy@ucy.ac.cy

ΠΡΟΣ
Τμήμα Αρχαιοτήτων
Λεωφόρος Μουσείου 1, 1097, Λευκωσία
antiquitiesdept@da.mcw.gov.cy
Λευκωσία, 20/05/2021

ΑΔΕΙΑ ΜΕΛΕΤΗΣ ΦΩΤΟΓΡΑΦΙΩΝ ΑΠΟ ΤΗΝ ΑΝΑΣΚΑΦΗ ΝΑΥΑΓΙΟΥ ΜΑΖΩΤΟΥ

Σας ενημερώνω με την παρούσα επιστολή ότι έχω χορηγήσει στην Ειρήνη Κατσούρη, μεταπτυχιακή φοιτήτρια του Πανεπιστημίου Κύπρου, άδεια μελέτης των ευρημάτων που περιλαμβάνονται στον παρακάτω κατάλογο, στο πλαίσιο εκπόνησης διατριβής μάστερ με συναφές θέμα.

Στέλλα Δεμέστιχα

Αναπληρώτρια Καθηγήτρια Ενάλιας Αρχαιολογίας
Διευθύντρια Ανασκαφής Ναυαγίου Μαζωτού

	DSC_4921.JPG Εύρημα: P0385		DSC_6506.JPG Εύρημα: P0273
	DSC_4968.JPG Εύρημα: P0353		DSC_5213.JPG Εύρημα: P0357
	DSC_6509.JPG Εύρημα: P0342		DSC_5240.JPG Εύρημα: P0314
	DSC_5216.JPG Εύρημα: P0310		DSC_6903.JPG Ευρήματα: P0310, P0295
	P4089700.JPG Εύρημα: P0295		DSC_6856.JPG Εύρημα: P0292
	DSC_5244.JPG Ευρήματα: P0220, P0371		DSC_6160.JPG Εύρημα: P0263
	DSC_6865.JPG Εύρημα: P0018		DSC_5271.JPG Ευρήματα: P0290, P0362
	DSC_5279.JPG Εύρημα: P0141		DSC_6610.JPG Εύρημα: P0385
	DSC_5282.JPG Εύρημα: P0151		DSC_6887.JPG Εύρημα: P0384
	DSC_6886.JPG Εύρημα: P0384		

ΚΥΠΡΙΑΚΗ ΔΗΜΟΚΡΑΤΙΑ
ΥΠΟΥΡΓΕΙΟ ΜΕΤΑΦΟΡΩΝ, ΕΠΙΚΟΙΝΩΝΙΩΝ ΚΑΙ ΕΡΓΩΝ

ΤΜΗΜΑ ΑΡΧΑΙΟΤΗΤΩΝ
1516 ΛΕΥΚΩΣΙΑ

Αρ. Φακ.: 14.01.001.23
Αρ. Τηλ.: 22865812
Αρ. Φαξ.: 22303148

31 Μαΐου 2021

Κα Ειρήνη Κατσούρη
katsouri.irene@ucy.ac.cy

Αγαπητή κυρία Κατσούρη,

ΘΕΜΑ: ΑΙΤΗΣΗ ΓΙΑ ΧΟΡΗΓΗΣΗ ΑΔΕΙΑΣ ΓΙΑ ΤΗ ΧΡΗΣΗ ΚΑΙ ΔΗΜΟΣΙΕΥΣΗ ΦΩΤΟΓΡΑΦΙΩΝ

Αναφέρομαι στο πιο πάνω θέμα σε συνέχεια ηλεκτρονικού μηνύματος σας ημερομηνίας 21 Μαΐου 2021 και επιθυμώ να σας ενημερώσω ότι το αίτημα σας εγκρίνεται με τον όρο όπως στην δημοσίευση αναφερθεί ότι οι συγκεκριμένες φωτογραφίες χρησιμοποιούνται με την άδεια του Τμήματος Αρχαιοτήτων.

Παρακαλώ όπως αποστείλετε αντίγραφο της δημοσίευσης σας στην Βιβλιοθήκη του Τμήματος Αρχαιοτήτων Κύπρου.

Με εκτίμηση,

Δρ. Μαρίνα Σολομίδου-Ιερωνυμίδου
Διευθύντρια
Τμήματος Αρχαιοτήτων